THE NATURE OF THE PASTE – AGGREGATE INTERFACE

NOVEMBER 1972 – NUMBER 40

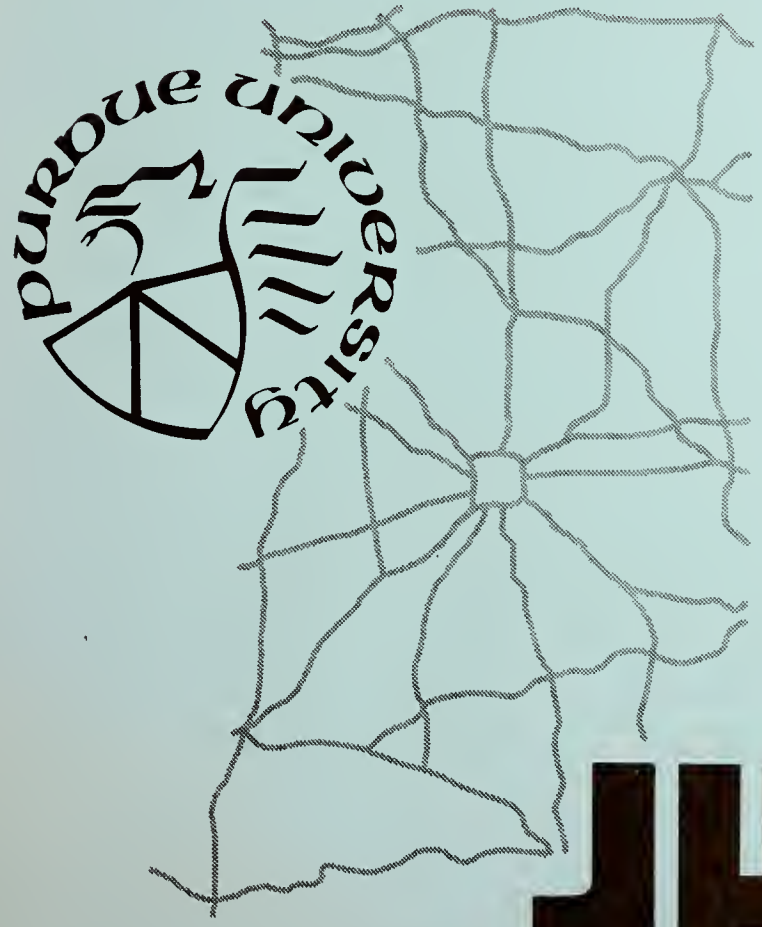

BY

DAVID W. HADLEY

JHRP

JOINT HIGHWAY RESEARCH PROJECT

PURDUE UNIVERSITY AND

INDIANA STATE HIGHWAY COMMISSION

Interim Report

THE NATURE OF THE PAST-AGGREGATE INTERFACE

TO: J. F. McLaughlin, Director
Joint Highway Research Project

November 9, 1972

Project: C-36-61E

FROM: H. L. Michael, Associate Director
Joint Highway Research Project

File: 5-14-5

The attached Report is an Interim one on the HPR Part I Research Study titled "Fundamental Studies of Portland Cement Concrete". The research reported was conducted as part of Phase II of this Study and is titled "The Nature of the Paste-Aggregate Interface". Mr. David W. Hadley authored the Report under the direction of Professors W. L. Dolch and Sidney Diamond.

The research reported herein was designed to determine the structure developed at the interface between hardened portland cement paste and aggregates, to study the effect of common variables on this structure, and to relate the structure at the interface to paste-aggregate bond. A scanning electron microscope-x-ray spectrometer combination, together with x-ray diffraction and optical microscopy, were used in conduct of this research. The Report details the results of the research.

As the Study was performed as an HPR one, copies of the Report will be forwarded for review, comment and acceptance to the ISHC and FHWA. The Report is submitted for acceptance as partial fulfillment of the objectives of Phase II of this Study.

Respectfully submitted,

Harold L. Michael
Associate Director

HLM:ms

cc:
W. L. Dolch
R. L. Eskew
W. H. Goetz
M. J. Gutzwiller
G. K. Hallock
R. H. Harrell
M. L. Hayes
C. W. Lovell
G. W. Marks
R. D. Miles
J. W. Miller
G. T. Satterly
C. F. Scholer
M. B. Scott
J. A. Spooner
N. W. Steinkamp
H. R. J. Walsh
E. J. Yoder

Digitized by the Internet Archive
in 2011 with funding from
LYRASIS members and Sloan Foundation; Indiana Department of Transportation

http://www.archive.org/details/natureofpastaggr00hadl

Interim Report

THE NATURE OF THE PASTE-AGGREGATE INTERFACE

by

David W. Hadley
Graduate Instructor in Research

Joint Highway Research Project

Project No.: C-36-61E

File No.: 5-14-5

Prepared as Part of an Investigation

Conducted by

Joint Highway Research Project
Engineering Experiment Station
Purdue University

In cooperation with the

Indiana State Highway Commission

and the

U.S. Department of Transportation
Federal Highway Administration

The opinions, findings and conclusions expressed in this publication are those of the authors and not necessarily those of the Federal Highway Administration.

Purdue University
West Lafayette, Indiana
November 9, 1972

TABLE OF CONTENTS

	Page
LIST OF TABLES	iv
LIST OF FIGURES	v
ABSTRACT	xi
CHAPTER I - INTRODUCTION	1
Purpose and Scope	1
Nomenclature	2
Literature Review	5
Paste-Aggregate Bond	5
Microcracking at the Paste-Aggregate Interface	6
Relationship Between Bond and Concrete Strength	7
Calcium Hydroxide at the Paste-Aggregate Interface	9
Scanning Electron Microscopy of Cement Paste	10
Chemical Reactions at the Paste-Aggregate Interface	13
Equipment and Procedures	15
Scanning Electron Microscopy	15
Equipment	16
Sample Preparation	16
Procedure	19
Energy Dispersive X-Ray Spectrometry	19
Equipment	21
Calibration	21
Sample Preparation	22
Procedure	22
X-Ray Powder Diffraction	26
Equipment	26
Sample Preparation and Procedures	26
Materials	27
Substrates	27
Cement	28
Mortar Sands	28

TABLE OF CONTENTS, cont.

Page

CHAPTER II - PRESENTATION AND DISCUSSION OF RESULTS . 30

Particle Sizes in Cement 30
The Nature and Development of the Interfacial Region; 0 - 28 Days 33
Hydrated for One Day 33
General Features 33
Interfacial Film 35
Partially Hydrated Grains 38
Fractured Grains 41
Massive Lime Crystals 49
Aggregations of Grains 55
Elemental Distribution 55
Mode of Fracture 58
Hydration for Three Days 59
Hydration for Seven Days 67
Hydrated Fourteen Days 78
Hydrated Twenty-eight Days 83
Early Development of Structure at the Interface . . 87
Sample Dried Immediately After Casting 87
Hydrated One Hour 93
Hydration for Four Hours 93
Hydration for Eight Hours 98
X-Ray Diffraction Studies of Lime Orientation . . . 103
Hydration of Artificial Cements 107
Morphology Within the Hydration Shells 108
Composition of Large Needles 112
Effect of Substrate Orientation 112
Effect of Water-Cement Ratio 116
The Bonding of Paste to Roughened Surfaces 116
The Structure Developed on Quartzite 120
The Structure Developed on Marble 141

CHAPTER III - SUMMARY AND CONCLUSIONS 156

Summary 156
Conclusions 168

LIST OF REFERENCES 170

APPENDIX 174

Ottawa Sand Mortars 174
Manufactured Calcite Sand Mortars 181

VITA 186

LIST OF TABLES

Table		Page
1.	Common Oxides and their Abbreviations	2
2.	Nomenclature and Abbreviations for Major Cement Compounds	3
3.	Physical and Chemical Properties of Cement 317	29
4.	Analysis of Platy Crystals	66

LIST OF FIGURES

Figure		Page
1.	Calibration for CaO/SiO_2 Ratio	23
2.	Calibration for CaO/SO_3 Ratio	24
3.	Calibration for CaO/Al_2O_3	25
4.	Size Distribution in Cement	31
5.	Size Distribution in Cement	32
6.	Surface of Glass Substrate - 1 Day	34
7.	Interfacial Film on Substrate - 1 Day	36
8.	Lime Film on Paste - 1 Day	37
9.	C-S-H Gel on Lime Film - 1 Day	39
10.	Partially Hydrated Cement Grains - 1 Day . . .	40
11.	Ruptured Partially Hydrated Grains - 1 Day . .	42
12.	Hydration Shell - 1 Day	43
13.	Hydration Shell and Remnant Grain - 1 Day . . .	44
14.	Hydration Shell and Remnant Grain - 1 Day . . .	45
15.	Hydration Shell and Remnant Grain - 1 Day . . .	46
16.	Hydration Shell and Remnant Grain - 1 Day . . .	47
17.	Hydration Shell and Remnant Grain - 1 Day . . .	48
18.	Layered Structure in Hydration Shell - 1 Day .	50
19.	Massive Lime Crystals - 1 Day	51
20.	Massive Lime Crystals - 1 Day	53
21.	Separation Through Lime Film - 1 Day	54

LIST OF FIGURES, cont.

Figure		Page
22.	Aggregation of Cement Grains - 1 Day	56
23.	Surface of Glass Substrate - 3 Days	60
24.	Hydration Shells with Ettringite - 3 Days	61
25.	Hydration Shell - 3 Days	62
26.	Platy Crystals - 3 Days	64
27.	Platy Crystals - 3 Days	65
28.	Support of Interfacial Film by Platy Crystals - 3 Days	68
29.	Surface of Glass Substrate - 7 Days	69
30.	Hydration Shell and C-S-H Gel - 7 Days	70
31.	Reticular Network Structure of C-S-H Gel - 7 Days	72
32.	Early Development of Reticular Network - 3 Days	73
33.	Surface of Interfacial Film - 7 Days	74
34.	Interfacial Film Supported by Platy Crystals - 7 Days	75
35.	Reticular Network Structure on Grain - 7 Days	76
36.	Surface of Glass Substrate - 14 Days	79
37.	C-S-H Gel on Interfacial Film - 14 Days	80
38.	Hydration Shell - 14 Days	81
39.	Hydration Shell - 14 Days	82
40.	Surface of Lime Film - 28 Days	84
41.	Ettringite Crystals - 28 Days	85
42.	Hydration Shell - 28 Days	86

LIST OF FIGURES, cont.

Figure		Page
43.	Surface of Glass Substrate - 0 Hours	88
44.	C-S-H Gel on Interfacial Film - 0 Hours	90
45.	Oriented Lime Platelets on Grain - 0 Hours	91
46.	Oriented Lime Platelets on Grain - 0 Hours	92
47.	Surface of Glass Substrate - 1 Hour	94
48.	C-S-H Gel on Interfacial Film - 1 Hour	95
49.	Oriented Lime Platelets on Grain - 1 Hour	96
50.	Surface of Grain Hydrated Four Hours	97
51.	Surface of Glass Substrate - 8 Hours	99
52.	Aggregation of Grains - 8 Hours	100
53.	Ruptured Partially Hydrated Grain - 8 Hours	101
54.	Hydration Shell and Remnant Grain - 8 Hours	102
55.	C-S-H Gel on Interfacial Film - 8 Hours	104
56.	Preferred Orientation of Lime	106
57.	Hydration Shell - Alite Paste - 3 Days	109
58.	Hydration Shell - Alite + Gypsum - 3 Days	110
59.	Hydration Shell - Alite + Gypsum + C_3A - 3 Days	111
60.	Alite + Gypsum Paste - 3 Days	113
61.	Alite + Gypsum + C_3A Paste - 3 Days	114
62.	Paste Cast Against Vertical Surface - 7 Days	115
63.	Roughened Glass Surface	118
64.	Roughened Glass Surface	119
65.	Roughened Glass Substrate - 1 Day	121

LIST OF FIGURES, cont.

Figure		Page
66.	Roughened Glass Substrate - 1 Day	122
67.	Roughened Glass Substrate - 3 Days	123
68.	Roughened Glass Substrate - 3 Days	124
69.	Roughened Glass Substrate - 7 Days	125
70.	Roughened Glass Substrate - 7 Days	126
71.	Roughened Glass Substrate - 14 Days	127
72.	Roughened Glass Substrate - 14 Days	128
73.	Roughened Glass Substrate - 28 Days	129
74.	Roughened Glass Substrate - 28 Days	130
75.	Quartzite Surface	131
76.	Quartzite Surface	132
77.	Quartzite Substrate - 1 Day	133
78.	Quartzite Substrate - 3 Days	134
79.	Quartzite Substrate - 7 Days	135
80.	Quartzite Substrate - 7 Days	136
81.	Quartzite Substrate - 14 Days	137
82.	Quartzite Substrate - 28 Days	138
83.	Paste Against Quartzite - 28 Days	139
84.	Paste Against Quartzite - 28 Days	140
85.	Paste Against Quartzite - 3 Days	142
86.	Marble Substrate	143
87.	Marble Substrate	144
88.	Marble Substrate - 1 Day	145
89.	Marble Substrate - 1 Day	146

LIST OF FIGURES, cont.

Figure Page

90. Separation Through Marble - 1 Day 147

91. Marble Substrate - 3 Days 148

92. Marble Substrate - 3 Days 149

93. Marble Substrate - 7 Days 151

94. Marble Substrate - 7 Days 152

95. Marble Substrate - 14 Days 153

96. Interface Region Immediately After Consolidation 157

97. Cement Grain at Interface 158

98. Interface After 1/2 Hour 160

99. Interface After Two Hours 161

100. Interface After Eight Hours 163

101. Interface After One Day 164

102. Interface After Three Days 166

103. Interface After Three Days 167

Appendix
Figure

104. Ottawa Sand Mortar - 1 Day 175

105. Ottawa Sand Mortar - 1 Day 176

106. Ottawa Sand Mortar - 3 Days 177

107. Ottawa Sand Mortar - 3 Days 178

108. Ottawa Sand Mortar - 7 Days 179

109. Ottawa Sand Mortar - 7 Days 180

110. Ottawa Sand Mortar - 14 Days 182

LIST OF FIGURES, cont.

Appendix
Figure Page

111. Ottawa Sand Mortar - 14 Days 183

112. Manufactured Calcite Sand Mortar - 1 Day . . . 184

113. Manufactured Calcite Sand Mortar - 1 Day . . . 185

ABSTRACT

Hadley, David Watson. Ph.D., Purdue University, August 1972. The Nature of the Paste-Aggregate Interface. Major Professor: W. L. Dolch.

The research was designed to determine the structure developed at the interface between hardened portland cement paste and aggregates, to study the effect of common variables on this structure, and to relate the structure at the interface to paste-aggregate bond.

The greater part of the research was done using a scanning electron microscope-x-ray spectrometer combination. X-ray diffraction and optical microscopy were used to a lesser extent.

A considerable volume of water-filled void space remains at the paste-aggregate interface after consolidation of the paste. The bonding of the paste to the aggregate is accomplished primarily through the filling of this space with the products of cement hydration.

The first feature to form in the interfacial void is a film of lime, about 1/4 micron thick, that is deposited directly on the surface of the aggregate. The lime in this film is almost perfectly oriented, with the c-axes normal to the aggregate surface. A layer of C-S-H gel is

subsequently deposited on the surface of the lime film lying toward the void, giving rise to a compound interfacial film.

Within four to eight hours of casting, large and randomly oriented crystals of lime begin to form in the interfacial void. As these crystals grow, they engulf and encapsulate partially hydrated cement grains. This process results in the progressive filling of the void and in the tying of the interfacial film to the main body of paste.

After one to three days, needles of ettringite and booklets of large platy hexagonal crystals are also deposited in the interfacial void space. The platy crystals are neither lime nor calcium monosulfate aluminate hydrate, but rather appear to be a complex solid solution of calcium, silica, alumina, and sulfur.

A complex shell of hydration products forms on the hydrating cement grains. This shell consists of an inner layer of lime and an outer layer of C-S-H gel. The lime in the shell is also oriented plane-parallel to the interface, but the degree of orientation decreases away from the interface. Random orientation is reached at about 200 microns. Small crystals of ettringite are believed to be encapsulated within the lime in the hydration shells.

With the exception of a few acicular crystals, no hydration products are deposited on the inner surface of

the hydration shells within the first 28 days. As the grains hydrate, a progressively larger void space develops within the shell. By 28 days, many of the hydration shells are completely hollow. It is not known if these features also form in the interior of the paste, nor if they are eventually filled.

The type of structure that develops at the interface is independent of the aggregate type, surface roughness, orientation of the interface, or water-cement ratio.

At early ages, fracture is mainly in the void space between the interfacial film and the main body of paste. As the interfacial void is filled, fracture moves progressively to the immediate vicinity of the interface. Once the void is filled, fracture is primarily a function of the properties of the aggregate. With strong aggregates, such as the siliceous rocks, fracture occurs through the lime portion of the interfacial film. With aggregates composed of minerals that have well developed cleavages, such as limestones, fracture is largely through the mineral cleavages. In no case does fracture occur at the true paste-aggregate interface.

CHAPTER I - INTRODUCTION

In this introductory chapter, the purpose and scope of the research will be stated, nomenclature will be discussed, pertinent literature will be reviewed, and the equipment, experimental techniques, and materails used will be described.

Purpose and Scope

The overall purpose of the research described in this thesis was to determine the nature of the interface between various aggregate materials and paste formed through the hydration of portland cement. Basic to this investigation were:

1. Study of the morphology and development of paste structure in the interface region.

2. Study of the influence of such factors as the nature and roughness of the aggregate surface, surface orientation, and water-cement ratio of the cement paste on the structure developed at the interface.

3. Study of the relationship between the structure at the interface and the bond between cement paste and aggregate.

Since it was recognized that chemical reactions between paste and aggregate occur, and especially at later ages would obscure relationships at the interface, this study was limited to samples cured for twenty-eight days or less.

Nomenclature

It is common practice in the cement industry and among those engaged in research relating to portland cement and concrete, to report analytical data on the basis of oxides of the elements present. Abbreviations for the more common oxides have been developed and are universally used in the literature. The common oxides and their abbreviations are listed in Table 1.

TABLE 1

COMMON OXIDES AND THEIR ABBREVIATIONS

Oxide	Abbreviation
CaO	C
SiO_2	S
Al_2O_3	A
Fe_2O_3	F
SO_3	$\bar{S}$
H_2O	H
MgO	M
Na_2O	N
K_2O	K

The major phases present in portland cement are commonly referred to in terms of combinations of the abbreviations for their constituent oxides. Tricalcium silicate ($3\ CaO \cdot SiO_2$), for example, would be called C_3S. The substituted forms of the anhydrous phases actually present in cement have also been given so called "mineral" names. Thus impure C_3S is called "alite". The abbreviations and "mineral" names for the principal cement compounds are listed in Table 2.

TABLE 2

NOMENCLATURE AND ABBREVIATIONS FOR MAJOR CEMENT COMPOUNDS

Chemical Composition	Abbreviation	"Mineral" Name
$3CaO \cdot SiO_2$	C_3S	Alite
$2CaO \cdot SiO_2$	C_2S	Belite
$3CaO \cdot Al_2O_3$	C_3A	Aluminate phase
$4CaO \cdot Al_2O_3 \cdot Fe_2O_3$ *	C_4AF	Ferrite phase

* actually solid solution series ranging roughly from C_2F to C_6A_2F.

A relatively complex system of nomenclature has also been developed for the hydration products of portland cement. A brief description of the principal hydration products and their nomenclature is given below:

Lime: One of the principal products of cement hydration is calcium hydroxide, which is normally referred to as

lime. The mineral name, portlandite, is also sometimes used.

C-S-H gel: Both silicate phases in cement hydrate to produce a poorly-crystallized and highly-substituted material referred to as calcium silicate hydrate gel. This material has a non-stoichiometric composition and an extremely high surface area. The x-ray diffraction pattern exhibits three broad peaks that correspond to the principal peaks for the mineral tobermorite. For this reason, some authors refer to it as "tobermorite gel" or "tobermoroid gel". Many modern workers use the hyphenated form, C-S-H gel, to convey the variable composition.

Sulfoaluminates: During early hydration, the aluminate phase in portland cement reacts with sulfate ion released from the gypsum added to cement to control the rate of hardening. The hydrated calcium aluminate sulfate that forms is of two types. The first formed product has the composition $C_3A \cdot 3\ C\bar{S} \cdot H_{32}$, and is called "high form" sulfoaluminate or ettringite.

The second form, which is produced by reaction of the ettringite with additional aluminate released by the hydrating C_3A, has the composition $C_3A \cdot C\bar{S} \cdot H_{12}$ and is referred to as "low form" sulfoaluminate or "monosulfoaluminate".

Literature Review

Paste-Aggregate Bond

Much of the published research dealing with relationships at the interface between hydrated cement paste and aggregates has dealt primarily with the question of paste-aggregate bond. (1-11) An excellent review on this subject was published by Alexander et al. (3), and further insight was provided by Scholer (11). The results of these studies are summarized below:

Aggregate Type. All investigators found that the bond strength varied with the type of aggregate. Normally, the bond developed with siliceous aggregates was greater than that with carbonate aggregates (3, 5, 11). Hsu and Slate (6), however, found, in the limited suite of rocks they tested, the greatest strength with a limestone.

With siliceous rocks, the bond increased with increasing silica content (3).

Variations in bond strengths within a group of limestone aggregates was found to be minor compared to the differences between limestone and quartzite aggregates (11).

Surface Texture. The bond to broken, sawed, or ground surface was found to be similar (3, 6, 11). Differences were attributed by Alexander et al. (3) to the amount of broken or disrupted material on the aggregate surface, rather than to surface roughness itself.

Although Alexander et al. (3) and Hsu and Slate (6) found the bond strength to be lower with highly polished aggregate surfaces, Scholer (11) found the opposite true in some instances.

Weathered Surfaces. Naturally weathered and water-worn surfaces gave appreciably lower bond strengths than fresh surfaces (3).

Curing Temperatures. Bond strength was found to be independent of curing temperature (3).

Age. The strength of the paste-aggregate bond was found to increase in bond strength to be relatively minor with carbonate aggregates.

Water-Cement Ratio. Bond strength was found to decrease with increasing water-cement ratio (3, 6). The effect was intensified with increasing aggregate size (3).

Drying of Test Specimen. A number of investigators found the apparent bond strength to decrease rapidly as the sample dried (3, 5, 6, 11).

Specimen Size. Tensile bond strength was found to be independent of specimen size, whereas shear bond strength decreased with increasing size (3).

Microcracking at the Paste-Aggregate Interface

It has been found that when concrete is subjected to a compressive stress, disruption of the concrete first appears in the form of microcracks at the interface between the mortar and the coarse aggregate particles (8, 12, 13,

14). These microcracks apparently represent bond failures, and have been found to some extent in concrete prior to any loading, presumably due to dimensional changes within the paste (8, 12).

Hsu et al. (12) reported that these bond cracks first begin to form in large numbers at about 30-50% of the ultimate load. Their formation continues to be the most important cracking mechanism until about 70% of the ultimate, at which point cracks begin to propogate through the paste. Even when continuous cracks have formed, however, the greater part of their length lies at the paste-coarse aggregate interface.

Scholer (11) found that the load at which large numbers of cracks began to form did not seem to be a function of the bond strength. The total area of separation, however, was related to the strength of the paste-aggregate bond.

Relationship Between Bond and Concrete Strengths

A number of investigators (3, 11, 15, 16) studied the relationship between the strength of the paste-aggregate bond and that of concrete.

Alexander and Taplin (2) fitted equations of the form:

$$Y = b_0 + b_1 m_1 + b_2 m_2$$

where:

m_1 = modulus of rupture of the Paste (lbs./in.^{2})

m_2 = modulus of rupture of the cement-aggregate bond (lbs./in.^{2})

when Y = modulus of rupture of concrete (lbs./in.^{2}),

b_o= 290, b_1 = 0.318, b_2 = 0.162

when Y = compressive strength of concrete (lbs./in.^{2}),

b_o= 480, b_1 = 2.08, b_2 = 1.02

Scholer (11) also found that the stronger the paste-aggregate bond, the stronger the concrete in both compression and flexure.

Using a novel approach, Nepper-Christensen and Nielsen (15) compared the strength of a concrete made with glass marbles with an identical mix in which the marbles had been coated with a 12 micron thick layer of a soft plastic to lessen the paste-aggregate bond. They found that the coating reduced the concrete strength by as much as 2.5 times. They noted, however, that deformation of the relatively thick and soft coating might have had an appreciable effect.

In a similar study, Darwin and Slate (16) coated coarse aggregate particles with both a thin (0.0004 in.) and a thick (0.001 in.) coating of polystyrene. They found that the thickness and deformability of the coating was a significant factor in strength reduction. Even with the thin, hard coating, however, the lowered bond strength with the coated particles caused a 10-15% reduction in compressive strength.

Calcium Hydroxide at the Paste-Aggregate Interface

Several investigators (5, 17, 18, 19, 20, 21, 22) have reported that the aggregate particles in concrete are often surrounded by a layer of calcium hydroxide. A comprehensive review of the occurrence of calcium hydroxide in concrete was prepared by Bache et al. (17), who reported that layers of calcium hydroxide up to fifty microns thick had been observed around aggregate particles.

Although Lyubimov and Pinus (18) stated that no layer of calcium hydroxide was observed around carbonate aggregate particles, Mather (19) reported that such layers do form on carbonate aggregates. She observed, however, that the layers that formed around carbonate aggregates were composed of much smaller crystals than those around siliceous aggregates such as granodiorite and diorite.

Farran (5) also noted the development of calcium hydroxide around carbonate aggregates and postulated that the bond between the calcium hydroxide and calcite was epitaxial. He based this assumption on the fact that when a calcium hydroxide film was allowed to partially carbonate, the calcite formed in optical continuity with the parent calcium hydroxide, indicating that a similar shared orientation might occur when calcium hydroxide was deposited on a calcite surface.

Colony (23) also noted the presence of calcium hydroxide at the paste-aggregate interface and concluded that

the presence of this layer was probably detrimental to the bond between the paste and the aggregate.

Hedin (24) and Martin (25) studied the precipitation of calcium hydroxide on the surfaces of a wide variety of aggregate materials. In these studies, the various aggregates were suspended in saturated solutions of calcium hydroxide and the increase in weight with time was noted. Martin (25) found the greatest increase in weight with marble and magnesite aggregates. Hedin (24) found that the amount of lime deposited increased markedly with increasing surface roughness.

Scanning Electron Microscopy of Cement Paste

Several investigators have studied the morphology of cement hydration products and the structure of cement paste by the use of the scanning electron microscope.

Chatterji and Jeffery (26-29), using a combination of scanning electron microscopy, transmission electron microscopy, and X-ray diffraction techniques, found that hardened paste was made up of a limited number of morphological elements. Two types of needles were recognized. The first was relatively large and was identified by electron diffraction as ettringite. The second type of needle, which was an order of magnitude smaller than the ettringite, was thought to be calcium silicate hydrate. In addition, platy hexagonal crystals were present and

were identified as calcium hydroxide and/or calcium monosulphate aluminate hydrate.

Diamond (30, 31) described additional morphological features. He found that the calcium silicate hydrate occurred as branching dendritic crystals and also as sponge-like bodies displaying what he termed a reticular network structure. He also noted the presence of massive crystals of calcium hydroxide that displayed prominant slip planes and appeared to encapsulate other elements of the paste as they grew. In a study of paste with a scanning electron microscope equipped for energy dispersive X-ray spectrometry, Diamond (31) was unable to detect either aluminum or sulfur in the large needle-like crystals identified as ettringite by Chatterji and Jeffery (26-29). He concluded that these large needles were actually composed of calcium hydroxide. Diamond also believed that small (approximately 1-5 micron) bodies in the paste represented spherulitic or globular clusters of calcium silicate hydrate gel, presumably formed from growth centers nucleated within large water-filled pores. The presence of such spherulitic clusters in cement paste had been postulated by Williamson (32).

Taplin (33) proposed that the hydration of portland cement occurs through both the deposition of hydration products in water-filled space between the cement grains and through the formation of a more dense hydration product

within the original boundaries of the cement grains. The two types of material were called the "outer" and "inner" hydration products, respectively. In a study of tricalcium silicate pastes, Williamson (34) described what appeared to be pseudomorphs of the original silicate grains, surrounded by hydration shells of varying morphology, and encapsulated in massive crystals of calcium hydroxide. He believed the pseudomorphous grains to represent the "inner" product, and the hydration shells the "outer" product postulated by Taplin (33). In a later extension of this work, Williamson (35) retained the terminology of "inner" product for material deposition within the original grain boundaries, while terming that portion of the "outer" product which constituted a visible hydration shell around the original grain the "columnar zone." Material in this zone was believed to grow perpendicular to the grain surface, and the term was derived from the zone of crystals that develop perpendicular to the walls of the mold in metal castings. Diamond (30) also described "inner" product as understood by Williamson.

Mills (36) described large rosette crystals of gel growing on the surface of cement grains after twenty-eight days hydration. Chatterji and Jeffery (28) stated that these rosettes, the individual crystals of which were up to three microns in length, were much too large to be gel.

They believed that the rosettes were actually composed of calcium hydroxide.

Berger et al. (37) studied fiber-reinforced cementitious composites and noted that the calcium hydroxide grew in intimate contact with the fibers. They suggested that similar lime growth might contribute to the bond of paste to aggregate in concrete.

In a recent study, Chatterji and Jeffery (29) studied the bond of cement to a variety of aggregates in mortars. Mortars containing natural sand, crushed limestone, basalt, or granite were cured for 7 days, 28 days or 6 months, were broken with a hammer, and the fracture surfaces were examined under the scanning electron microscope. They found with all the aggregates a progressively greater proportion of the fracture taking place at the cement-aggregate interface as the age of the samples increased. They also reported significant etching of the aggregate surface at later ages, especially with the crushed limestone aggregate. Similar etching of the aggregate surface was noted by Farran (5).

Chemical Reactions at the Paste-Aggregate Interface

The pore solutions in concrete are highly alkaline, due to the calcium and alkali metal hydroxides released into the solution during the hydration of portland cement. This highly alkaline environment is, from a geological standpoint, unusual, and the silicate rocks normally used

as concrete aggregates would necessarily be metastable in the concrete environment. This metastability is reflected in the high solubility of both silica and alumina in solutions of high pH (38). The mobilization of silicon and aluminum at the interface almost certainly leads to some degree of chemical reactivity between common siliceous aggregates and the cement paste.

Recent work on the alkali reactivity of the carbonate rocks (39) has shown that both dolomite and calcite also enter its chemical reactions at the interface.

It seems probable, therefore, that chemical reactions between the aggregate and the enclosing cement paste are common. Etching of the aggregate surfaces at later ages was noted on a wide variety of aggregate types by Farran (5) and by Chatterji and Jeffery (29) and provides experimental evidence to support this view.

While the amount of reaction taking place with the majority of aggregates is minor, the effect of even limited reactivity on such factors as cement to aggregate bond and microcracking might well be significant, especially at later ages. It was for this reason that it was decided to limit the scope of the present investigation to include only samples cured for 28 days or less.

Equipment and Procedures

In this section the equipment used will be listed, and techniques and procedures will be described.

Scanning Electron Microscopy

The major research tool in the investigation described in this thesis was the scanning electron microscope. This instrument has a number of important advantages over optical and transmission electron microscopes. Factors especially important in this investigation were:

1. Ease of sample preparation: In order to study surfaces of the type investigated in this work with a transmission electron microscope, it would be necessary to prepare surface replicas. The area of surface investigated with replicas is small, their preparation time consuming, and with rough surfaces there is considerable introduction of artifacts and loss of resolution. With surfaces showing the great amount of relief that was present in many of the samples used in this study, preparation of replicas would, in fact, be almost impossible. By contrast, sample preparation for scanning electron microscopy consists simply of coating the sample surface with a thin film of some conducting material.

2. Depth of field: The depth of field with the scanning electron microscope varies with magnification from roughly one thousand microns at 100X to over ten microns

at 10,000X. By comparison, the depth of field with a binocular optical microscope is only about one hundred and fifty microns at 100X. (40) Depth of field with a transmission electron microscope would be limited by the maximum relief that could be successfully replicated.

3. Range of magnification: Magnifications ranging from 60X to about 100,000X are possible with the scanning electron microscope. Although the transmission electron microscope gives magnifications between 600X to about 250,000X, work at lower magnifications is hampered by interference due to grid bars and the field of view is further limited by the small apertures necessary for contrast. The utility of optical microscopy is, of course, limited by the upper limit of useful magnification which is about 2,500X at most.

4. Analytical capabilities: The usefulness of the scanning electron microscope can be greatly enhanced by modification so as to permit elemental analysis through X-ray spectrometry. This subject will be discussed in detail later.

Equipment. The instrument used was a Jeolco SMU-3 Scanning Electron Microscope equipped for display on either cathod ray tubes or a television monitor.

Sample Preparation. The samples for scanning electron microscopy were of two principal types.

The most commonly used samples were prepared by casting a pat of neat cement paste, roughly 1/2 inch in diameter, on the surface of an aggregate substrate. Unless otherwise noted, pastes were prepared at a water-cement ratio of 0.5 and were mixed by hand in a glass beaker for five minutes. The substrate surfaces were cleaned prior to casting by scrubbing with distilled water and lens paper and were allowed to air dry. Owing to the high fluidity of the pastes, consolidation was limited to tapping the substrate gently with a spatula.

In one series of samples, a water-cement ratio of 0.25 was used. The paste for these samples was mixed by shaking the cement and water for five minutes in a closed container on a model 5110 Red Devil paint mixer. After casting on the substrate surface, the low water-cement ratio pastes were consolidated on a vibrating table.

Immediately after casting, the samples were placed over water in petri dishes, the dishes were sealed with a plastic film, and the samples were allowed to cure for eight hours. The samples were then removed and stored under saturated calcium hydroxide solution until ready for separation. Samples were cured for one, three, seven, fourteen, or twenty-eight days.

In the preliminary portions of the study, the paste was separated from the substrate with a hammer and chisel. The two halves of the sample were then oven dried.

Examination of these samples under the scanning electron microscope disclosed that there had been a significant deposition of calcium hydroxide at the drying surfaces subsequent to separation. To avoid this problem, it was decided to thoroughly dry the samples before separation. In this way, the pore solutions would be drawn away from the interface and toward the upper surface of the sample, thus preventing spurious deposits in the interface region. The drying was effected by storing the samples over magnesium perchlorate in a desiccator. This technique did prevent the spurious deposition of lime at the interface. In addition, it was found that the stresses produced through the shrinkage of the paste under these severe drying conditions were sufficiently strong to cause an almost complete separation of the paste from the aggregate substrate. The two halves of the sample could be separated after drying by simply tapping the sample gently against the bench top. This technique was used for all samples described in this thesis.

The second type of sample used was small mortar cylinders. Mortars were prepared with a water-cement ratio of 0.5 and with one part cement to three parts standard Ottawa sand (or an equivalent volume of manufactured calcite sand) by weight. The mortars were mixed in accordance with ASTM C-190, and cast in tapered plastic test tubes roughly four inches long and 1/2 inch in diameter.

Immediately after casting the sample was consolidated on a vibrating table for one minute, and the test tube was sealed with a rubber stopper. After twenty-four hours, the sample was removed from the test tube and cured under a saturated solution of calcium hydroxide for three, seven, fourteen or twenty-eight days. After the curing period, the mortar samples were oven-dried and then fractured in flexure. The fractured specimen was trimmed to a workable size with a hammer and chisel.

Samples were coated with a layer of carbon, followed by a layer of a gold-palladium mixture. After coating, the samples were stored in a desiccator over magnesium perchlorate and Mallcosorb (a carbon dioxide absorbent) until used.

Procedure. The sample was mounted in the sample chamber of the microscope and was oriented so that the sample surface was essentially perpendicular to the electron beam. Using the television monitor, the entire surface of the sample was then inspected. Once the overall nature of the sample had been determined, representative fields were chosen, the signal was channeled to the cathode ray tubes, and photographs were taken.

Energy Dispersive X-Ray Spectrometry

As was mentioned earlier, the utility of the scanning electron microscope can be greatly increased by modifying

the instrument to provide the capability for energy dispersive X-ray analysis. In this system, a detector is mounted in the specimen chamber of the microscope close to the specimen stage. The electron beam of the microscope excites the specimen which generates characteristic x-rays. The detector, in this case a cryogenic semiconductor, generates electrical impulses that are proportional in height to the energies of the X-ray photons emitted by the specimen. A multichannel analyzer splits these pulses into narrow energy channels and accumulates the number of pulses for each channel. The resulting spectrum can be displayed on a cathode ray tube, printed out by a teletypewriter, or fed to a computer for processing. The elements present are identified on the basis of their x-ray spectra, and quantitative analyses are made on the basis of relative peak intensities after corrections for background, matrix effects etc. have been made.

Diamond (31) studied the application of the scanning electron microscope - energy dispersive x-ray spectrometer combination to the study of cement paste and found that the ratios of the gross peak heights of the K α peaks were linear functions of the oxide ratios for calcium as compared to silicon, sulfur, and aluminum. He also found matrix effects were unimportant in the cement system.

Although the diameter of the electron beam in the scanning electron microscope is of the order of several

hundred angstrom units at the voltages normally applied, the beam excites a significantly larger area of the sample. Diamond (31) calculated that the diameter of the area excited in solid material for calcium Kα and less energetic radiation was about one and a half microns. Unfortunately, most of the morphological units encountered in this study were significantly smaller than this, making quantitative analysis of many of the observed features impossible. However, it was possible to ascertain the broad picture of elemental distribution among the various morphological units.

Equipment. The microscope was equipped with a Nuclear Diode Model 707 Element-Dispersive X-Ray Analysis attachment.

Calibration. The scheme for calibration and analysis was essentially that developed by Diamond (31). The analysis was set up on the basis of ratios rather than absolute composition. As is the normal practice in cement chemistry, analyses were expressed as oxide rather than elemental ratios.

Using the standards described by Diamond (31), calibration curves were set up for CaO/SiO_2, CaO/SO_3, and CaO/Al_2O_3 by plotting count ratios against mole ratios for each pair of elements. Diamond (31) based his curves on the gross peak heights; the curves in this investigation were based on integrated intensity. The calibration

curves are shown on Figures 1 - 3. The solid points represent the average of ten determinations. The dashed vertical lines show the range in measured values.

Sample Preparation. The essentially qualitative analyses that constituted the bulk of the work were performed on the standard specimens for scanning electron microscopy, already described. An interference between one of the spectral lines for gold and the principal line for sulfur was found not to be a significant problem. Since the interfering gold line was produced by the gold in the gold-palladium coating, it was possible to use the realtive intensity of an unobstructed palladium line as an internal standard from which the intensity due to gold at the sulfur position could be estimated. Since the intensity of the sulfur line was at least an order of magnitude greater than the intensity for the gold with all sulfur bearing phases, these phases could be identified with confidence.

For those samples on which quantitative analyses were performed, and for the standard samples used in the derivation of the calibration curves, the sample was coated only with carbon.

Procedure. After locating appropriate areas for analysis on the television monitor, the field was centered on the cathode ray tube and the electron beam was moved onto the area to be analyzed. For quantitative

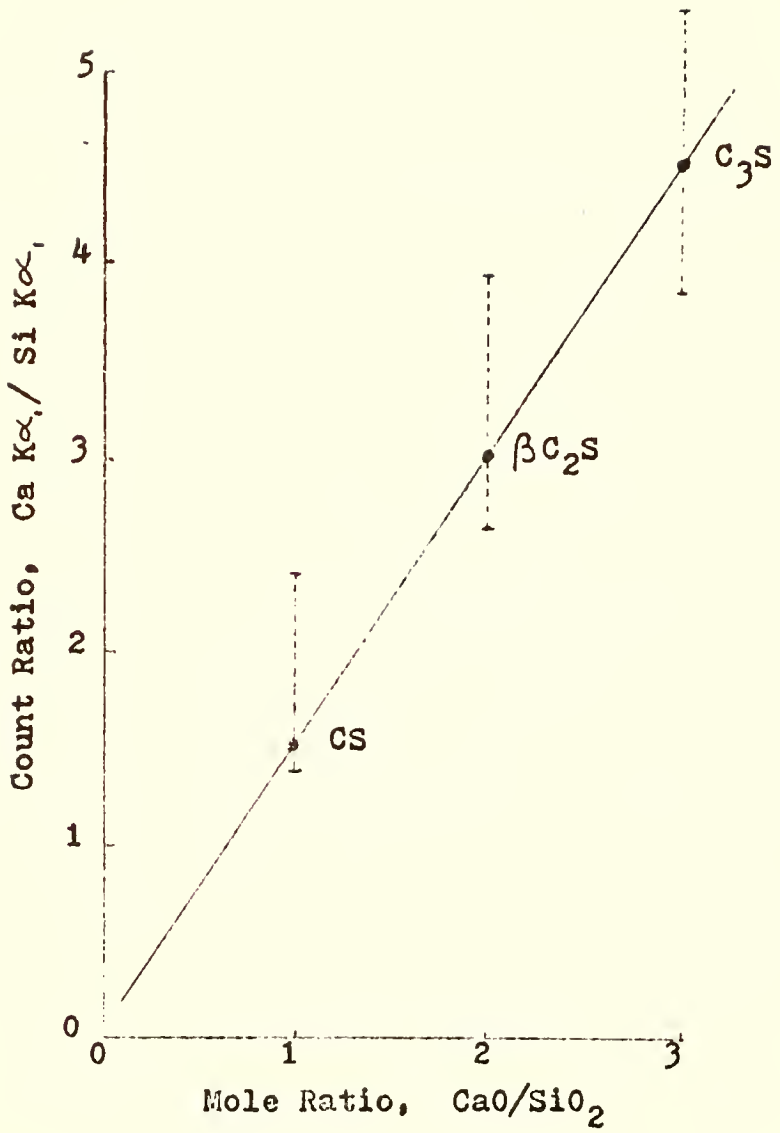

Figure 1. Calibration for CaO/SiO_2 Ratio

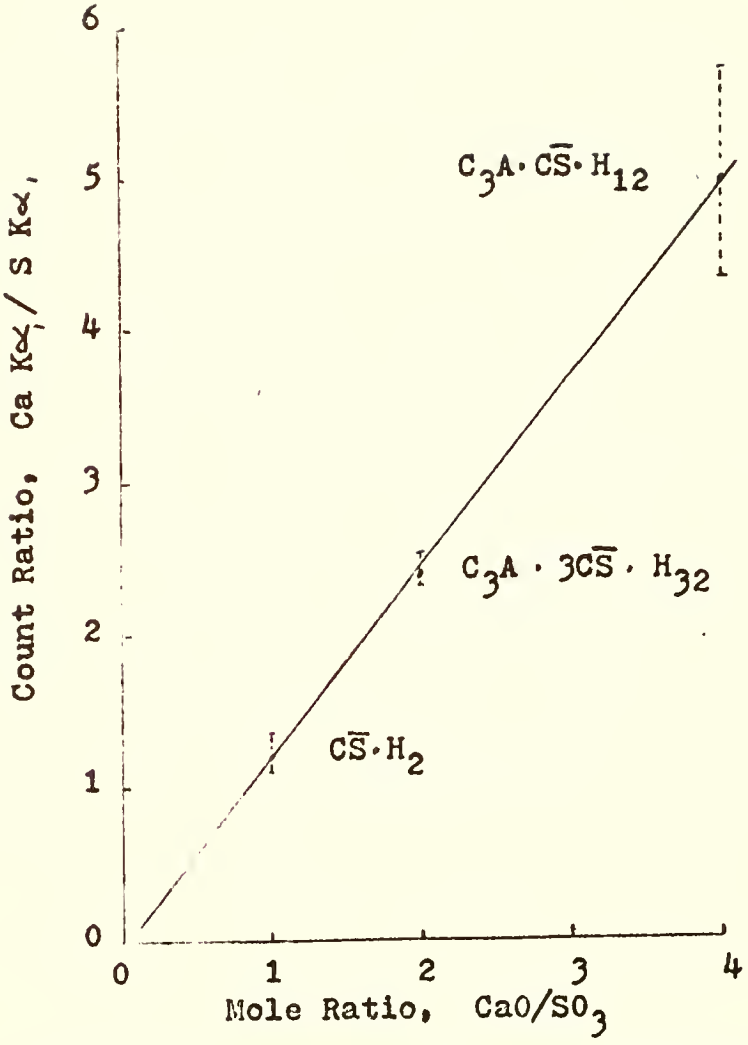

Figure 2. Calibration for CaO/SO_3 Ratio

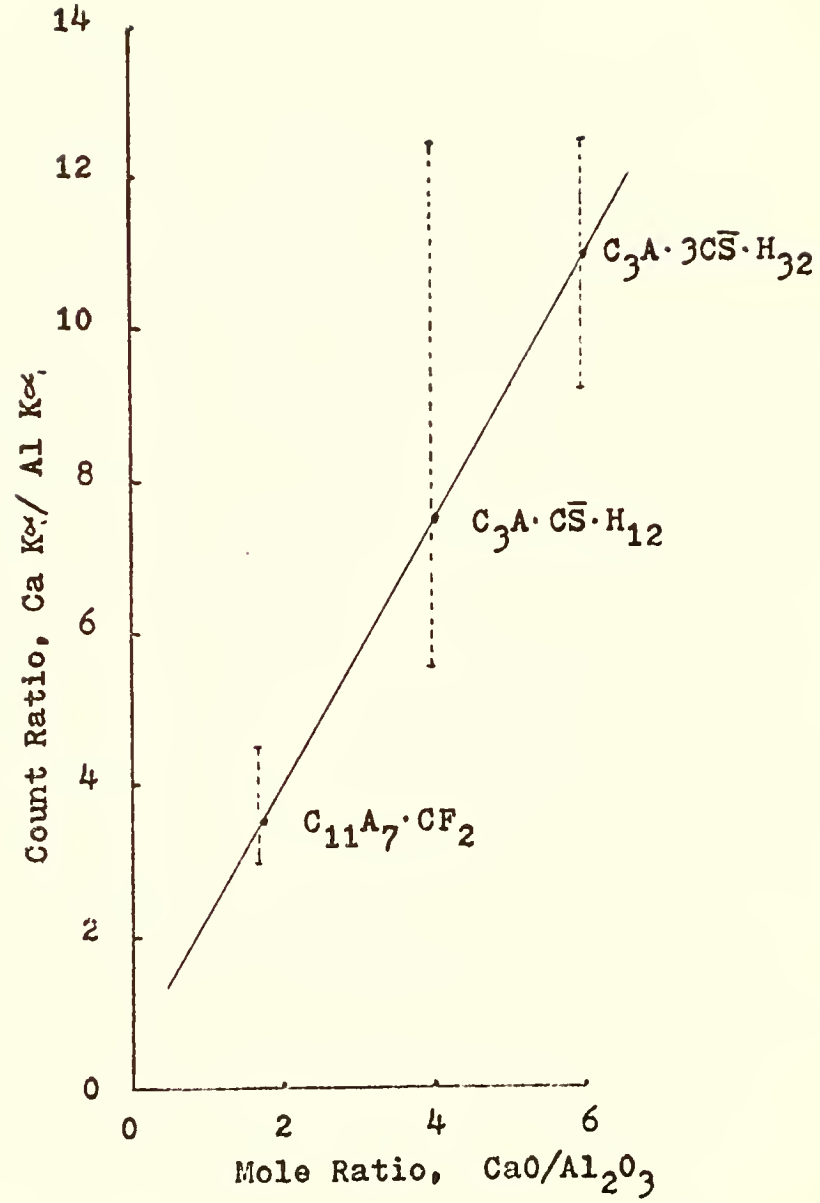

Figure 3. Calibration Curve for CaO/Al_2O_3

determinations, the signal from the detector was channeled into the computer, and the integrated intensities were computed. All quantitative determinations were based on the average of ten analyses, each of which involved at least 25,000 counts.

For qualitative determinations of elemental distribution, the signal from the detector was displayed on the cathode ray tube, the intensity of the interfering gold peak was estimated, and the elements present were noted. Many analyses were run on each of the basic morphological units recognized, and the results of these analyses were sufficiently consistent to allow confidence in assigning compositions to the features observed.

X-Ray Powder Diffraction

X-ray diffraction was used to determine the crystalline phases present in the interface region and to study the degree and depth of orientation of the calcium hydroxide deposited at and near the interface.

Equipment. The instrument used was a General Electric XRD-5 equipped with a high intensity copper tube.

Sample Preparation and Procedures. The samples used for x-ray diffraction were identical to those used for scanning electron microscopy. After separation by drying, the interfacial regions of both the paste and the substrate were analyzed.

A measure of the degree of orientation of the calcium hydroxide at the interface was obtained by determining the ratio of the gross peak heights of the (00.1) and (10.2) peaks.

To determine the variation in degree of orientation as a function of distance from the interface, a small stainless steel ball bearing was attached to the upper surface of the dried paste with epoxy resin. Layers of paste, 30-40 microns thick, were then removed from the fracture surface by grinding it against a glass plate using No. 1200 grinding compound with acetone as the vehicle. The thickness of the sample was determined after the removal of each layer of paste by measuring on a small comparator using a glass plate for the lower surface and the attached ball bearing as a gauge point. Peak height ratios were obtained after each layer had been removed.

Materials

Substrates

The following materials, all purchased from Ward's Natural Science Establishment, Inc., were used as substrates in the samples for scanning electron microscopy:

Petrographic Microscope Slides

White Marble, coarse crystalline, Georgia.

This is an almost pure calcitic marble containing no dolomite detectable by x-ray diffraction and only trace amounts of graphite and apatite.

Quartzite, Montana

This rock is a well cemented orthoquartzite consisting of angular quartz grains cemented with cryptocrystalline silica.

Cement

The cement was a locally available Type I cement, obtained in quantity from a single clinker batch from the manufacturer. The laboratory designation was Cement 317. The physical and chemical properties of the cement as supplied by the manufacturer are given in Table 3.

Mortar Sands

Ottawa Sand, 20-30 mesh; Ottawa Silica Co., Ottawa, Ill.

Manufactured Calcite Sand, 20-30 mesh; This sand was prepared from a high calcium limestone coarse aggregate supplied by the Bloomington Crushed Stone Co., Bloomington, Indiana.

TABLE 3

PHYSICAL AND CHEMICAL PROPERTIES OF CEMENT 317

Physical Properties

Fineness, No. 325 sieve	95.9 percent
Specific Surface, Blaine	3380 sq. cm./gm.
Initial set	3 hr. 15 min.
Final set	5 hr. 5 min.

Chemical Analysis

Compound	percentage present
Silicon dioxide, SiO_2	21.76
Aluminum oxide, Al_2O_3	5.41
Ferric oxide, Fe_2O_3	1.97
Calcium oxide, CaO	65.30
Magnesium oxide, MgO	1.11
Sulfur trioxide, SO_3	2.43
Loss on ignition	1.78
Total Alkalies, as Na_2O	0.38

Calculated Compound Composition

Compound	percentage present
Tricalcium Silicate, C_3S	51.20
Dicalcium Silicate, C_2S	23.83
Tricalcium Aluminate, C_3A	11.00
Tetracalcium Aluminoferrite, C_4AF	5.99
Calcium Sulfate, $CaSO_4$	4.13

CHAPTER II - PRESENTATION AND DISCUSSION OF RESULTS

Particle Sizes in Cement

Figures 4 and 5 are views at two magnifications of the anhydrous cement. It can be seen that although the greater part of the cement is made up of grains ten microns or larger in diameter, there are large numbers of smaller grains, ranging down to fractions of a micron in diameter, and adhering to the larger grains.

These smaller grains are significant for several reasons. Because of their small size, many pass through the network of larger grains during sedimentation and consolidation after casting, and therefore tend to be concentrated at the interface on samples cast against horizontal surfaces. Secondly, the chances are good that the majority of these small grains are essentially monomineralic. For these reasons, much of the analysis that follows was based primarily on the study of the smaller grains.

Diamond (30) reported small (1-5 micron) globular clusters with the surface morphology of C-S-H gel. Primarily because he considered these features too small to represent hydrated cement grains, he concluded they were

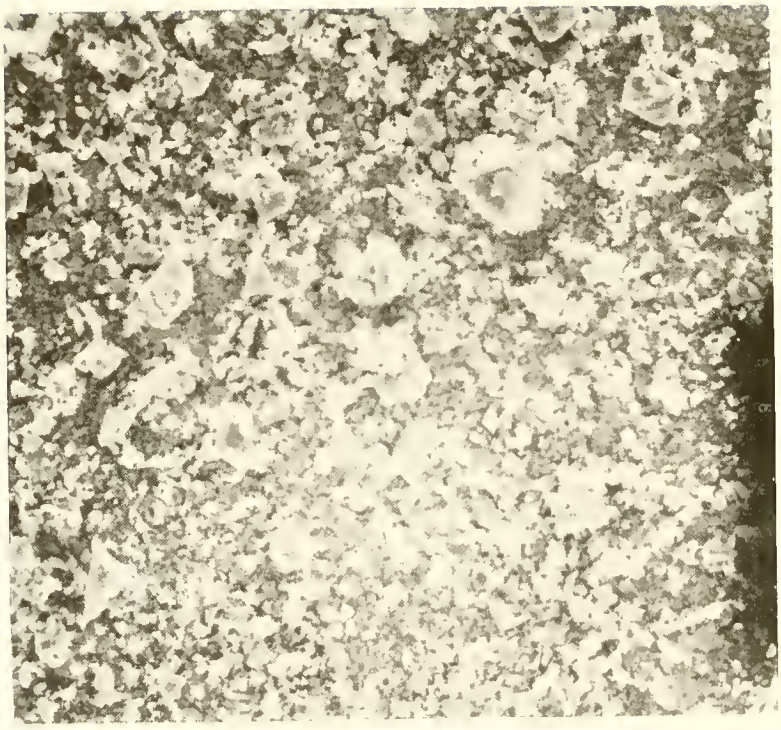

10μ

Figure 4. Size Distribution in Cement

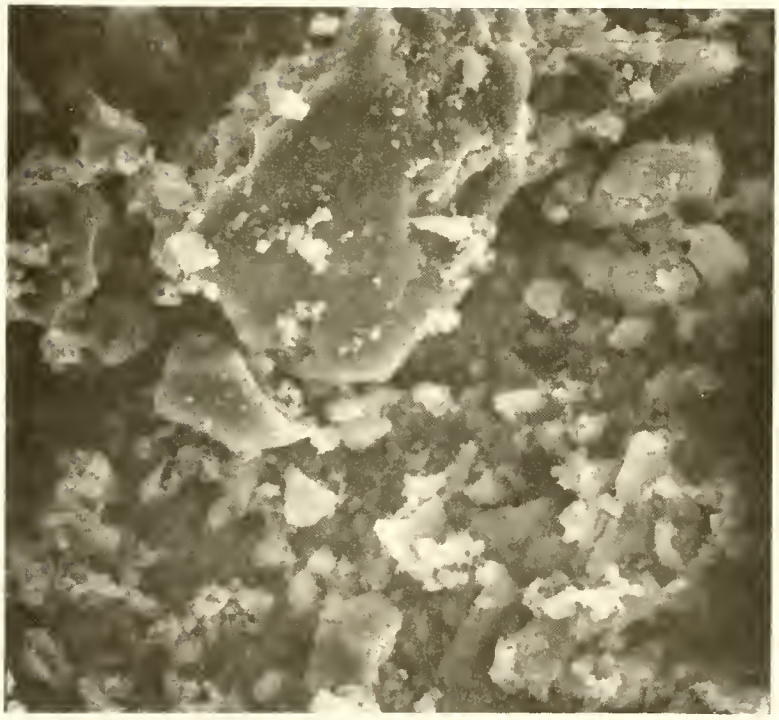

10μ

Figure 5. Size Distribution in Cement

spherulites that had formed through nucleation in water filled space.

The presence in the cement of large numbers of extremely small grains would suggest that many of the features previously described as spherulites may actually be hydrated cement grains.

The Nature and Development of the Interfacial Region; 0 - 28 Days

The work described in this section was based on the study of samples consisting of neat cement paste with a water-cement ratio of 0.5, cast against horizontal glass microscope slides. The glass substrate was used because the smooth surface greatly facilitated the interpretation of the complex relationships at and near the interface. All the features that will be described were also found when the paste was cast against crystalline silicate and carbonate substrates.

Hydrated One Day

General features. A low magnification view of the surface of the glass substrate is shown on Figure 6. The black areas represent relatively clear glass, the grey areas consist of cement hydration products deposited at the interface, and the white blobs are cement grains and aggregations of grains together with adhering hydration products. These and associated features will be described below.

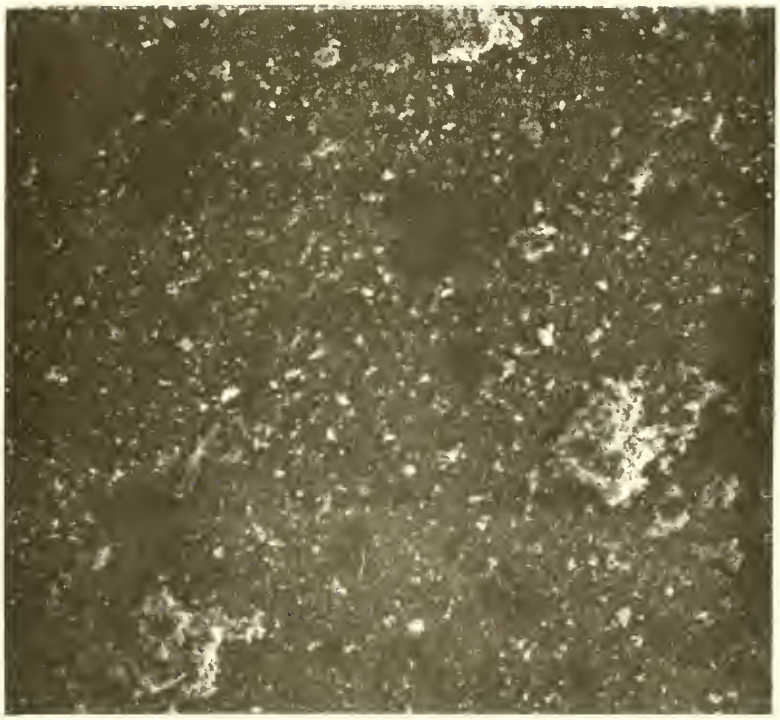

100 μ

Figure 6. Surface of Glass Substrate - 1 Day

Interfacial film. Relationships at the paste-aggregate interface are shown on Figure 7. This field, which is an enlarged view of a boundary between black and grey areas on Figure 6, shows that a two-layered film of cement hydration products has been deposited on the surface of the glass slide. This film consists of a lower, light-colored and massive layer, lying directly on the glass and backed with a second layer of small sheaf-like crystals.

The reverse side of this film can be seen in Figure 8, which is a view of the paste side of the specimen. The large, smooth, and dark bodies are portions of the interfacial film that have pulled loose from the glass slide. The areas from which this material has pulled loose are the black areas on Figures 6 and 7.

X-ray diffraction studies were run on companion specimens. The light colored film lying directly on the glass consisted of lime crystals, deposited in an almost perfect plane-parallel orientation, with their c-axes perpendicular to the surface of the glass.

In preliminary studies, paste was also cast against calcite, dolomite, siderite, quartz, orthoclase, microcline, albite, biotite, muscovite, phlogopite, fluorite, galena, teflon, polyethylene, and mercury surfaces. In every instance it was found that a lime film had been deposited at the paste-aggregate interface, and x-ray diffraction studies showed the film to be highly oriented.

μ

Figure 7. Interfacial Film on Substrate - 1 Day

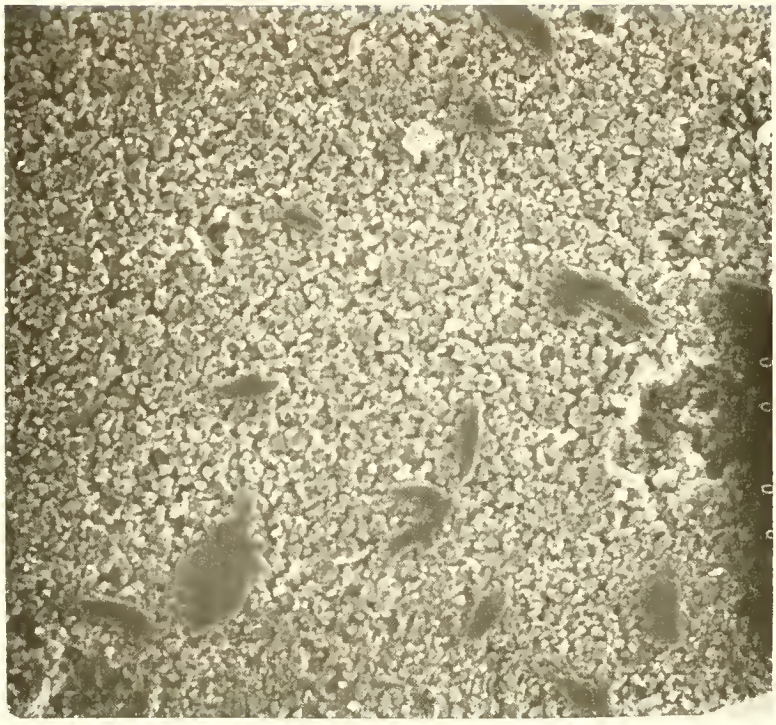

100 μ

Figure 8. Lime Film on Paste - 1 Day

A high mangification view of the fine-grained material on the surface of the lime film away from the glass is shown on Figure 9. Notice that many of the sheaf-like bundles give the impression of being rolled sheets. This is the material described as "small needles" by Chatterji and Jeffery (26-29) and as "branching dendritic particles" by Diamond (30-31). Both writers identified this material as C-S-H gel.

The geometrical relationship of the two components of the interfacial film indicates that there has been a sequential deposition from solution of the products of cement hydration at the interface. An early deposition of lime was followed by the subsequent deposition of the calcium silicate hydrate. For the sake of simplicity, the composite film of highly oriented lime with its backing of C-S-H gel will be referred to as the interfacial film in the remainder of this report.

Partially Hydrated Grains. Figure 10 is a view of the substrate showing partially hydrated grains of cement lying on the surface of the interfacial film. The bright appearance of these grains is due to their position as topographic highs. The C-S-H gel on the surface of these grains appears identical to that of the underlying interfacial film. The upper surfaces of the grains shown on Figure 10 show no sign of having been ruptured, indicating that they were not in direct contact with the overlying paste at the time of separation.

Figure 9. C-S-H Gel on Lime Film - 1 Day

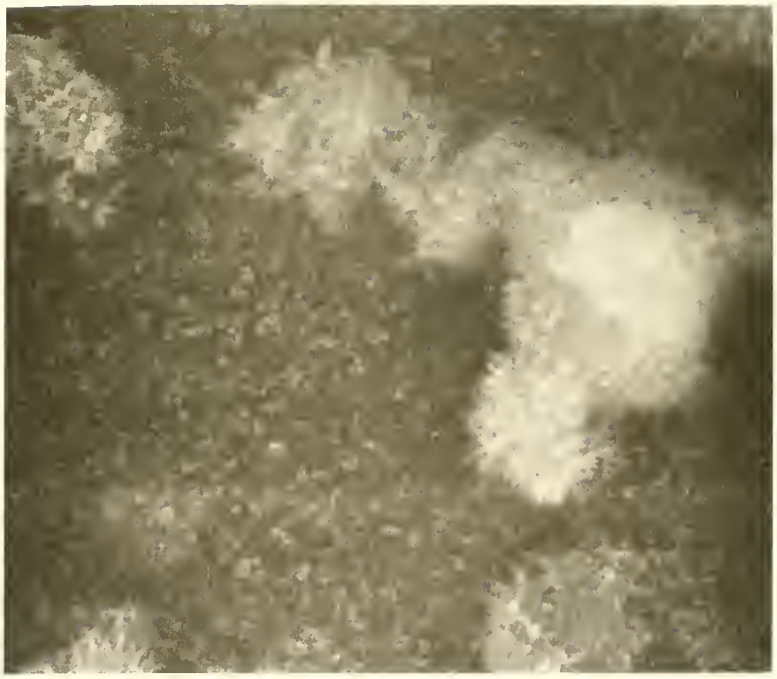

1μ

Figure 10. Partially Hydrated Cement Grains - 1 Day

Fractured grains. Cement grains that clearly were in contact with both the interfacial film and the bulk of the paste are shown on Figure 11. Many grains shown on this field have been ruptured, and many give the appearance of being hollow. These features are sockets from which the remnant cement grains have been pulled loose from the surrounding jacket of cement hydration products. An example at higher magnifications is shown in Figure 12.

Examination of grains of this type has provided insight into the spatial distribution of cement hydration products and the structure of cement paste. An informative example of a partially hydrated and ruptured cement grain is shown in Figure 13. This shows a grain in which the hydration shell has been partially pulled away during separation, exposing the interior structure. Note that the remnant grain has been largely rounded by solution, and that it is significantly smaller than the cavity in which it rests. Notice also that the remnant grain is joined to the surrounding hydration products by several acicular crystals. The presence of these acicular crystals is helpful in indicating the void space within a hydration shell when the remnant grain has pulled away. In all instances observed, a considerable void has been found between the remnant grains and their jackets of hydration product. Additional examples are shown in Figures 14 through 17.

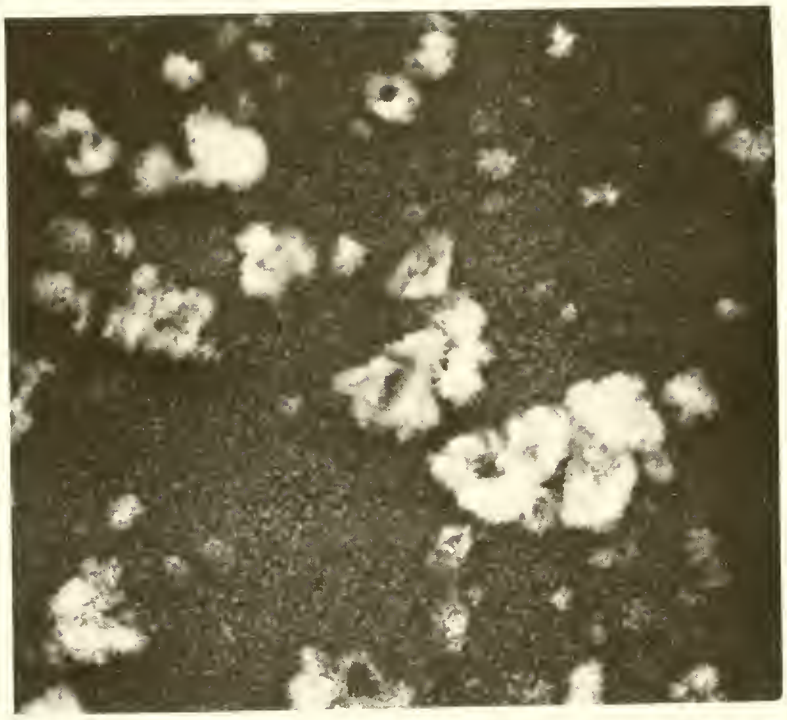

Figure 11. Ruptured Partially Hydrated Grains - 1 Day

μ

Figure 12. Hydration Shell - 1 Day

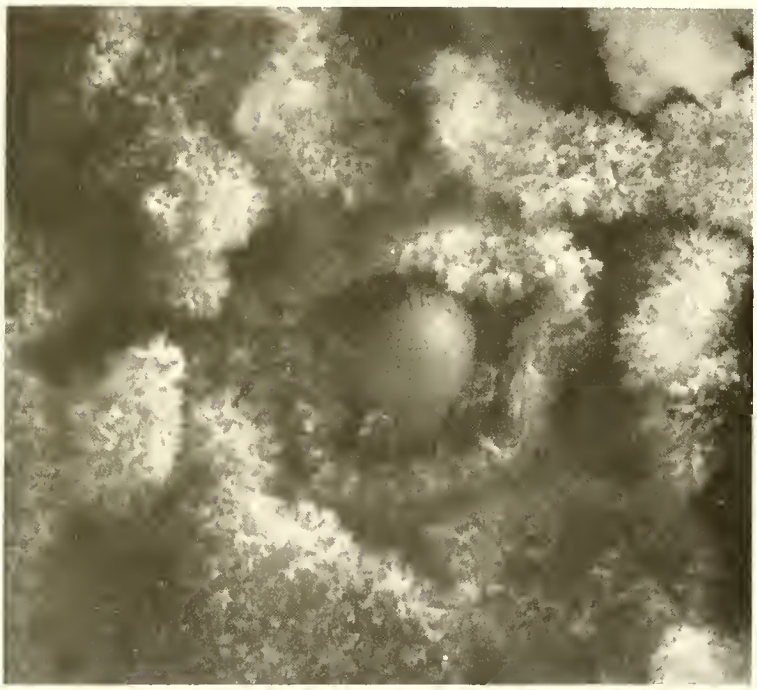

$\underline{\mu}$

Figure 13. Hydration Shell and Remnant Grain - 1 Day

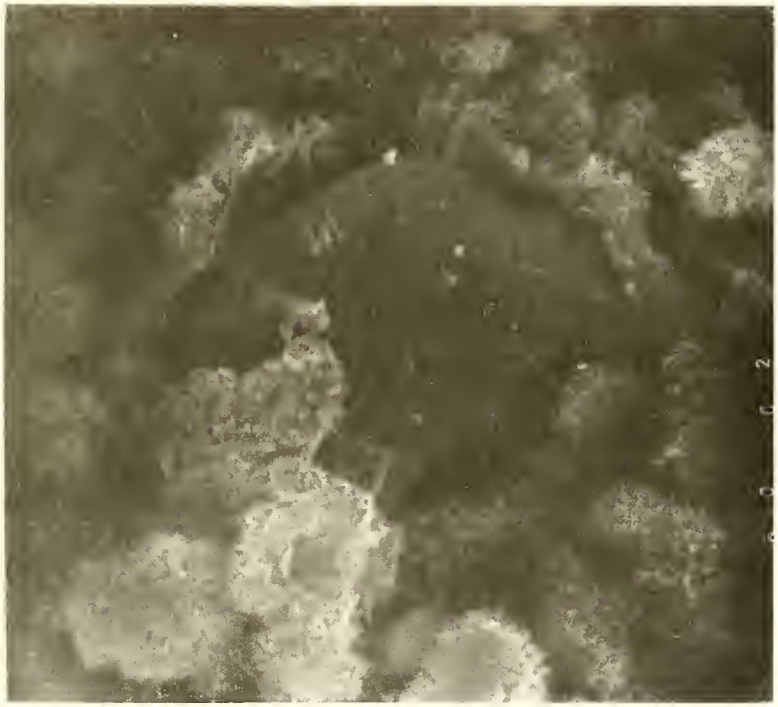

μ

Figure 14. Hydration Shell and Remnant Grain - 1 Day

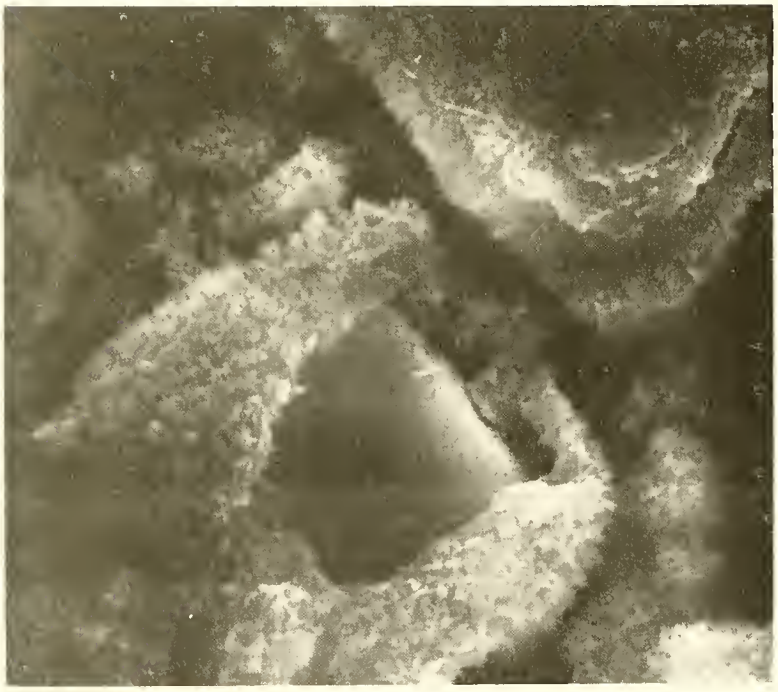

$\underline{\mu}$

Figure 15. Hydration Shell and Remnant Grain - 1 Day

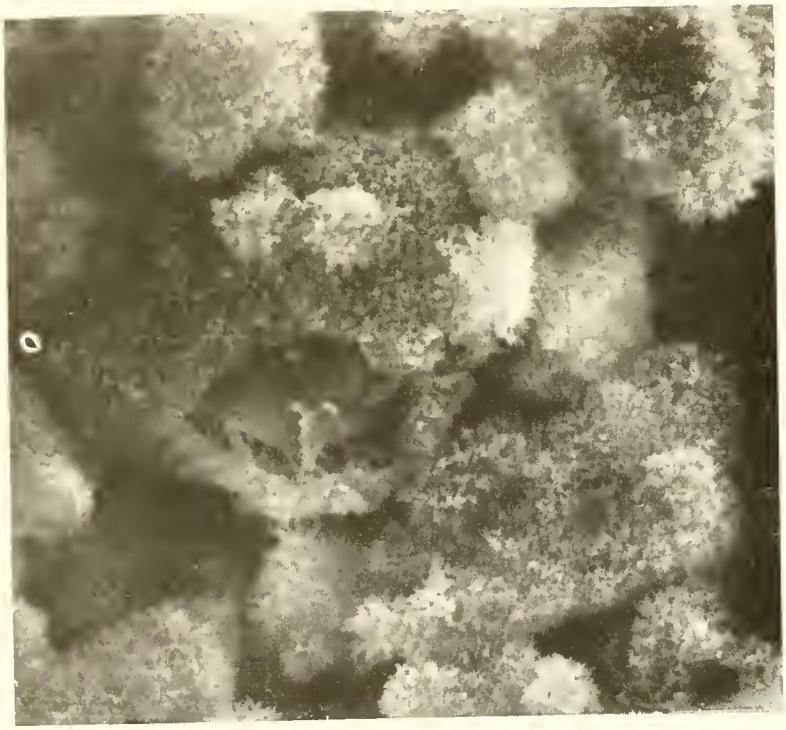

μ

Figure 16. Hydration Shell and Remnant Grain - 1 Day

1 μ

Figure 17. Hydration Shell and Remnant Grain - 1 Day

An additional feature observed on the fractured grains is shown in Figure 18. Here it can be seen that the jacket of hydration products has a layered structure, consisting of a massive interior portion and an exterior fuzzy mass of sheaf-like crystals. X-ray diffraction studies, to be described in detail later, show that the inner and massive material is predominantly lime. The outer portion was identified as C-S-H gel on the basis of its morphology. The inner surface of the lime portion of the shell presumably represents the original grain boundary, and therefore the composite shell would correspond to the "outer product" of Taplin (33) and to the "columnar zone" described by Williamson (35).

Massive lime crystals. Careful examination of the paste portion of the sample was undertaken to determine why certain portions of the interfacial film had pulled loose from the glass slide, as shown in Figures 6 and 7. It was found that the areas of the interfacial film that had remained with the paste at separation were backed by and welded to the bulk of the paste with massive crystals of lime. A good example is shown on Figure 19, which was taken with the sample tilted at 25 degrees. This photomicrograph shows the junction of three lime crystals, each of which is capped with the thin, horizontal, interfacial film. The regions between the lime crystals contain

μ

Figure 18. Layered Structure in Hydration Shell - 1 Day

μI

Figure 19. Massive Lime Crystals - 1 Day

partially hydrated cement grains, and in these areas the interfacial film has remained with the glass substrate.

A similar field is shown on Figure 20, which was also taken with the sample tilted 25 degrees. Notice that as the lime crystals grow they engulf and encapsulate the partially hydrated cement grains lying between them. Notice also that in both Figures 19 and 20 the bulk of the cement grains lie well below the level of the interface as defined by the surface of the interfacial film. This gives a good indication of the large amount of water-filled void space at the interface.

The regions of the glass slide from which the interfacial film had been pulled loose were also examined. Figure 21 shows a high magnification view of such an area. It can be seen that rather than separating at the true interface, the fracture has actually been through the lime portion of the interfacial film. This interpretation was substantiated by x-ray spectrographic analyses of both areas such as that shown on Figure 21 and of the surface of identical glass slides upon which no paste had been cast. These analyses showed a considerably higher calcium concentration on the areas of the slide from which the interfacial film had been pulled loose. It is apparent, therefore, that little or no separation has taken place at the true paste-aggregate interface.

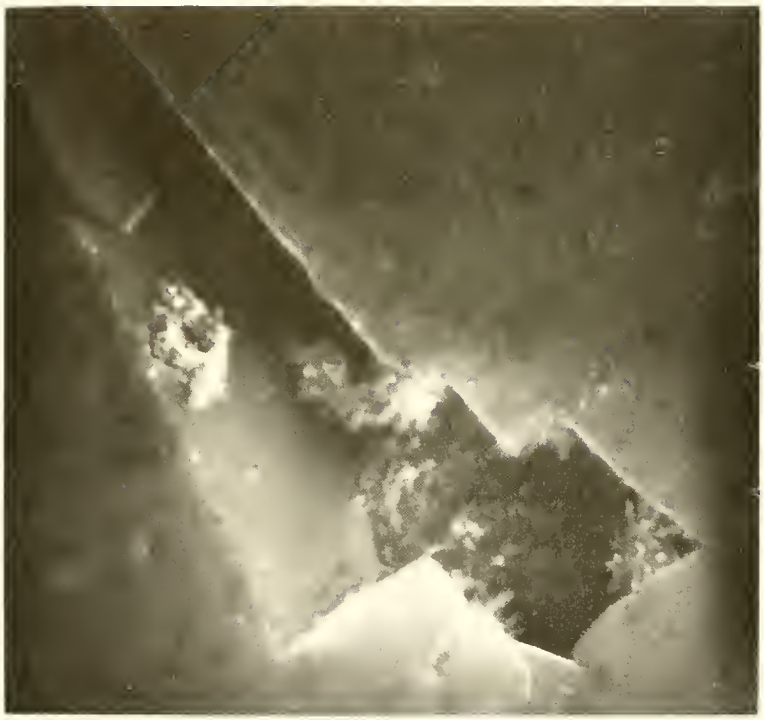

μ

Figure 20. Massive Lime Crystals - 1 Day

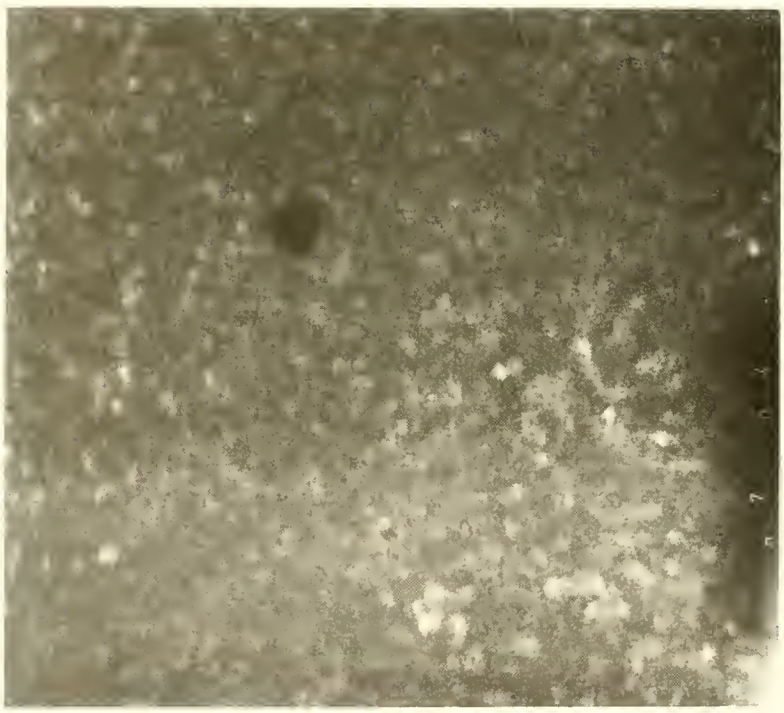

μ

Figure 21. Separation Through Lime Film - 1 Day

Aggregations of grains. In addition to the individual cement grains and small clusters of grains observed on the glass surface shown in Figure 6, there were also a number of larger aggregations, consisting of hundreds or thousands of grains. Many of these aggregations are roughly conical, with their bases at the interface. A view of the side of one of these aggregations is shown on Figure 22. This view shows large hexagonal crystals identified by x-ray spectrometry as lime, growing out past the edge of the aggregation. Since these crystals could only have formed through growth in water-filled space, it seems probable that the aggregations were separated from the main body of the paste by cracks before drying. The origin of these cracks is unknown, although syneresis cracking or bridging and differential settlement are possibilities.

Elemental distribution. In the course of examining the one day old samples, qualitative x-ray spectrographic analyses were run on the various features that have been described. The elemental distribution within the various features is given below:

Lime film: Since the lime film was backed with C-S-H gel, it was not possible to determine whether there was silica within the lime. No aluminum or sulfur were detected.

C-S-H gel on lime film: Although Diamond (31) found that sulfur was a ubiquitous component of the C-S-H gel in the fractured samples he studied, neither sulfur nor

10 μ

Figure 22. Aggregation of Cement Grains - 1 Day

aluminum was detected in the gel backing the lime film at the interface.

Lime crystals: Although a few instances were encountered where the massive lime crystals were pure, the majority of the analyses showed varying degrees of contamination with silicon, aluminum, and to a lesser degree, sulfur. This finding is probably due to the presence of cement grains and their coatings of hydration products encapsulated in the lime. In contrast, the platy hexagonal lime crystals such as were shown on Figure 22 were found to be extremely pure.

Hydration shells: Although shown by x-ray diffraction to be composed primarily of lime, analyses of the massive inner layer on the hydration shells showed a relatively high sulfur and aluminum content. Owing to the presence of C-S-H gel on the exterior of the hydration shells, no analysis for silica was possible.

X-ray diffraction of one day old pastes shows the presence of ettringite in the interfacial region. Since the hydration shells are the only morphological units containing aluminum and sulfur, it seems probable that the presence of these elements in the shell reflects the presence of encapsulated crystals of ettringite.

Analyses of the C-S-H gel on the exterior of the hydration shells also show sulfur and aluminum, but at a much lower level. Since the gel coatings, such as shown

in Figure 18, are less than a micron thick, analysis of the gel would also involve considerable excitation of the underlying massive layer. Possibly, therefore, the gel does not contain sulfur or aluminum, and the spectra for these elements may simply reflect their presence in the underlying massive layer.

Unbroken partially hydrated grains: Analyses for these phases are essentially identical to those obtained on the exteriors of the hydration shells.

Mode of fracture. At the end of the first day, fracture occurred largely in the void space lying between the composite interfacial film and the main body of paste. If cement grains were in contact with both the interfacial film and the bulk of the paste, fracture occurred through the grains. In areas in which the film was tied to the paste through the growth of large lime crystals, failure occurred close to the true interface, but even in such locations, the fracture actually occurred within the lime portion of the interfacial film.

In isolated areas, the fracture surface was found to move into the body of the paste. It is believed that in these instances fracture followed preexisting cracks, presumably formed through self-desiccation or differential consolidation of the paste.

It is interesting to note that in no case did fracture occur at the true paste-aggregate interface.

Hydrated Three Days

Figure 23 is a low magnification view of the surface of the glass slide. Comparison with Figure 6 shows that a considerably larger portion of the interfacial film has been pulled away with the paste portion of the separate after three days hydration.

Figure 24 is a higher magnification view of the surface of the slide. Several fractured hydration shells are visible, and it should be noted that there has been no appreciable filling of the interior voids between one and three days. Another view of a fractured shell is shown in Figure 25, which shows the paste portion of the separate. Note that the acicular crystals in the void have been bridged about half the distance to the center of the cavity, indicating that after three days the remnant grain was small.

Figures 24 and 25 also show the presence of long acicular crystals growing out from the surface of the grains. These are the type of crystals that Chatterji and Jeffery (26-29) called ettringite on the basis of electron diffraction. Diamond (31) was unable to detect sulfur or aluminum in crystals of this type and concluded that they were crystals of lime. The writer was also unable to detect sulfur or aluminum, but feels that this is probably attributable to the small size of the crystals. On the basis of their morphology, the diffraction results of

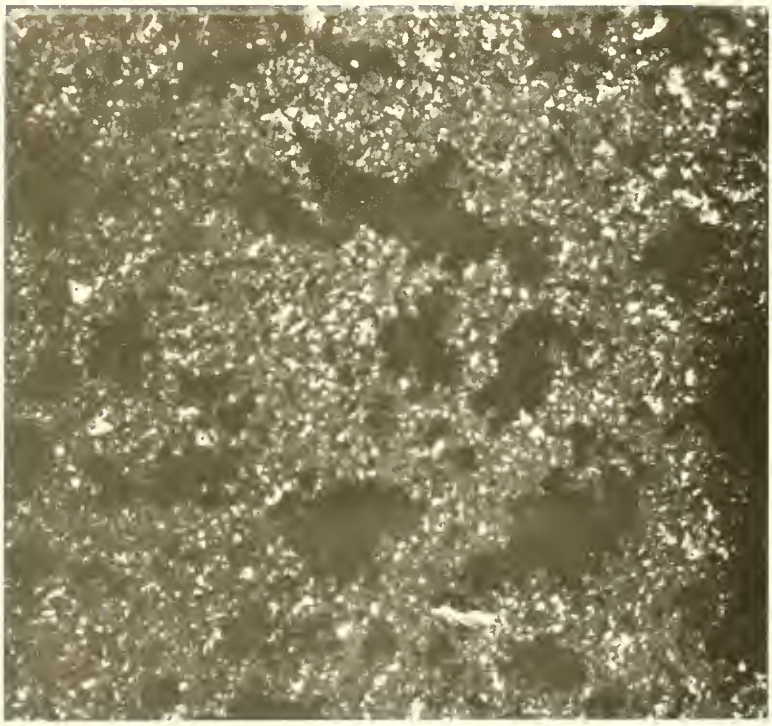

100 μ

Figure 23. Surface of Glass Substrate - 3 Days

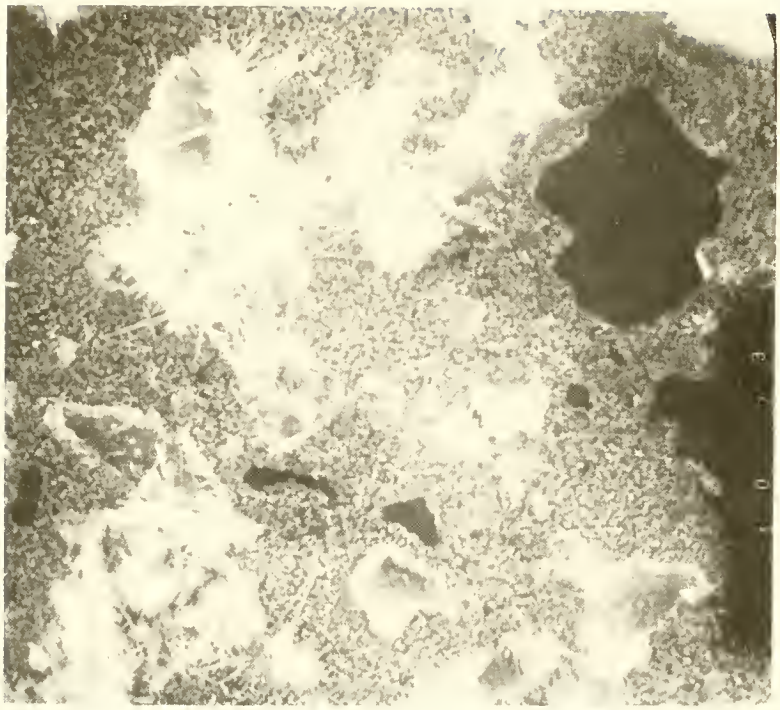

Figure 24. Hydration Shells with Ettringite - 3 Days

1 μ

Figure 25. Hydration Shell - 3 Days

Chatterji and Jeffery (26-29), and studies with artificial systems to be described later, the writer feels safe in calling these crystals ettringite.

Another type of crystal that is first evident after three days hydration is shown in Figure 26. Here we see platy, often slightly curved, hexagonal crystals growing in a sub-parallel array, with their c-axes roughly parallel to the interface. Another view of crystals of this type is shown in Figure 27. In this case, growth has been outward from the body of the paste. Notice that the upper surfaces of many of these crystals are extremely irregular as compared to the equivalent faces shown in Figure 26. This would indicate that the crystals were in contact with the interfacial film before separation and that in the course of separation the fracture surface passed through the platy crystals near the interface. Although the morphology of these crystals is similar to that shown by the lime crystals on Figure 22, x-ray spectrographic analyses show that the crystals shown on Figures 26 and 27 contain appreciable amounts of silica, alumina and sulfur.

Quantitative analyses were run on ten of the largest booklets of platy crystals. The results of these analyses are summarized in Table 4.

1 μ

Figure 26. Platy Crystals - 3 Days

Figure 27. Platy Crystals - 3 Days

TABLE 4

ANALYSIS OF PLATY CRYSTALS

Mole Ratios:	CaO/SiO_2	CaO/Al_2O_3	CaO/SO_3
highest value:	6.8	15.2	11.1
lowest value:	3.1	7.4	6.4
average value:	4.2	9.9	8.1

Large platy hexagonal crystals of the type under discussion were identified on the basis of morphology as either lime or monosulfate aluminate hydrate by Chatterji and Jeffery (26-29). The levels of sulfur and aluminum shown in Table 4 are much too low for a sulfoaluminate, and the extreme range in measured compositions makes it unlikely that the platy crystals represent a single compound. These crystals probably represent a complex solid solution.

None of the large aggregations of grains found to remain with the glass portion of the sample after one day were observed on the three day sample. This result may reflect autogenous healing of the cracks that initially caused the isolation of these aggregations.

Although the increased area of the interfacial film remaining with the paste on the three day sample is largely the result of continuing development of massive lime

crystals at the interface, the packets of platy crystals also seem to play some part in tying the film to the overlying paste. On Figure 28 for example, several packets of platy crystals can be seen projecting out from the area of attached film, indicating that some of the support for the film comes from this source.

The period from one to three days seems to be typified by the continued deposition of C-S-H gel at the interface and on grain surfaces, by the continued growth of massive lime crystals, and by the appearance of large ettringite needles and of packets of platy crystals, rich in sulfur, aluminum, and silica. The net result of these processes is a significant filling of the void space at the interface, and a corresponding increase in the proportion of the interfacial film that remains with the paste on separation.

Hydration for Seven Days

The surface of the glass slide separated from the paste after hydration for seven days in shown on Figure 29. Much of the glass is not exposed, and the surface of the paste portion of the separate now shows a glass-like reflectance.

Figure 30 shows a fractured hydration shell lying on the interfacial film. The shell appears identical to those already shown, and shows that there has been little or no additional filling of the interior. Notice in Figure 30

10 μ

Figure 28. Support of Interfacial Film by Platy Crystals - 3 Days

Figure 29. Surface of Glass Substrate - 7 Days

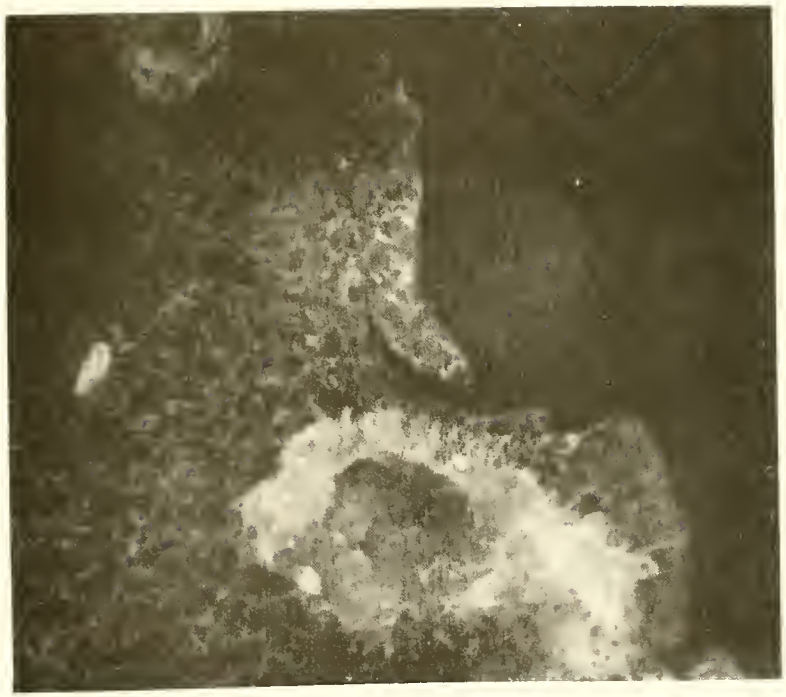

μ

Figure 30. Hydration Shell and C-S-H Gel - 7 Days

that the appearance of the C-S-H gel has changed appreciably. A high magnification view of this material is shown in Figure 31 and comparison with Figure 7 shows that the texture has coarsened, and that a cell-like structure has begun to develop. Figure 32 is a view of the C-S-H gel at the interface after three days and shows an intermediate step in the development of what Diamond (30) has termed a "reticular network structure." X-ray spectrographic analysis showed that the composition of the interfacial film remained unchanged from one to seven days. Figure 33 shows a low magnification view of the surface of the lime film, and Figure 34 a view down into one of the small areas in which the interfacial film has pulled away with the glass. Notice in Figure 34 that around the edges of the opening, separation has been deep within the lime portion of the film, leaving a thin transparent layer. By looking through this layer it can be seen that the interfacial film is tied to the bulk of the paste by platy crystals. Notice on the grain shown on Figure 35 that the C-S-H gel on the cement grains has also started to develop the reticular network structure shown by the gel on the interfacial film.

X-ray spectrographic analyses of the platy crystals exposed on the seven day samples showed that all contained significant amounts of sulfur and aluminum. No platy

1μ

Figure 31. Reticular Network Structure of C-S-H Gel - 7 Days

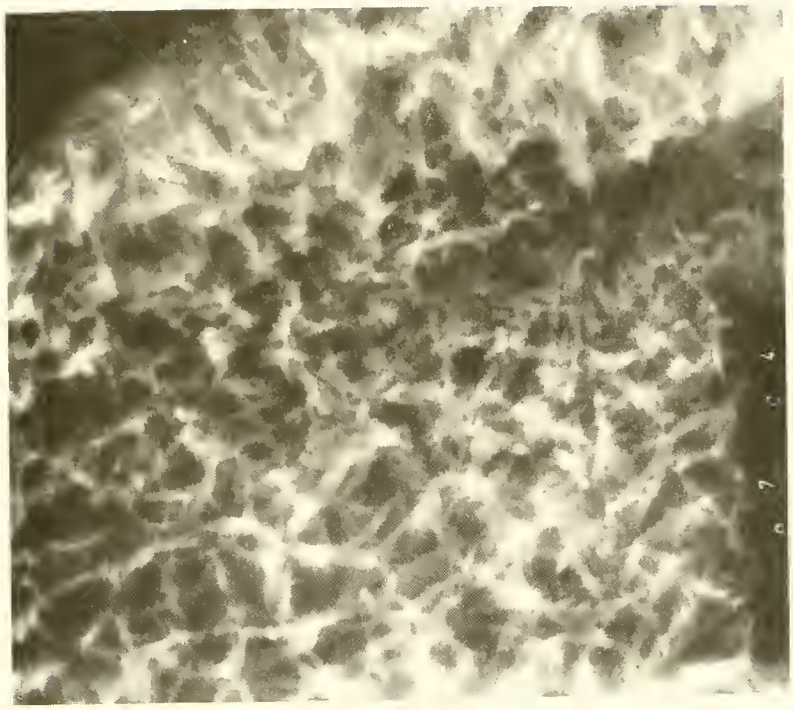

μ

Figure 32. Early Development of Reticular Network - 3 Days

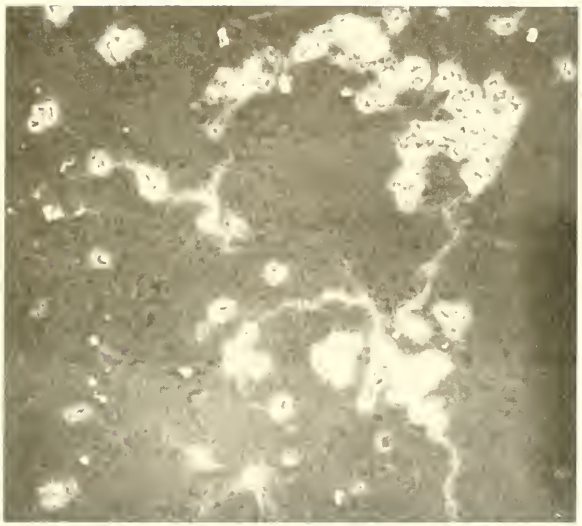

100 μ

Figure 33. Surface of Interfacial Film - 7 Days

Figure 34. Interfacial Film Supported by Platy Crystals - 7 Days

μ

Figure 35. Reticular Network Structure on Grain - 7 Days

crystals of pure lime, such as were found on the one day sample (Figure 22), were present.

It is interesting to note that after seven days hydration, roughly ten percent of the cement grains analyzed showed no sulfur or aluminum in the C-S-H gel coating. This result is interpreted as meaning that the gel on these particles had become sufficiently thick to mask the sulfur and aluminum in the underlying massive layer, and indicates strongly that sulfur and aluminum do not substitute into the C-S-H gel. If this interpretation is correct there are several significant corollaries. Diamond (31) reported that the C-S-H gel contained considerably more calcium than was previously believed. It may well be that the high lime-silica ratios he obtained were the result of picking up calcium radiation from the lime underlying the gel.

As was mentioned earlier, there is some question as to whether the smaller gel-coated features are spherulites or hydrated cement grains. If the C-S-H gel does not contain sulfur and aluminum in detectable amounts, then analysis of spherulites, which would be composed entirely of gel, should show the spherulites to be free of these elements. This is not the case. The feature shown in Figure 35, for example, contained appreciable quantities of both elements. Detection of these elements would suggest that in features such as that in Figure 35, the C-S-H

gel is underlain by a sulfur and aluminum bearing layer, and that the features are, in fact, small hydrated cement grains.

During the period from three to seven days, the only apparent alteration to the structure in the region of the paste-aggregate interface was the development of the reticular network structure on the C-S-H gel, and the continued development of massive lime, platy crystals, and ettringite. This growth resulted in the development of an increased bond between the interfacial film and the bulk of the paste that is reflected in the increased tendency for fracture to occur in the lime portion of the interfacial film.

Hydrated Fourteen Days

The appearance of the glass substrate after hydration for fourteen days is shown on Figure 36. Only a few small isolated areas of the interfacial film remain with the glass. Figure 37 is a view of one of these areas and shows that the C-S-H gel portion of the film shows little change.

Figures 38 and 39 are views down two of the few holes on the film surface. Prominent on both fields are fractured, empty hydration shells, little changed in appearance from those studied on earlier samples. Notice also the increased abundance of platy crystals and ettringite needles.

100 μ

Figure 36. Surface of Glass Substrate - 14 Days

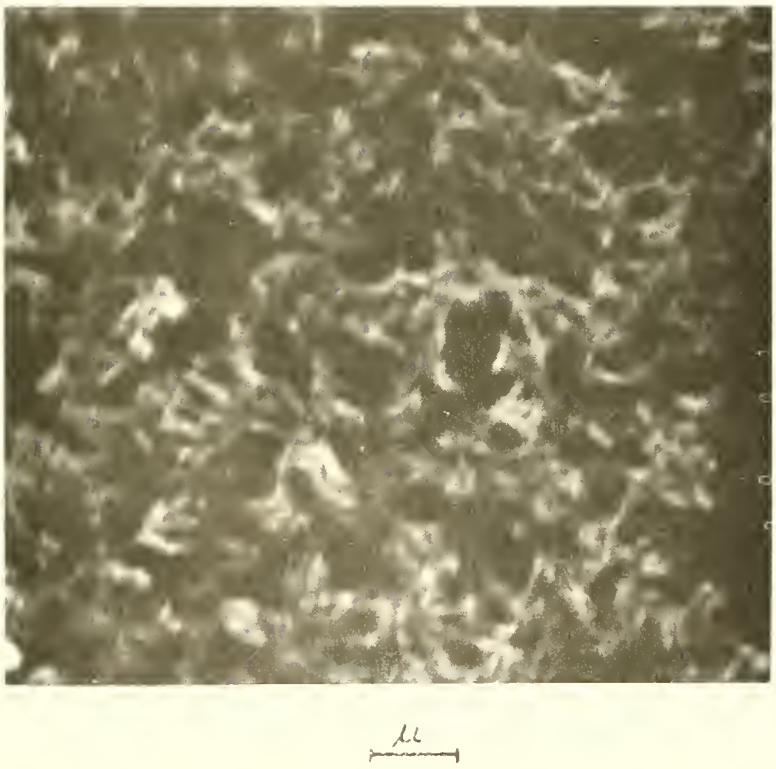

Figure 37. C-S-H Gel on Interfacial Film - 14 Days

Figure 38. Hydration Shell - 14 Days

μ

Figure 39. Hydration Shell - 14 Days

The only alteration of structure near the interface between seven and fourteen days was the continued tying together of the structure by the growth of plates, needles, and massive crystals of lime.

Hydrated Twenty-eight Days

The surface of the lime film developed at the interface after hydration for twenty-eight days is shown in Figure 40. The bonding of the paste to the interfacial film is virtually complete. The only place it was possible to view the interior of the sample was at the extreme "feather edge" of the paste pat. Here the consolidation would be at a minimum, and the forces at separation would be almost pure shear. A view down one of these openings is shown on Figure 41. The major feature in this field is a complex network of ettringite crystals, several of which show definite hexagonal outlines. Prominant is a large spherulite. An analysis was run with the beam centered on the central "hub" of the radiating crystals, and even though this feature is relatively large, no sulfur or aluminum was detected.

Figure 42 shows a fractured hydration shell. Dimly seen within this hollow body is an acicular crystal projecting to the center of the void and indicating that the cement grain that initially filled the cavity has completely dissolved. There is still no indication of additional

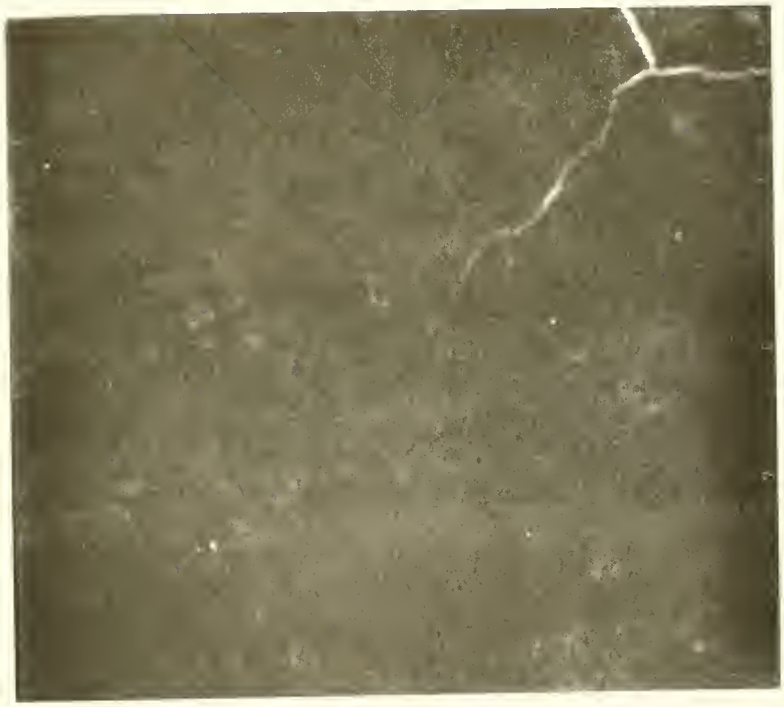

100μ

Figure 40. Surface of Lime film - 28 Days

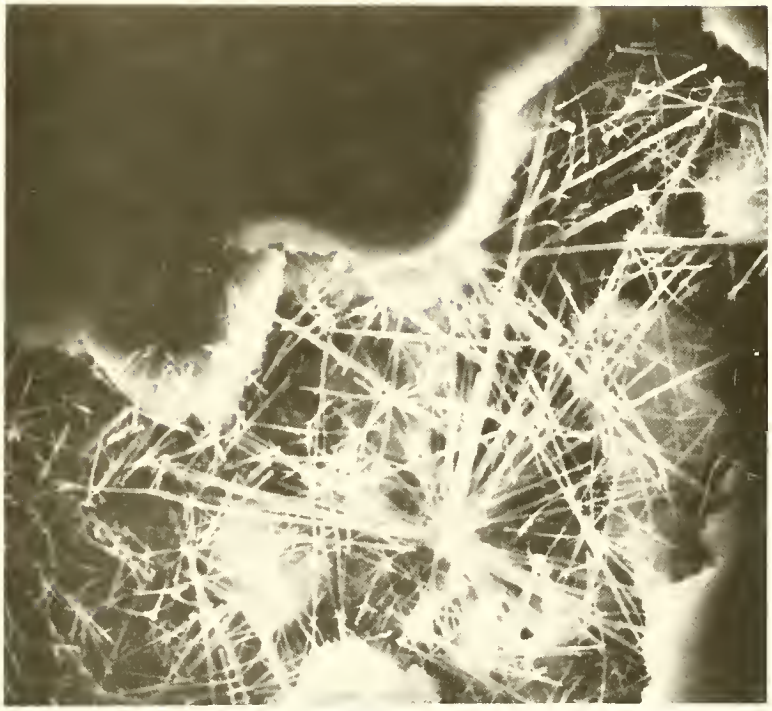

Figure 41. Ettringite Crystals - 28 Days

μ

Figure 42. Hydration Shell - 28 Days

deposition of material within the shell other than the acicular crystal.

The period from fourteen to twenty-eight days is apparently typified by the continued filling of interparticle void space to the point where the interfacial film is securely bonded to the main body of the paste.

Early Development of Structure at the Interface

As shown in the preceeding section, the basic framework of the structure ultimately developed at the interface was relatively well-established on samples hydrated for as little as twenty-four hours before drying. In order to study the earlier stages of development of this structure, samples were dried immediately after casting, and after one, four, and eight hours hydration. All these pastes had a water-cement ratio of 0.5 and were cast against horizontal glass slides. The time designations for these samples refer to the time the sample was allowed to hydrate before drying was initiated. The "zero hour" sample, for example, was placed in the desiccator immediately after casting.

Sample Dried Immediately After Casting

Figure 43 shows the surface of the glass substrate of the sample that was dried immediately after casting. Notice that the interfacial film was already well developed, and that almost all of the film had remained with the substrate.

100 μ

Figure 43. Surface of Glass Substrate - 0 Hours

Notice also the large number of isolated cement grains and small aggregations of grains tied to the substrate through the growth of the interfacial film.

Figure 44 shows the C-S-H gel on the interfacial film. The crystals show a needle-like habit in contrast to the sheaf-like appearance at one to three days and the reticular network structure that develops at later ages.

Figures 45 and 46 show views at two magnifications of the surface of a cement grain. The surface of the grain is covered with small platy crystals, all of which are oriented roughly parallel to the interface. X-ray diffraction studies of pastes of this age show the plates to be composed of calcium hydroxide, and also substantiate a high degree of orientation of the platelets.

Although, as shown in Figure 44, the deposition of lime at the interface has already been supplanted by the deposition of C-S-H gel on the interfacial film, no gel is yet evident on the surfaces of the cement grains; the reason for this is not known. X-ray spectrographic analysis shows, however, that although no sulfur is present in the interfacial film, sulfur and aluminum are present in the platelets developing on the grains. The presence of these elements in the embryonic hydration shell may make this surface less attractive as a site for gel deposition.

μ

Figure 44. C-S-H Gel on Interfacial Film - 0 Hours

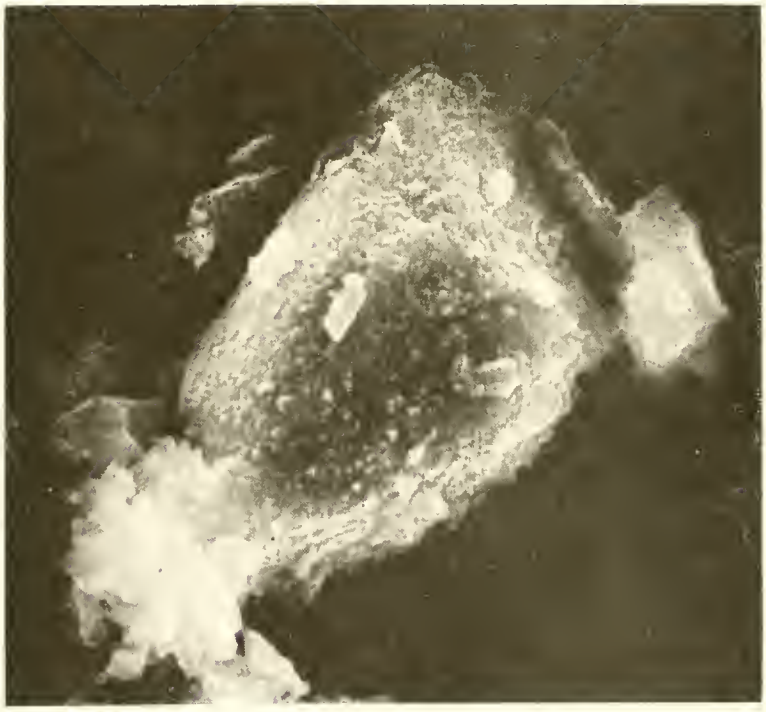

μ

Figure 45. Oriented Lime Platelets on Grain - 0 Hours

Figure 46. Oriented Lime Platelets on Grain - 0 Hours

Hydrated One Hour

The surface of the glass slide after hydration of the paste pat for one hour is shown in Figure 47. Practically all the interfacial film still remained with the substrate. Notice also the increased number of small aggregations of grains as opposed to the field shown in Figure 43 for the zero hour sample.

The C-S-H gel at the interface after one hour hydration is shown in Figure 48. The gel crystals were still needle-like. Notice the small platelets capping some of the aggregations of gel needles and lying roughly parallel to the interface. These platelets are probably lime, and their presence indicates contemporaneous deposition of lime and C-S-H gel during the later stages of development of the interfacial film.

The surface of a cement grain after hydration for one hour is shown in Figure 49. The platy habit of the lime and the high degree of orientation are evident. Notice that there was still little or no evidence of gel deposition on the developing hydration shell.

Hydration for Four Hours

The surface of a calcium silicate grain hydrated for four hours is shown in Figure 50. The plates of calcium hydroxide were well developed, and some small crystals of C-S-H gel were starting to develop. The appearance of the

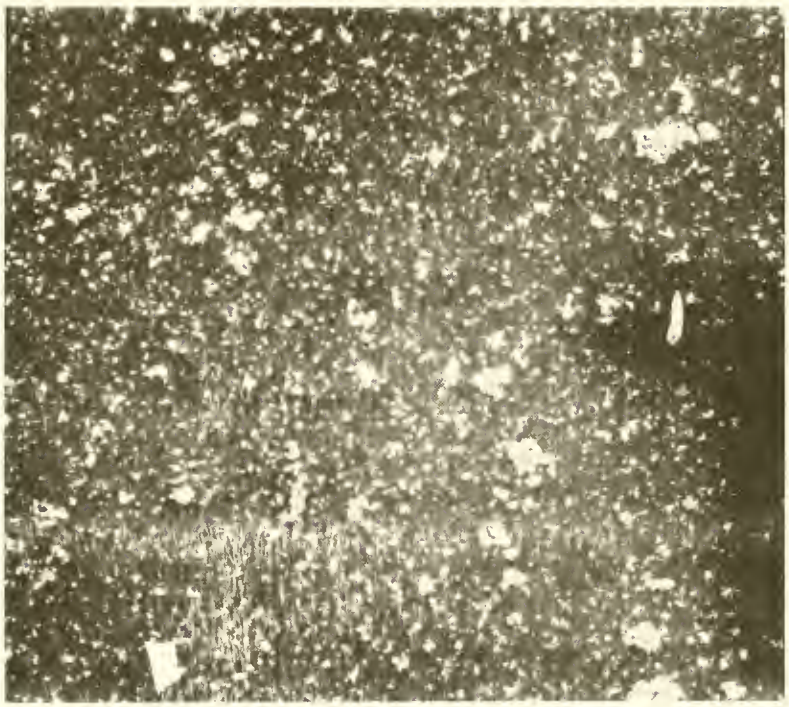

Figure 47. Surface of Glass Substrate - 1 Hour

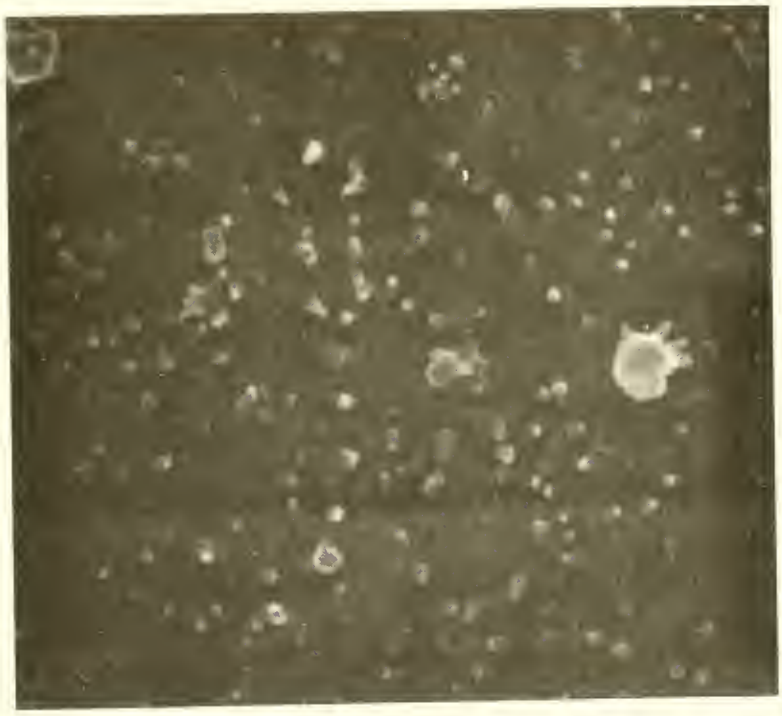

μ

Figure 48. C-S-H Gel on Interfacial Film - 1 Hour

μ

Figure 49. Oriented Lime Platelets on Grain - 1 Hour

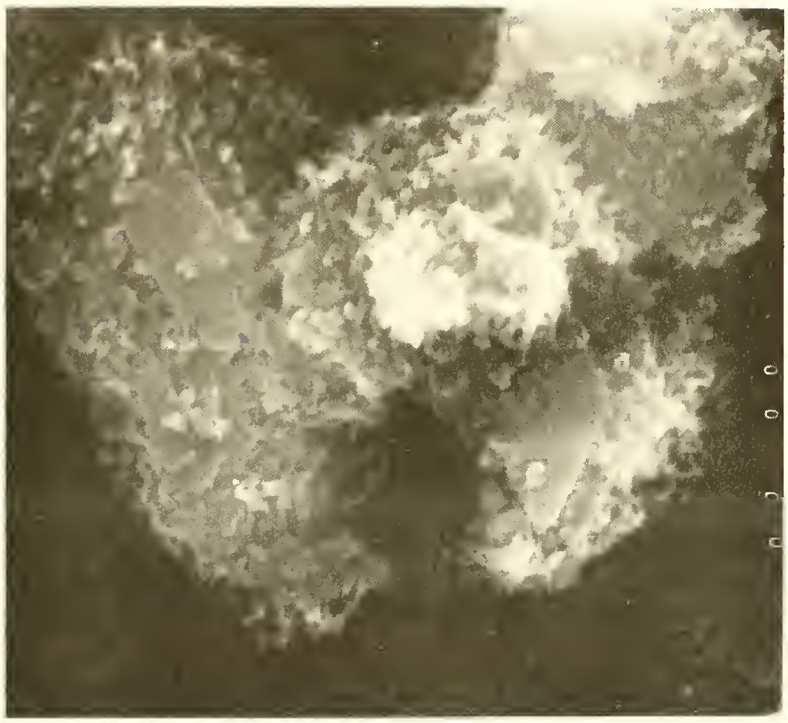

μ

Figure 50. Surface of Grain Hydrated Four Hours

gel on the interfacial film and the continuity of the film were the same as for the one hour sample.

Hydration for Eight Hours

The surface of the glass substrate after hydration of the pat for eight hours is shown on Figure 51. In several areas the interfacial film had pulled away from the glass on separation. Since it has been found that this occurs only when the paste is tied to the film by massive lime crystals, it seems the massive lime first appears sometime between four and eight hours after casting.

Figure 51 also shows the first appearance of large aggregations of cement grains of the type mentioned previously and shown in Figure 22. The large aggregation in the center of the field in Figure 51 is shown at a higher magnification in Figure 52. This aggregation is over one hundred microns high. Notice the fractured grain at the apex of the aggregation. This grain is shown at a still higher magnification in Figure 53. The hydration shell on the grain had been partially pulled away from the remnant cement grain during separation. The crack along the left side of the remnant grain represents the early development of void space between the remnant grain and the hydration shell. This void is shown also along the upper left hand corner of the grain in Figure 53, and at a higher magnification in Figure 54.

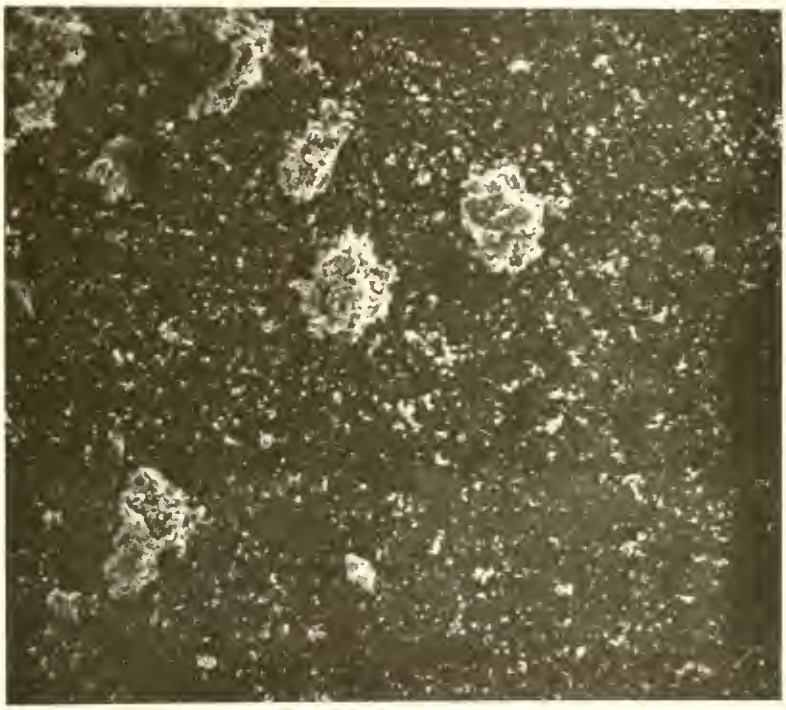

100μ

Figure 51. Surface of Glass Substrate - 8 Hours

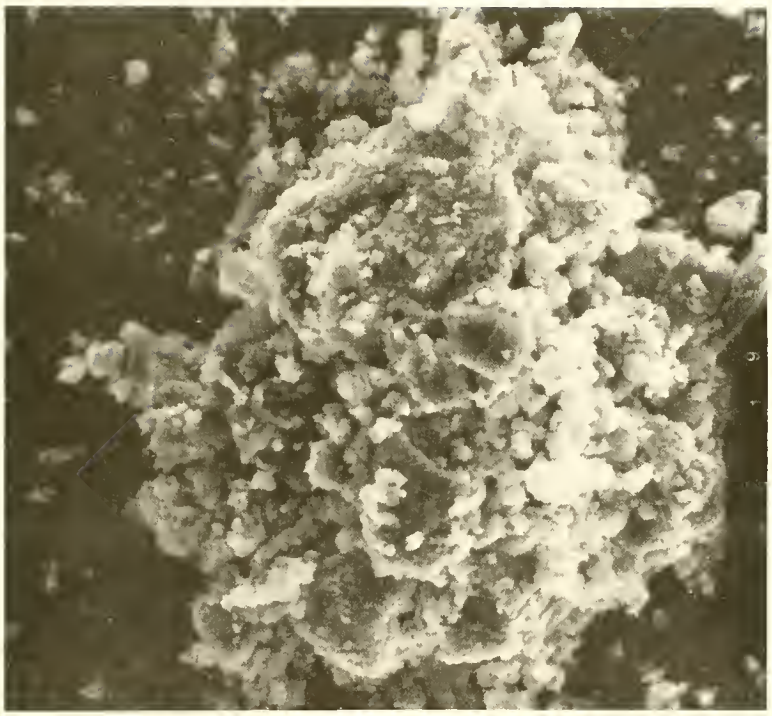

10 μ

Figure 52. Aggregation of Grains - 8 Hours

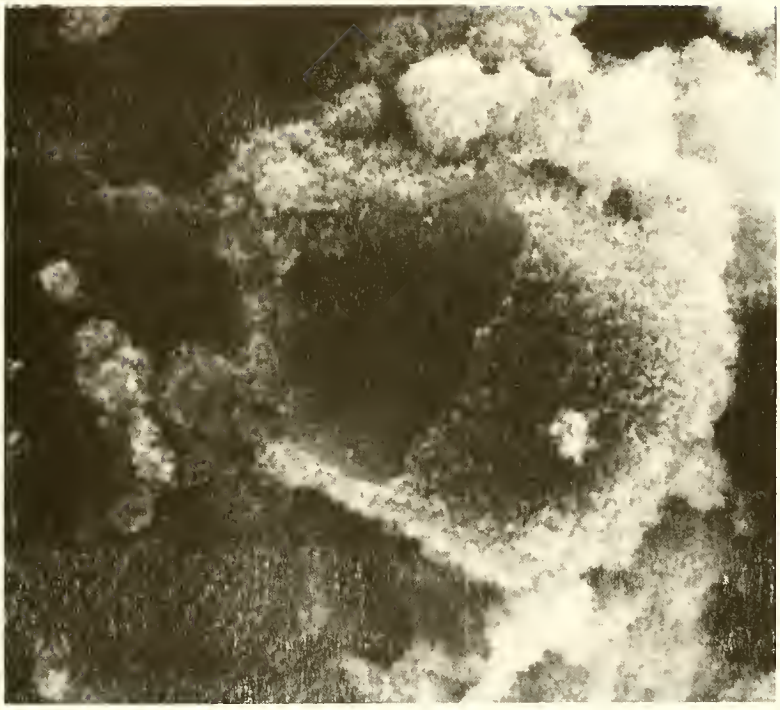

1 μ

Figure 53. Ruptured Partially Hydrated Grain - 8 Hours

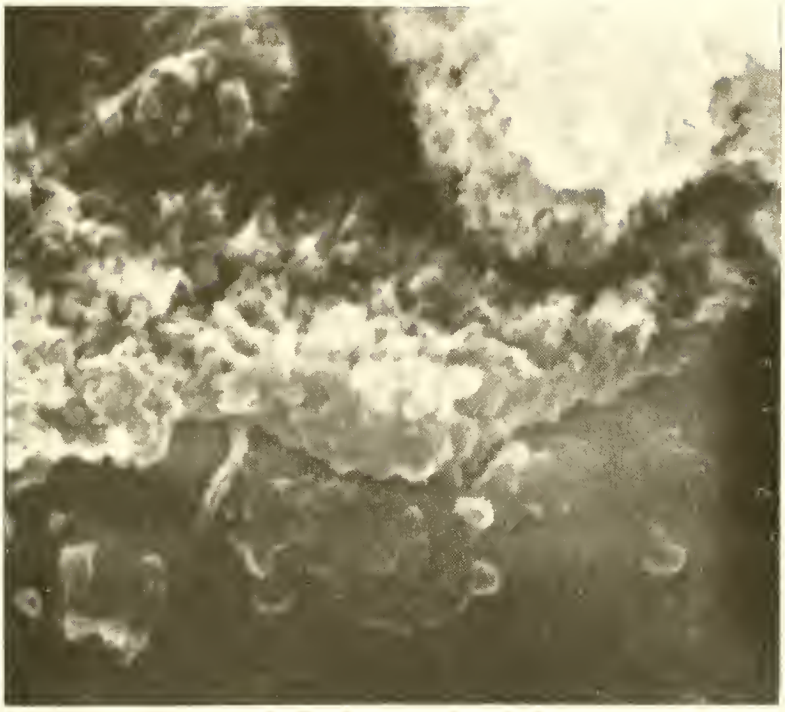

1μ

Figure 54. Hydration Shell and Remnant Grain - 8 Hours

Inspection of Figures 53 and 54 shows that most of the features observed on the hydration shells discussed previously are present after eight hours hydration. Apparent on the surface of the remnant grain, especially in Figure 53, are scattered stubby crystals that represent the early stage of development of the interior acicular crystals that join the remnant grain to the hydration shell. On Figure 54 can be seen the interior void, the massive layer of lime showing a considerable degree of preferred orientation, and the exterior layer of C-S-H gel.

The highly oriented nature of the lime in the hydration shell of this grain is significant since, as was shown in Figure 52, it lies a considerable distance from the interface.

Figure 55 shows the nature of the C-S-H gel developed on the interfacial film after hydration for eight hours. The crystals of gel were loosing their needle-like aspect and beginning to assume the sheaf-like appearance observed on the one day sample.

X-ray Diffraction Studies of Lime Orientation

As was mentioned in the preceeding section, scanning electron microscopy indicated that the lime in the inner portions of the hydration shells showed preferred orientation, even on grains lying a considerable distance from the interface. The orientation of the calcium hydroxide

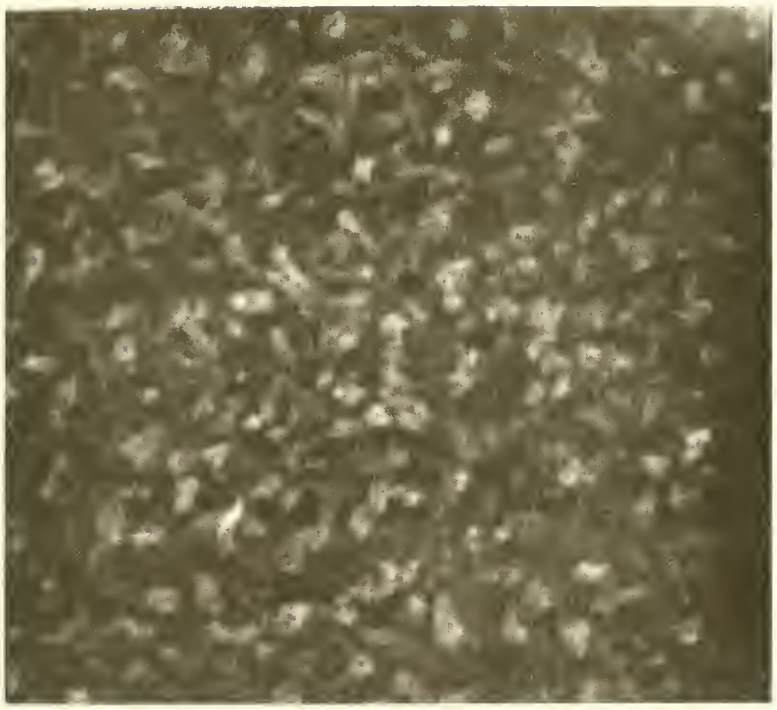

μ

Figure 55. C-S-H Gel on Interfacial Film - 8 Hours

in the paste was investigated using the x-ray techniques outlined in the introductory chapter.

The degree of preferred orientation of the calcium hydroxide, as measured by the peak height ratios of the (00·1) and (10.2) diffraction peaks, is shown as a function of distance from the paste-aggregate interface in Figure 56. The sample was a paste with a water-cement ratio of 0.5, cast against a horizontal glass surface, and hydrated for two months before separation.

Examination of the interfacial film adhering to the substrate with samples separated at early ages has shown the lime in the film to be perfectly oriented. Since the surface of the lime film at later ages showed no evidence of recrystallization, it was assumed that the orientation at the interface on the sample under investigation was also perfect.

As is shown in Figure 56, the degree of orientation drops off sharply immediately behind the interfacial film. This is due to the presence in this region of large and randomly oriented lime crystals, which mask the high degree of orientation that scanning electron microscopy has shown is to be present in the hydration shells near the interface.

This masking effect continues to predominate for about the first 35 microns inward from the interface. Between 35 and 70 microns, the relative quantity of randomly-oriented massive lime crystals progressively decreases.

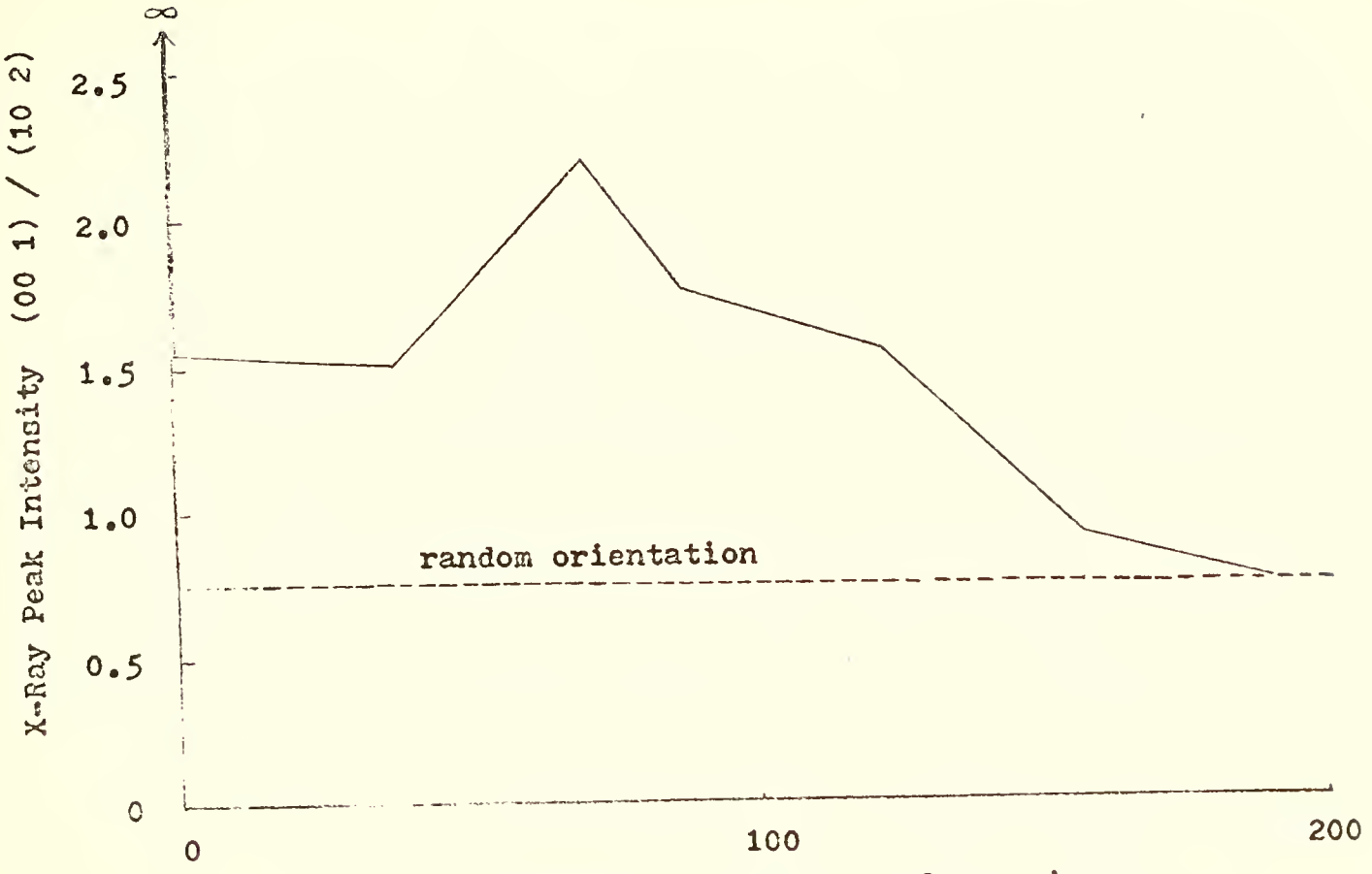

Figure 56. Preferred Orientation of Lime

The high degree of orientation of the lime in the hydration shells becomes progressively more apparent as the masking effect due to the massive lime decreases. This results in an upward trend in the orientation curve between 35 and 70 microns from the interface. At 70 microns, the effective outer limit of the massive lime is reached, and the orientation curve attains its maximum value. From the peak at 70 microns, the curve shows a steady decline in the degree of preferred orientation away from the interface. Random orientation was reached at a distance of approximately 200 microns from the paste-aggregate interface.

In summary, the lime in the interfacial film is perfectly oriented. The degree of preferred orientation of the lime in the hydration shells is also high at the interface, but shows a progressive decrease away from the interface, reaching random orientation at a distance of about 200 microns. A layer of randomly oriented massive lime crystals masks the high level of orientation in the shells in the first 70 microns away from the interface.

Hydration of Artificial Cements

To gain additional insight into the distribution of sulfur and aluminum in the morphological units observed in the work already described, the hydration of artificial cements was studied.

Three artificial cements were used. The first was composed of only alite, the second contained alite with a

2% gypsum replacement by weight, and the third contained alite, 2% gypsum, and 13% C_3A. All pastes were prepared at a water-cement ratio of 0.5 and were cast against horizontal glass slides. The significant information derived from these studies is given below.

Morphology Within the Hydration Shells

The interior of a fractured hydration shell observed on the three day old sample of alite paste is shown in Figure 57. The predominant features within the shell are platy crystals, growing roughly perpendicular to the interior surface of the shell.

Figure 58 shows an equivalent hydration shell, also three days old, and formed with the alite-gypsum mixture. The interior of this shell contains a number of prismatic crystals, much larger in cross-section than the acicular crystals observed in hydration shells formed in portland cement pastes. It is not known whether the alteration of crystal habit brought about by the introduction of sulphate represents a change in composition as well. If sulfate was present within the prismatic crystals, it was at a level too low for detection with the x-ray spectrometer.

The interior of a shell formed with the alite-gypsum-C_3A paste at three days is shown on Figure 59. This shell contains a large number of acicular crystals of the type seen in portland cement pastes. X-ray spectrographic

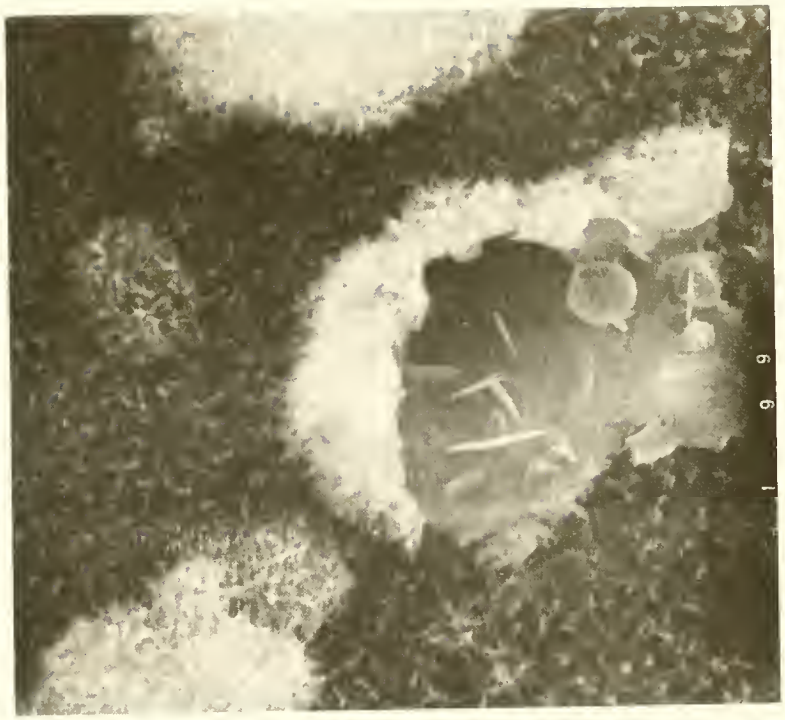

μ

Figure 57. Hydration Shell - Alite Paste - 3 Days

μ

Figure 58. Hydration Shell - Alite + Gypsum - 3 Days

μ

Figure 59. Hydration Shell - Alite + Gypsum + C_3A 3 Days

analysis does show the presence of both sulfur and aluminum within this shell.

Composition of Large Needles

Figure 60 is a view of the paste side of the alite-gypsum sample after three days hydration. Figure 61 is a view of the equivalent alite-gypsum-C_3A paste. The large number of needle-like crystals on the surface of the grains shown on Figure 61 and the complete absence of such crystals on the grains shown on Figure 60 would seem to offer substantial support to the view that the large needles are ettringite.

Effect of Substrate Orientation

To investigate the influence of the orientation of the aggregate surface on the structure at the paste-aggregate interface, specimens were cast against vertical glass surfaces. Mixing, casting, curing, and drying procedures were identical to those used in the preparation of the specimens cast against horizontal surfaces.

Examination of these samples showed that they were, in all respects, identical to the samples cast horizontally. Figure 62 is a streo-pair of the surface of a seven day old paste, cast against a vertical glass surface. In this figure can be recognized the compound interfacial film, needles of ettringite, a platey hexagonal crystal, and a fractured hydration shell showing an interior void containing

$\underline{\mu}$

Figure 60. Alite + Gypsum Paste - 3 Days

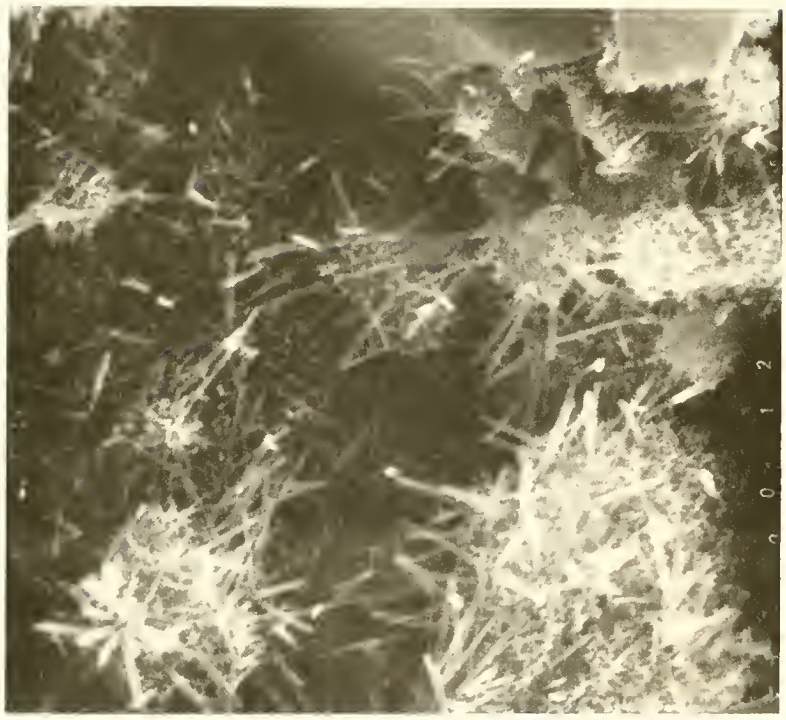

μ

Figure 61. Alite + Gypsum + C_3A Paste - 3 Days

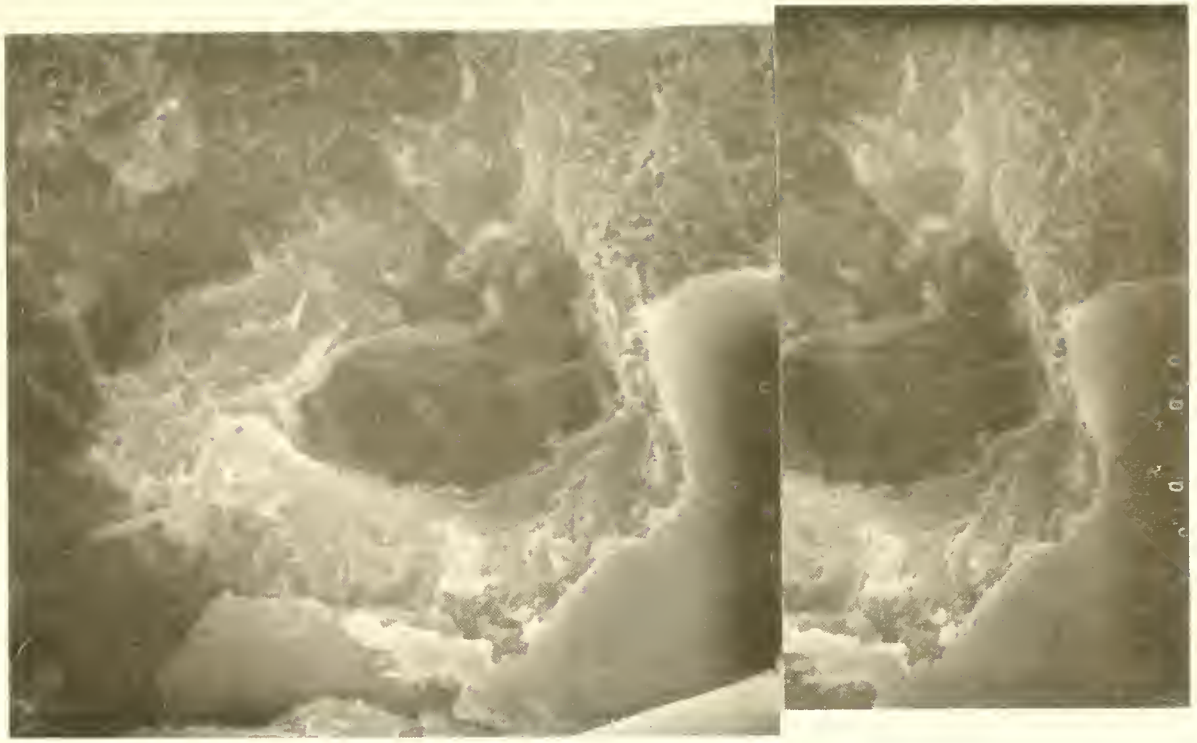

μ

Figure 62. Paste Cast Against Vertical Surface - 7 Days

acicular crystals. The layered structure of oriented lime is evident in the massive inner layer of the hydration shell, and the plates of lime are oriented parallel to the interfacial film and the interface. X-ray studies confirm that the lime in the interfacial film is oriented parallel to the interface.

In summary, the orientation of the substrate had no effect on the structure developed at the interface or on the orientation of any of the elements of that structure.

Effect of Water-Cement Ratio

In order to investigate the effect of variation of the water-cement ratio of the paste on the structure at the paste-aggregate interface, specimens were cast with a water-cement ratio of 0·25. Examination of these samples showed that the only apparent effect of the significant reduction in the water content of the paste was a drastic decrease in the amount of void space at the interface. As a result of the reduction in void space, a greatly increased percentage of the interfacial film was found to remain with the paste at separation. The paste was almost completely tied to the interfacial film at 7 days, as opposed to twenty-eight days for the samples with a 0·5 water-cement ratio.

The Bonding of Paste to Roughened Surfaces

Once the nature of the structure developed at the interface between cement paste and the smooth surfaces of

the glass slides had been established, the effect of surface roughness was investigated. Sand grains and crushed stone surfaces were studied under the scanning electron microscope, and the surfaces were compared with those produced by grinding the surfaces of glass slides with grinding compounds of various sizes. This work established that the surface obtained by grinding the slides against a glass plate with #240 grinding compound produced a surface similar to that displayed by the natural aggregates. Figures 63 and 64 show the glass surface after grinding.

Samples were prepared with a paste having a water-cement ratio of 0·5 and cast against horizontal roughened glass surfaces. Separation was initiated after one, three, seven, fourteen, and twenty-eight days hydration. It was found that even with the roughened surfaces, separation of the paste from the slide could be achieved by simply tapping the sample against the bench top after drying.

Study of these samples showed that the structure developed in the interfacial region with the roughened substrate was completely analogous to that observed with the smooth glass slides. A compound interfacial film formed at the interface, and the lime conformed to the surface perfectly. Needles of ettringite and platy crystals appeared at three days, and the percentage of the interfacial film remaining with the paste on separation increased with time. X-ray spectrometry of the surface indicated

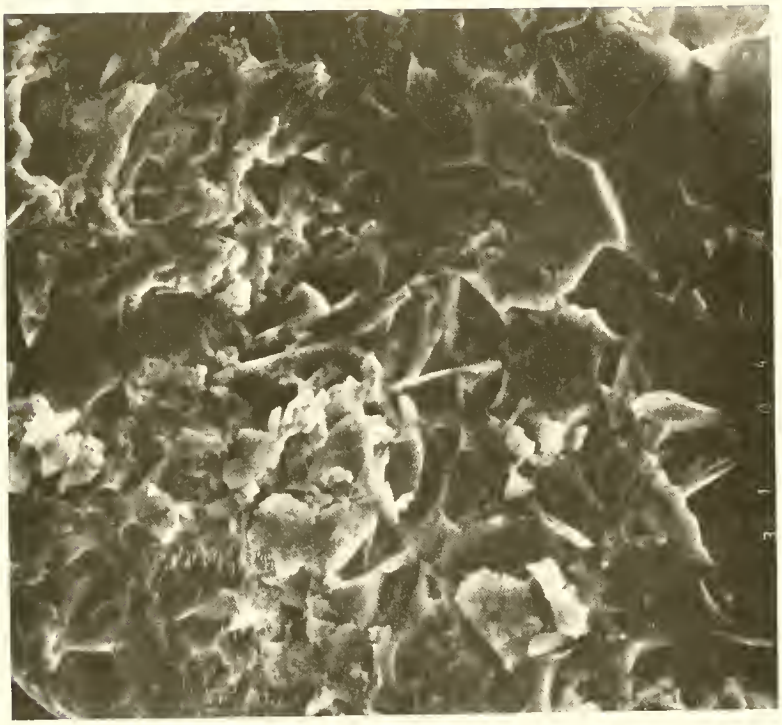

10 μ

Figure 63. Roughened Glass Surface

μ

Figure 64. Roughened Glass Surface

that separation took place within the lime film, leaving a thin residual layer of lime on the substrate surface. X-ray diffraction showed that, in spite of the roughened surface, the lime in the paste showed a preferred orientation, with the c-axes tending to be normal to the gross, or original, surface of the substrate. The degree of orientation was only slightly less than that shown by samples cast against a smooth surface. Figures 65 through 74 show the surface of the roughened substrate from one through twenty-eight days.

The Structure Developed on Quartzite

All the work described to this point was done using glass slides as the substrate. In order more closely to approach the conditions present in concrete, samples were prepared by casting a 0·5 water-cement ratio paste against a quartzite surface that had been roughened with #240 grinding compound.

Examination of these samples showed them to be equivalent in all respects to the samples cast against the roughened glass. The surface of the quartzite substrate is shown on Figures 75 and 76 and Figures 77 through 80 show the surface of the substrate after separation from the paste at one through fourteen days. Figures 81 and 82 show the substrate at twenty-eight days and Figures 83 and 84 show the surface of the paste at the same age. Notice the extent to which the surface of the paste reflects the substrate surface with which it was in contact. (These pairs

10 μ

Figure 65. Roughened Glass Substrate - 1 Day

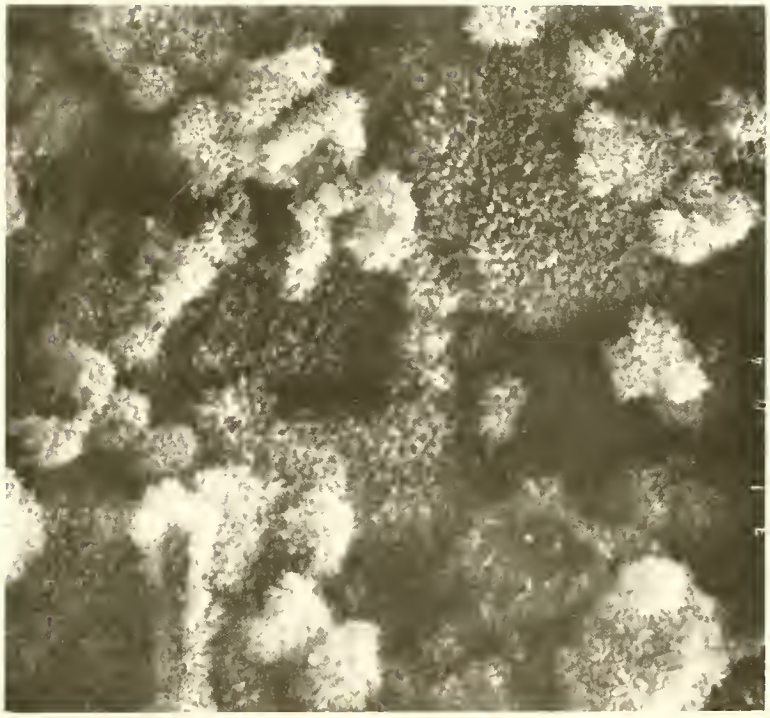

1 μ

Figure 66. Roughened Glass Substrate - 1 Day

10 μ

Figure 67. Roughened Glass Substrate - 3 Days

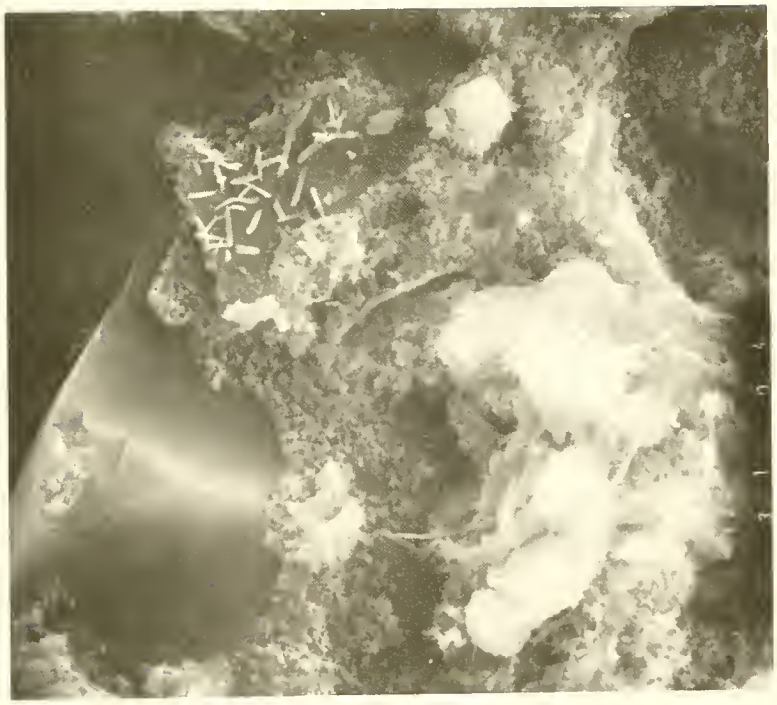

μ1

Figure 68. Roughened Glass Substrate - 3 Days

Figure 69. Roughened Glass Substrate - 7 Days

μ

Figure 70. Roughened Glass Substrate - 7 Days

Figure 71. Roughened Glass Substrate - 14 Days

μ

Figure 72. Roughened Glass Substrate - 14 Days

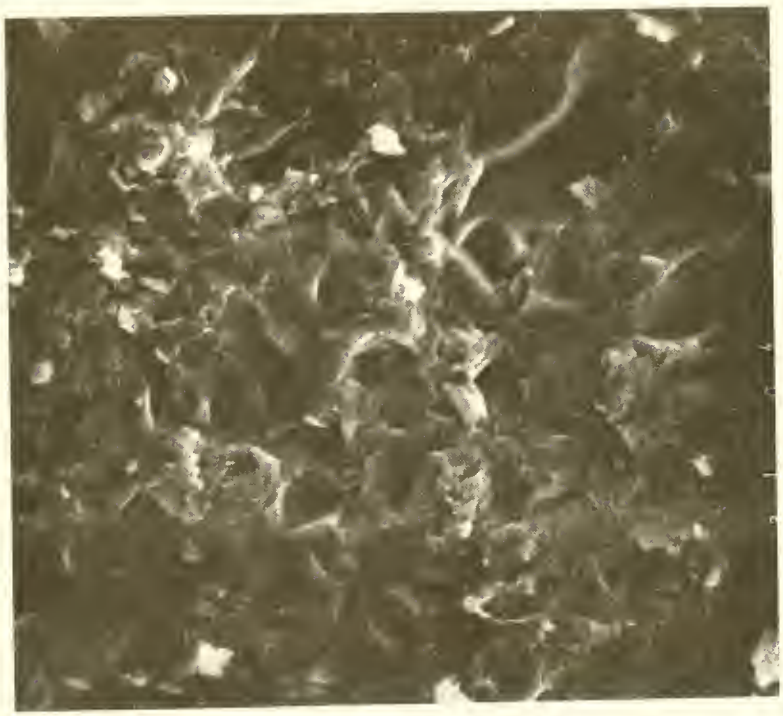

Figure 73. Roughened Glass Substrate - 28 Days

μ

Figure 74. Roughened Glass Substrate - 28 Days

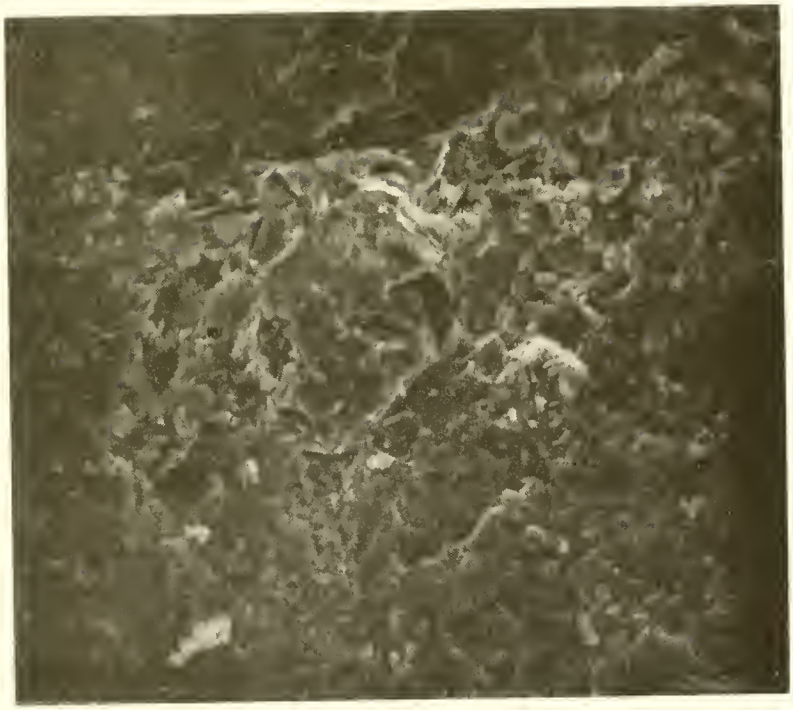

10 μ

Figure 75. Quartzite Surface

10 μ

Figure 76. Quartzite Surface

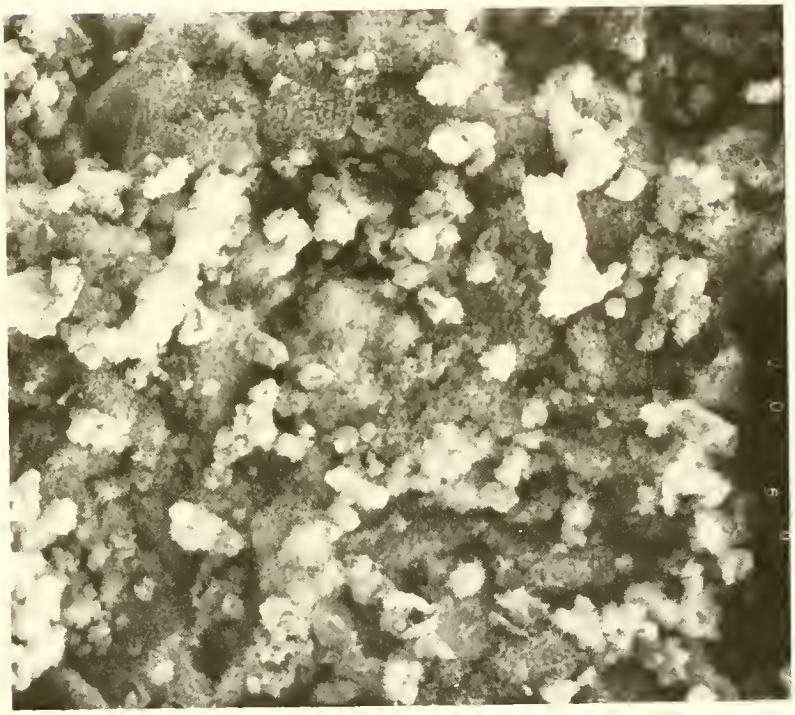

10 μ

Figure 77. Quartzite Substrate - 1 Day

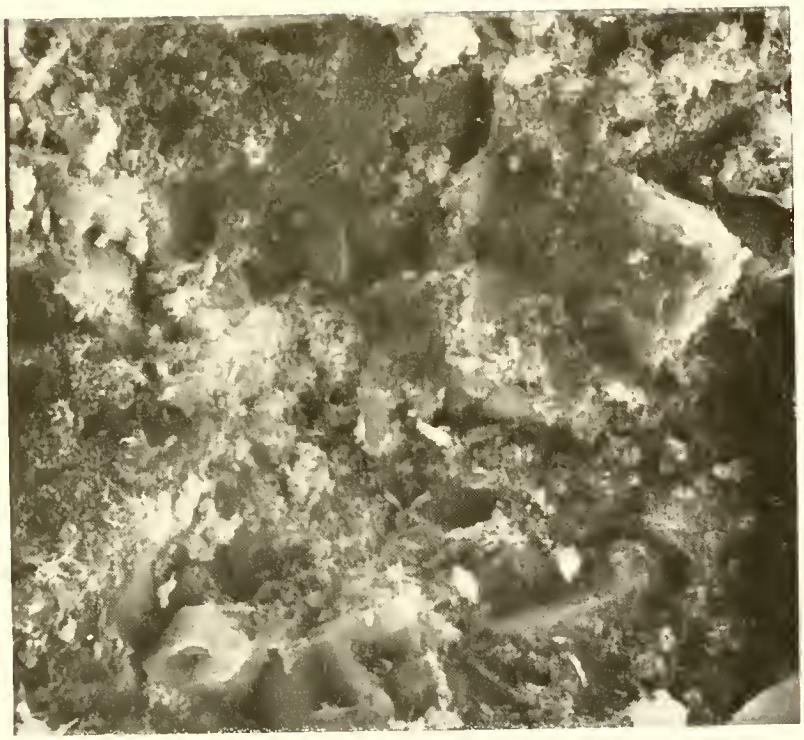

10 μ

Figure 78. Quartzite Substrate - 3 Days

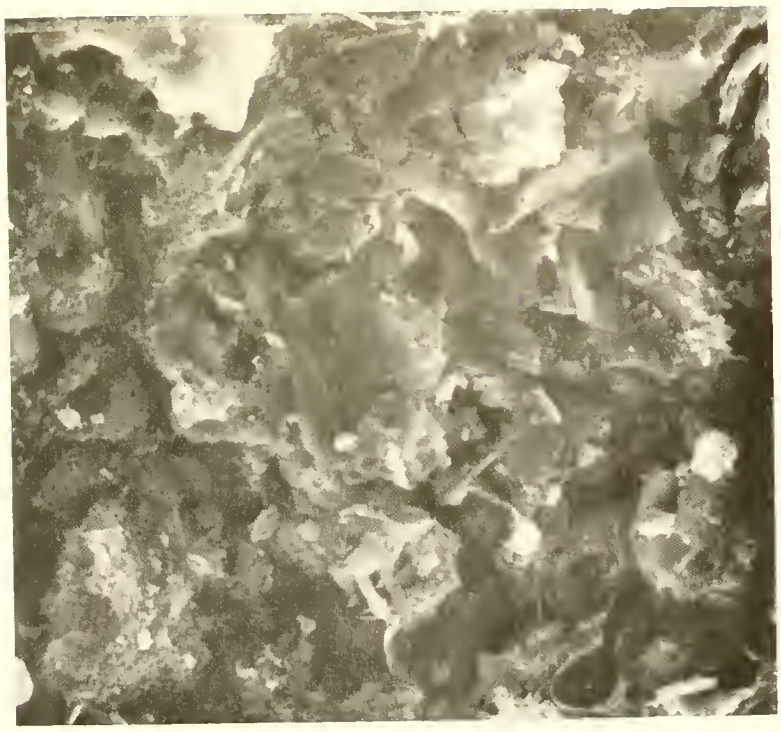

10 μ

Figure 79. Quartzite Substrate - 7 Days

10 μ

Figure 80. Quartzite Substrate - 14 Days

10 μ

Figure 81. Quartzite Substrate - 28 Days

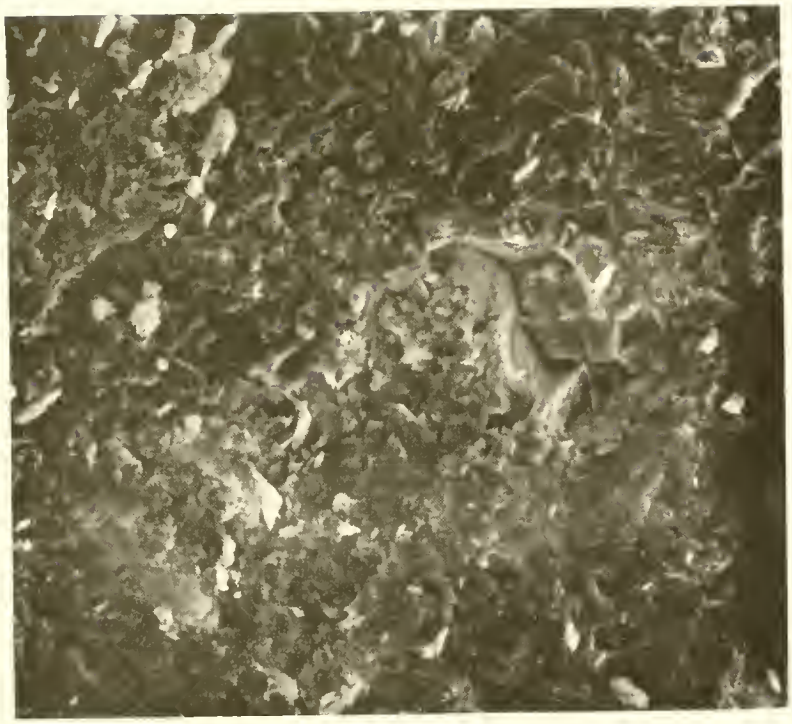

10 μ

Figure 82. Quartzite Substrate - 28 Days

10 μ

Figure 83. Paste Against Quartzite - 28 Days

10 μ

Figure 84. Paste Against Quartzite - 28 Days

of photomicrographs were not taken of the same fields, but show the general conformity of the paste at the interface to the substrate surface.)

Figure 85 shows the surface of the paste cast against quartzite and hydrated three days. All the elements of the structure described for the samples on glass are shown. The interfacial film, massive lime crystals, fractured hydration shells with interior needles, crystals of ettringite, and packets of platy crystals can be recognized.

The Structure Developed on Marble

To investigate the structure at the interface with carbonate aggregates, samples were cast against roughened marble. The nature of the marble substrate is shown on Figures 86 and 87. Figures 88 and 89 show the surface of the marble substrate after the removal of the paste at one day. The surface appears much the same as that developed on the glass and quartzite surfaces. Figure 90 shows the paste side of the one day sample. Prominant on this field is a large fragment of calcite that was plucked from the surface of the substrate at separation. The surface of the marble after three days is shown on Figures 91 and 92. It can be seen that a much greater proportion of the aggregate surface has been exposed after hydration for three days than was the case with the siliceous substrates. Examination of the paste side of the sample showed that the majority of the fracture had taken place along cleavage planes in the

Figure 85. Paste Against Quartzite - 3 Days

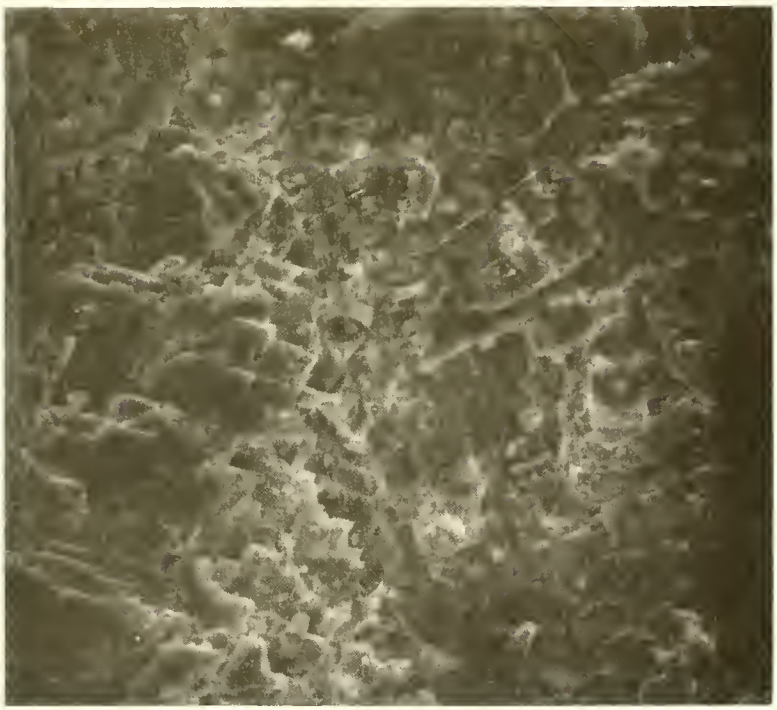

10μ

Figure 86. Marble Substrate

10μ

Figure 87. Marble Substrate

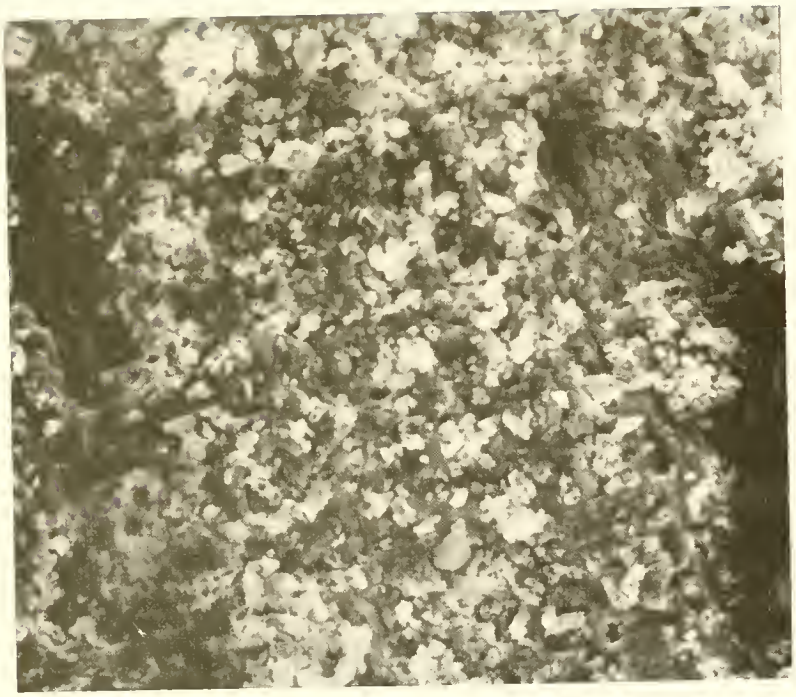

10μ

Figure 88. Marble Substrate - 1 Day

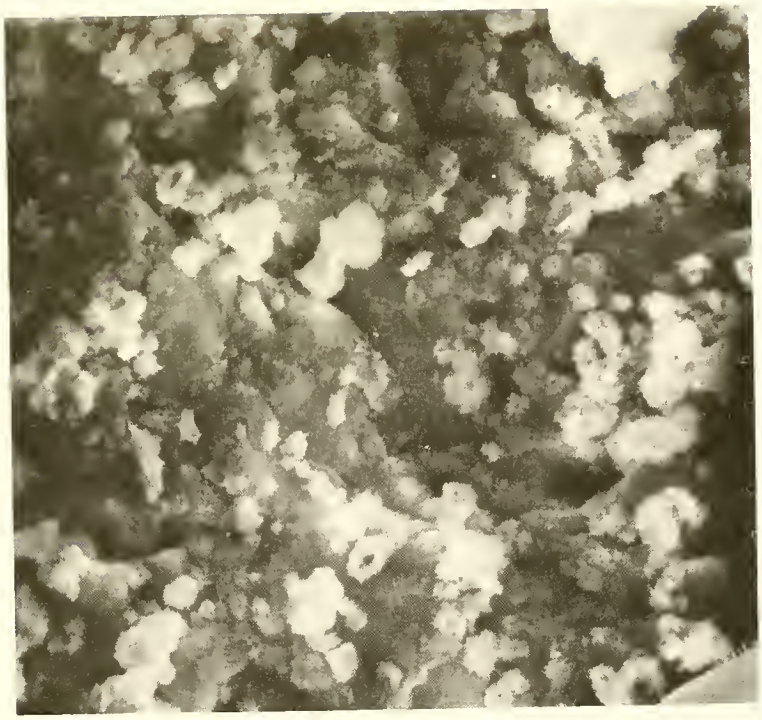

10 μ

Figure 89. Marble Substrate - 1 Day

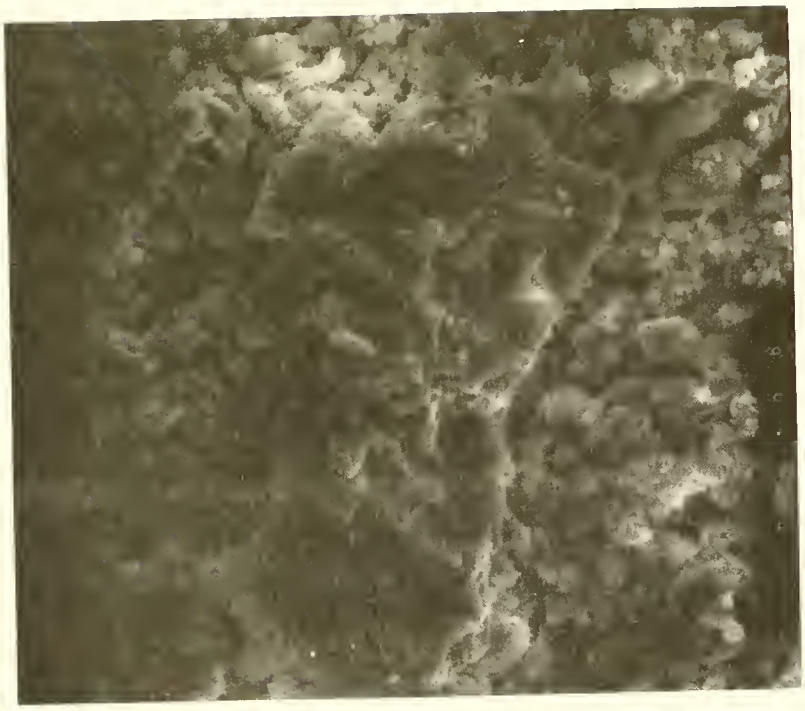

10 μ

Figure 90. Separation Through Marble - 1 Day

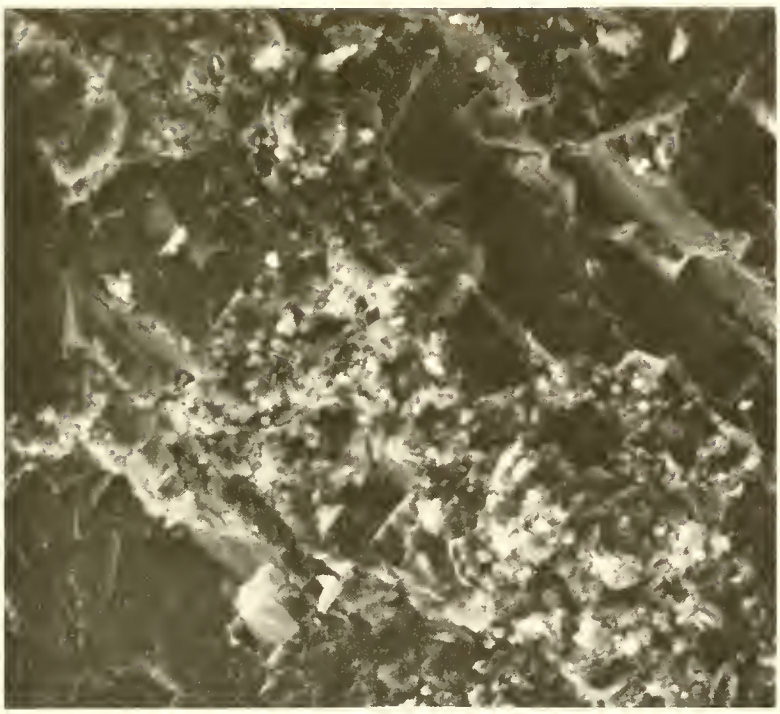

Figure 91. Marble Substrate - 3 Days

10 μ

Figure 92. Marble Substrate - 3 Days

marble, rather than at the interface. The substrate surface at 7 days is shown on Figures 93 and 94. Notice that the majority of the aggregate surface is exposed, and that fracture has occurred through the rock rather than at the interface. Figure 95 shows the substrate surface at fourteen days, and it can be seen that no paste remains on the surface. Examination of the paste side of the sample showed that fracture had been entirely through the rock.

The strong tendency of calcite to fracture through the mineral rather than at or near the interface was noted by Farran (5), who thought this mode of fracture to be the result of an unusually strong bond developed between calcite and the paste. In the work described earlier, however, in which paste was cast against a wide variety of mineral surfaces, the writer found that separation took place largely within the aggregate with all of those minerals showing well developed cleavages, such as dolomite, siderite, muscovite, biotite, phlogopite, fluorite, and galena.

Both ottawa silica sand mortars and manufactured calcite sand mortars were also studied and were found to show no features not already described. Descriptions are included as an appendix.

This work has raised a number of questions of importance to our understanding of the hydration of portland cement and the structure of cement paste.

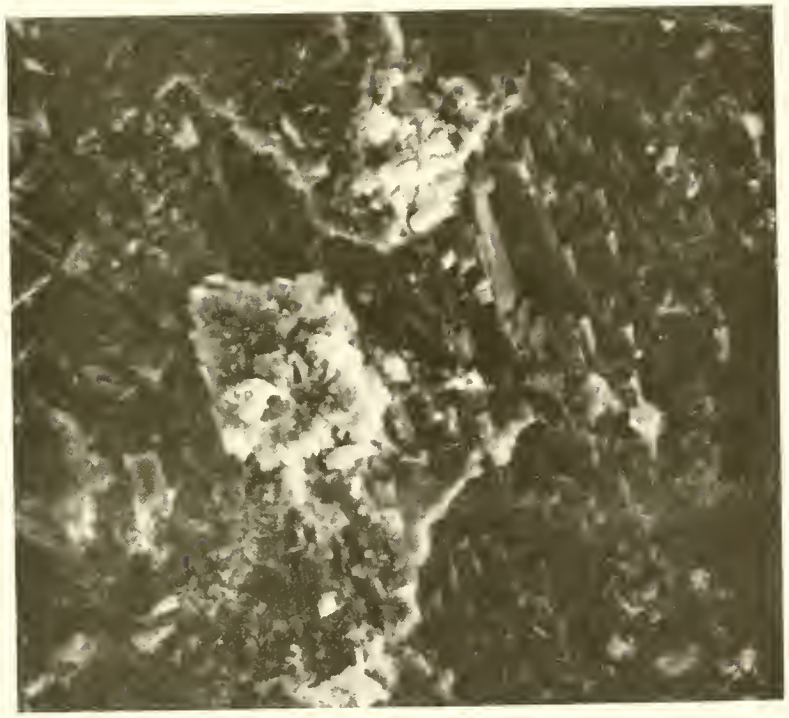

10 μ

Figure 93. Marble Substrate - 7 Days

10 μ

Figure 94. Marble Substrate - 7 Days

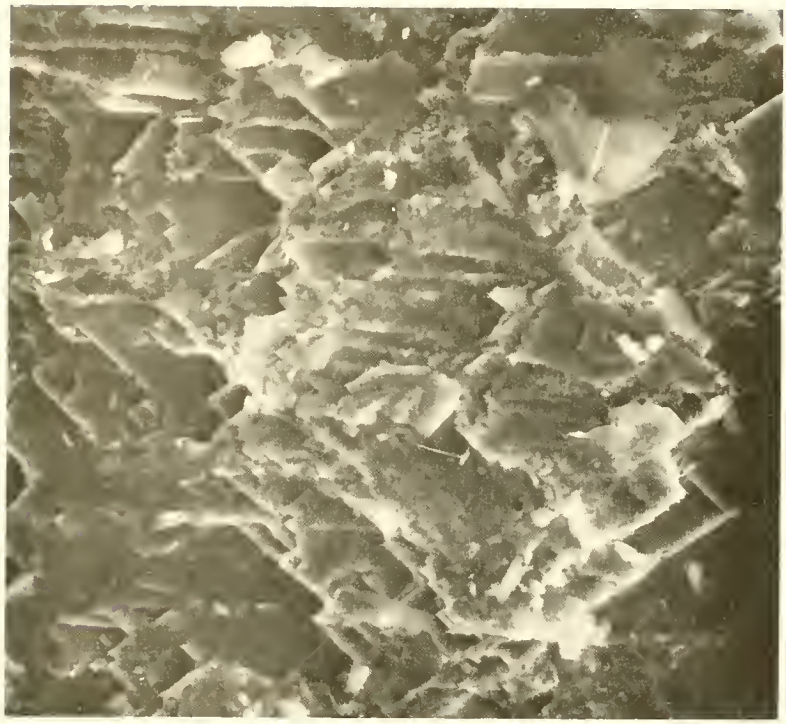

10 μ

Figure 95. Marble Substrate - 14 Days

Principal among these are questions concerning the origin, distribution, and longevity of the essentially hollow hydration shells. Since these shells were observed with all varieties of substrates and at various paste ages, they probably are not artifacts produced by the particular sample preparation procedures. If the shells are typical of the paste as a whole, it means that the hydration of portland cement takes place entirely through solution and subsequent deposition at sites relatively far away from the parent anhydrous cement grains. This is different from the commonly held picture of "isomorphous hydration", in which much of the calcium silicate hydrate is thought to be deposited within the original grain boundaries (41).

The origin of the void space within the shells is difficult to understand. Logically, the saturation of calcium and silicate would be highest in the immediate vicinity of the dissolving grain, and the C-S-H gel should preferentially be deposited on the inner surface of the lime layer that forms on the grain surface early in the hydration process. Instead, the dissolved components from the grain apparently diffuse through the hydration shell and are deposited as gel on the lime film at the interface. At later ages, after gel begins to form on the exterior of the oriented lime of the hydration shell, the inner surface still remains devoid of gel.

An important question is whether the hollow shells occur throughout the body of the paste, or are restricted to the immediate vicinity of the interface. Many fracture surfaces of the bulk paste were examined. No hydration shells of the type under discussion were recognized. The structure of the bulk paste is, however, so massive, especially in older pastes, that the recognition of individual morphological units of the type observed near the interface is difficult. Thus, while no hollow hydration shells were found within the bulk paste, neither were any filled hydration shells or "pseudomorphous grains" as described by Williamson (34) and Diamond (31). In this connection, it is possible that the features pictured by these authors, rather than being pseudomorphs, actually are remnant grains, prevented from further hydration by encapsulation in large lime crystals.

The question of whether the hollow hydration shells persist at later ages is also unanswered, since the paste at ages of greater than twenty-eight days is so massive that no fine structure could be observed.

Of lesser importance, but equally puzzling, is the question of the preferred orientation shown by the lime in the interfacial film and in the massive inner portion of the hydration shells near the interface.

CHAPTER III - SUMMARY AND CONCLUSIONS

Summary

During the sedimentation and consolidation of cement paste, (and, presumably, concrete as well) the grains are in a flocculated state, which brings about bridging near the paste-substrate (aggregate) interface and results in the development of a considerable volume of water-filled void space at the interface. Figure 96 is a diagrammatic sketch showing relationships at the interface immediately after casting and consolidation. On this figure is seen the open structure of the paste and the void space at the interface. Notice also the small isolated grain lying on the interface and not connected directly to the overlying grains. This grain is shown in an enlarged scale in Figure 97, which shows the grain to be separated from the aggregate surface by a thin water film.

Almost immediately after casting, a thin film of lime begins to develop at the interface. The lime in this film shows an almost perfect plane-parallel orientation, with the c-axes of the crystals normal to the interface. At a somewhat later time, but still within the first hour, small spicules of C-S-H gel begin to appear on the lime film still developing at the interface. Concurrently, small plates of

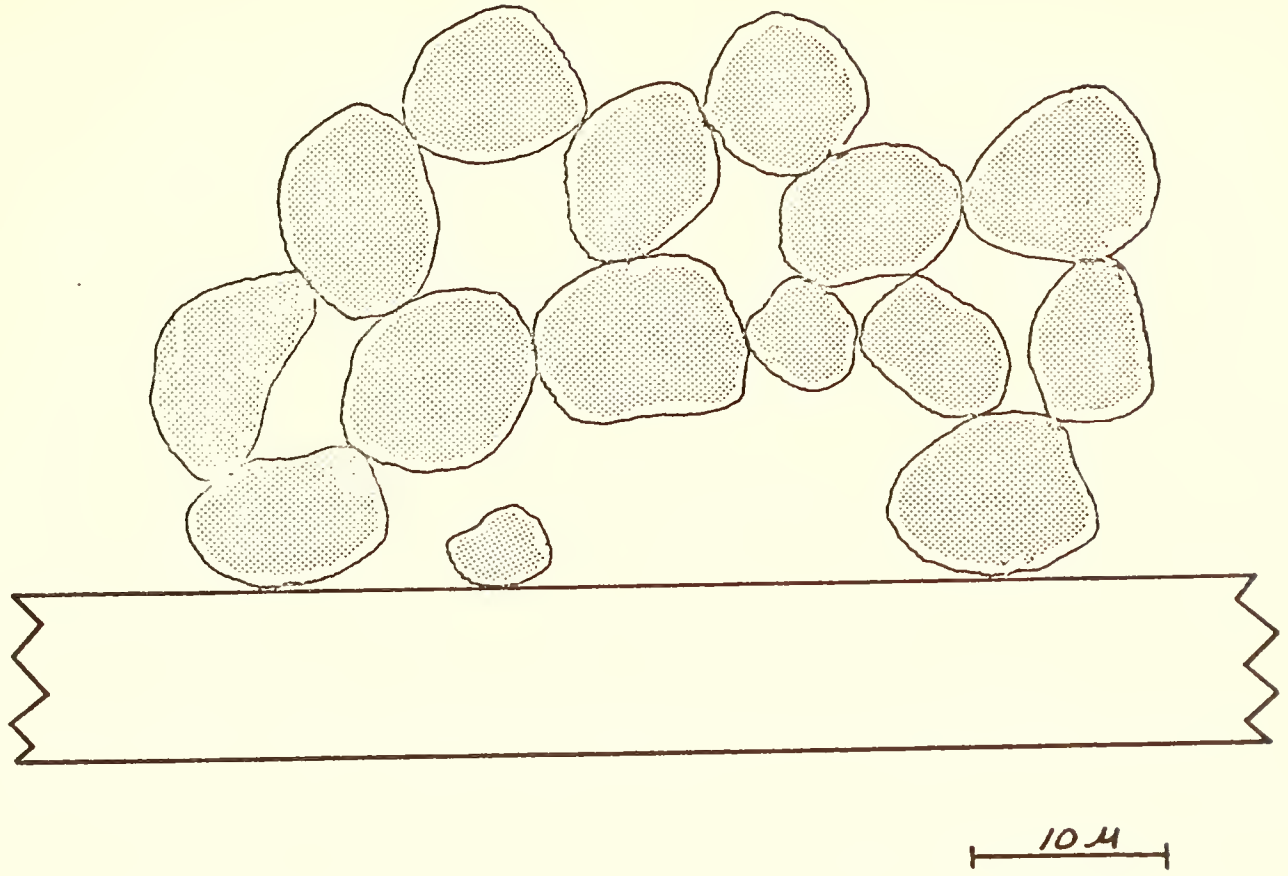

Figure 96. Interface Region Immediately After Consolidation

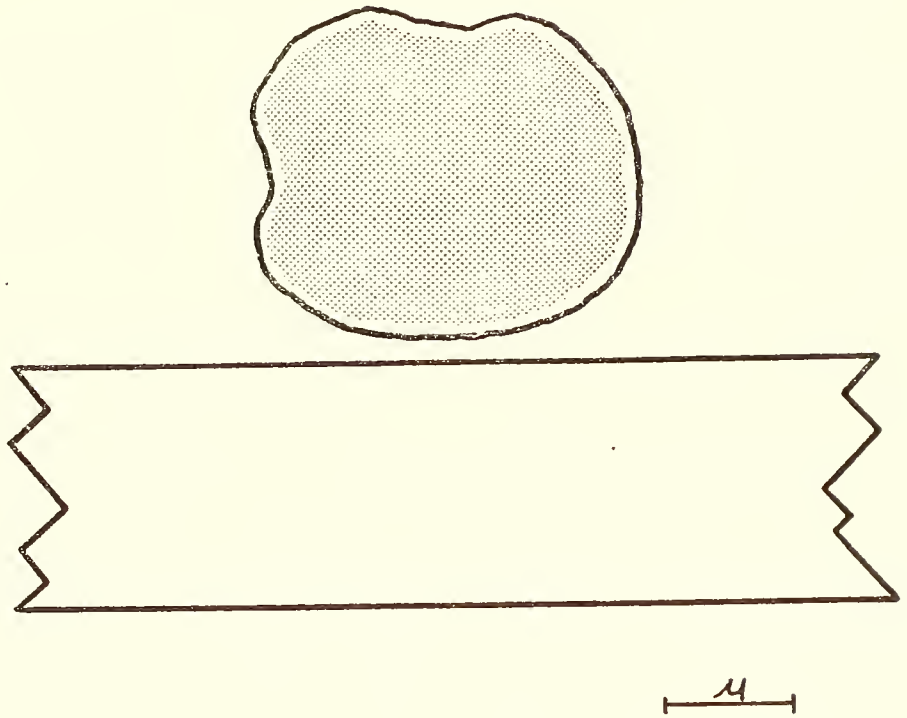

Figure 97. Cement Grain at Interface

lime begin to form on the surface of the hydrating cement grains. These crystals also show a considerable degree of preferred orientation, with their c-axes perpendicular to the aggregate interface. The degree of orientation is less perfect than that found in the interfacial lime film, and decreases with increasing distance from the interface. Random orientation is reached roughly two hundred microns from the interface. Although the lime in the interfacial film is fairly pure, that precipitating on the surface of the hydrating grains contains appreciable quantities of aluminum and sulfur, probably as the result of encapsulated crystals of ettringite. The general appearance of the region after less than an hour's hydration is shown diagrammatically on Figure 98.

The same region after about two hours hydration is shown in Figure 99. The continued deposition of C-S-H gel on the surface of the lime film at the interface blocks this region for further lime deposition. The result is the formation of a composite interfacial film, consisting of a layer of highly oriented lime, normally about a quarter of a micron thick, backed with a layer of gel.

Also shown on Figure 99 is the continued deposition of oriented lime on the surface of the cement grains, leading to the development of a massive layer of lime surrounding the grain. As the grain hydrates, a void space begins to develop between the inner surface of the lime hydration

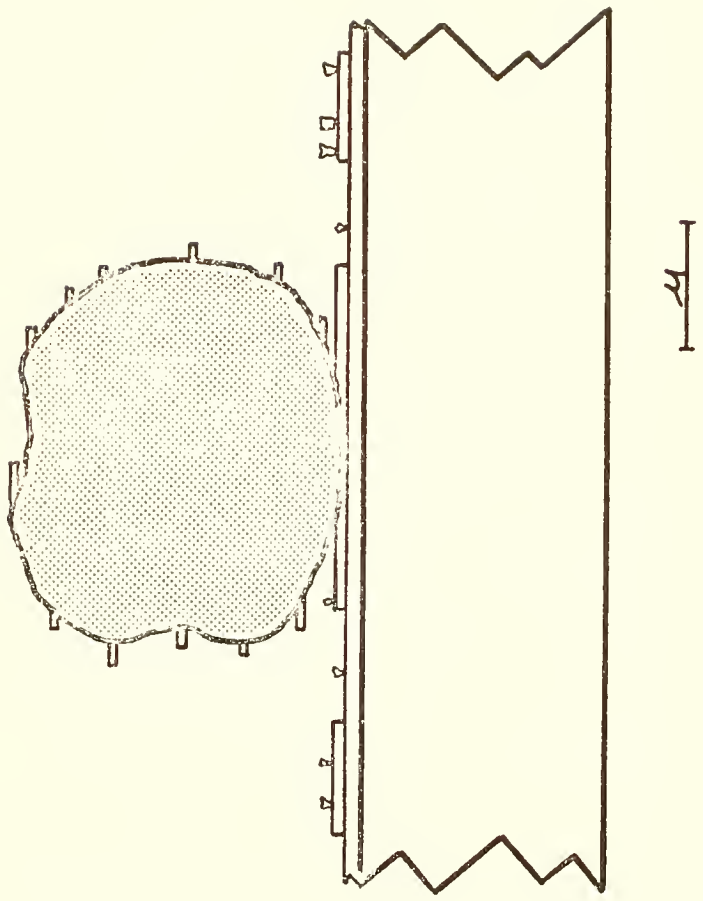

Figure 98. Interface After ½ Hour

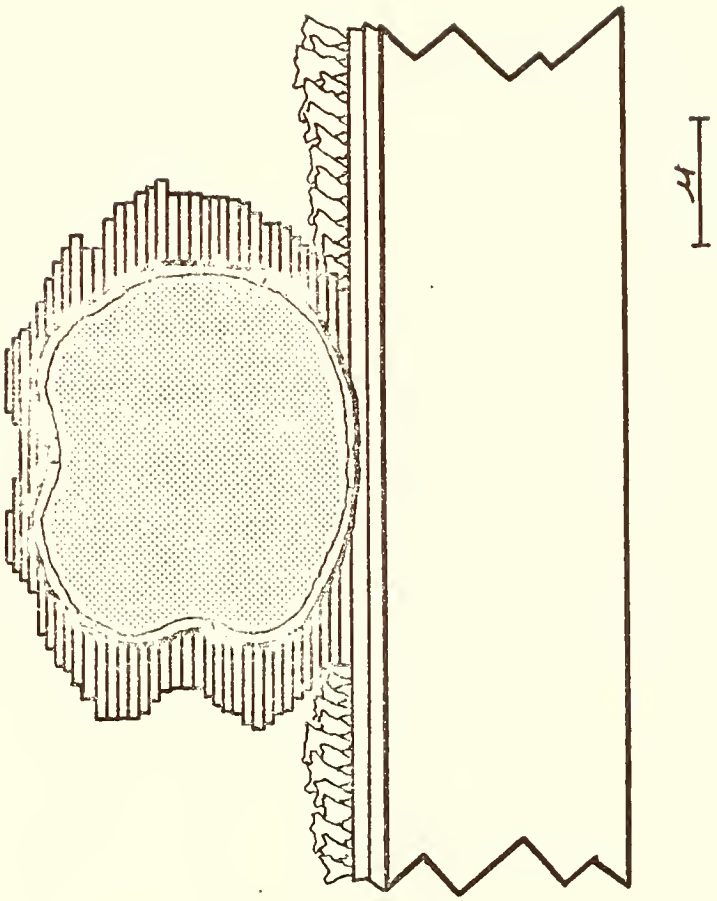

Figure 99. Interface After Two Hours

shell, which represents the original grain boundary, and the remnant cement grain. The remnant grain is tied to the hydration shell by small acicular crystals.

The appearance of the interface region after eight to twenty-four hours hydration is shown in Figures 100 and 101. The layer of massive lime surrounding the cement grain is now also coated with C-S-H gel. Gel has not, however, been deposited on the inner surface of the hydration shell. Consequently, the void between the shell and the remnant grain has increased in size. The remnant grain is still tied to the hydration shell by acicular crystals. Another prominant feature of the interface region after about eight hours is large and massive, randomly oriented crystals of lime. Such a crystal is shown in Figure 101. As the massive lime crystals grow, they engulf and encapsulate cement grains and their surrounding hydration shells.

Fracture at the paste-aggregate interface after about one day takes place largely through the void space lying between the interfacial film and the overlying paste. In regions where the bulk of the paste is tied to the aggregate by cement grains such as that shown on the right hand side of Figure 101, fracture takes place through the grain. In regions where the interface is tied to the paste through the growth of massive lime crystals, fracture takes place through the lime portion of the interfacial film, leaving a thin layer of lime adhering to the aggregate. If, however,

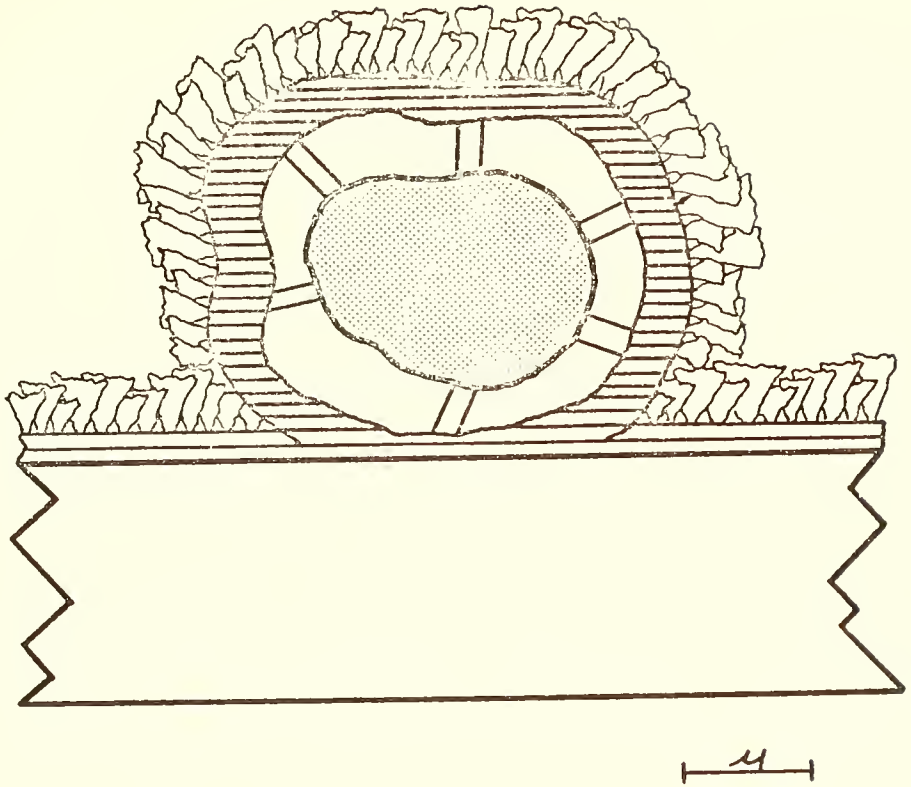

Figure 100. Interface After Eight Hours

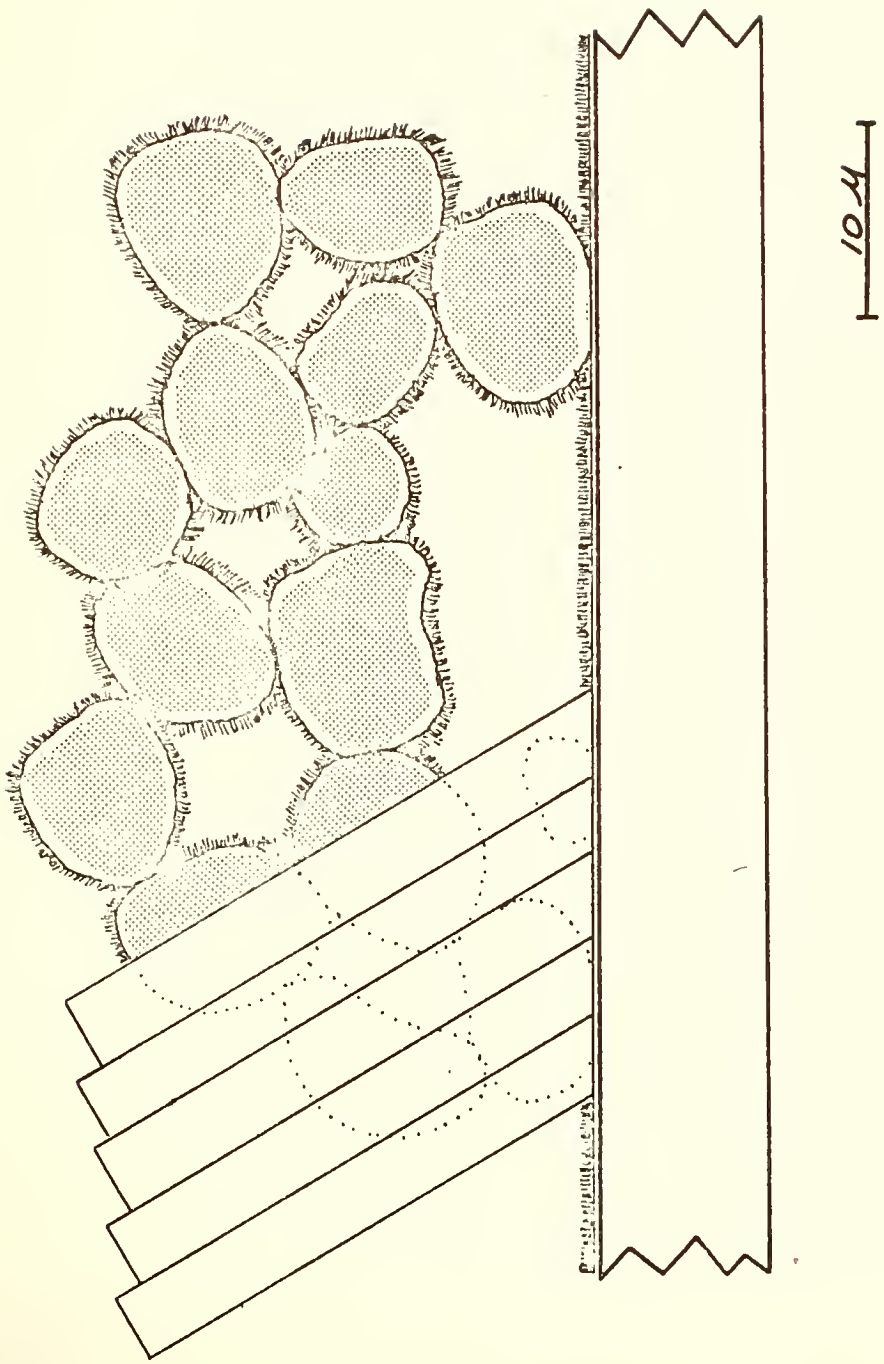

Figure 101. Interface After One Day

the aggregate has well-developed cleavages, such as are found with calcite and dolomite, fracture, rather than occuring in the lime film, will take place within the body of the aggregate along the cleavage planes of the minerals.

The relationships after about three days are shown in Figures 102 and 103. In Figure 102 the smaller cement grain has completely hydrated, leaving a shell of hydration products empty except for the acicular crystals. Large needle-like crystals of ettringite have developed on the exterior surfaces of the hydration shells. An additional feature can be seen in Figure 103. Large hexagonal plates, usually occuring in packets or booklets, have begun to form in the void space near the interface. These plates are rich in sulphur, aluminum and silicon, and probably represent a complex solid solution.

Owing to the continued development of massive lime, as well as some tying of the paste to the aggregate through the growth of platy crystals and ettringite needles, progressively greater proportions of the interfacial film remain with the paste upon fracture. By twenty-eight days, fracture is almost completely in the immediate vicinity of the paste-aggregate interface.

With strong aggregates such as the siliceous rocks, fracture occurs through the lime portion of the interfacial film. With aggregates having well developed cleavages, such as limestone and dolomite, fracture will be primarily along

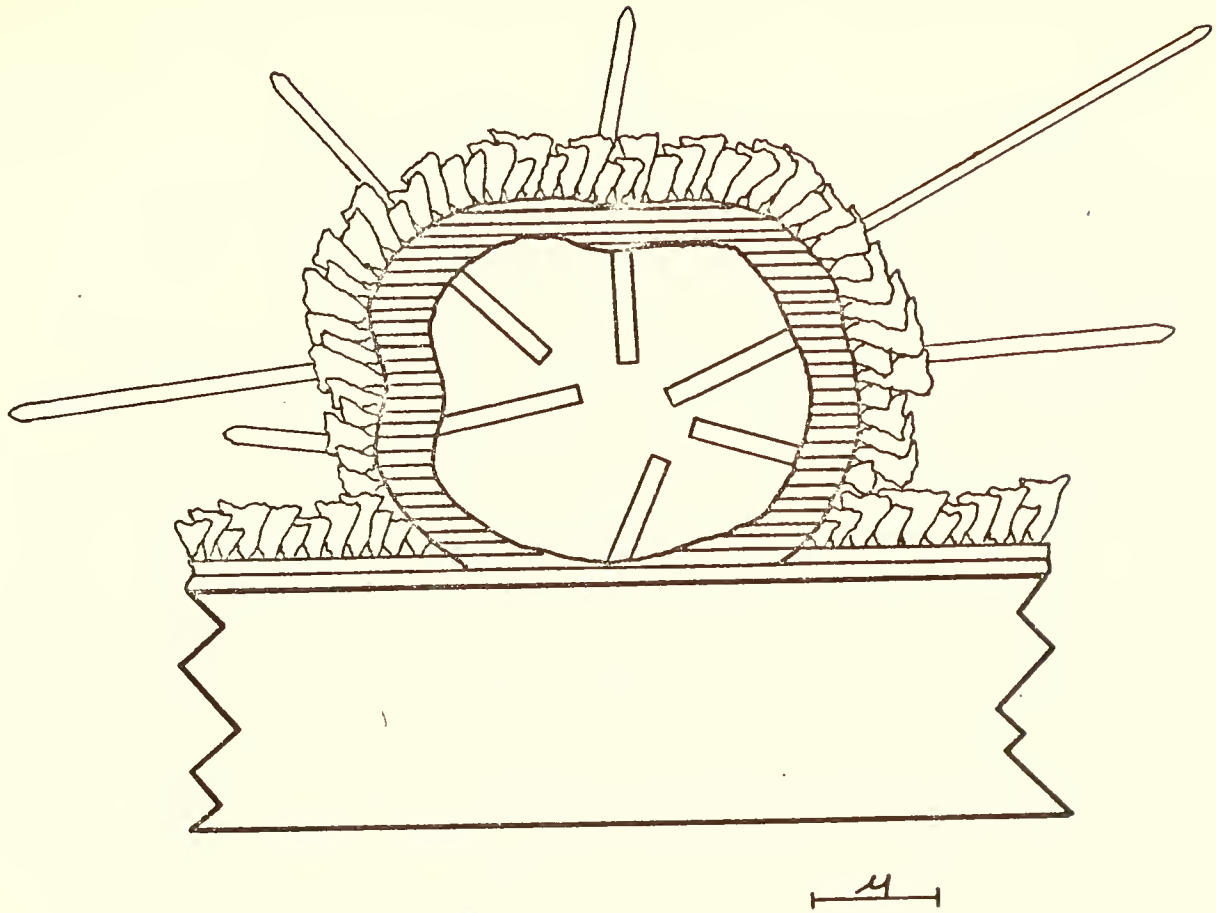

Figure 102. Interface After Three Days

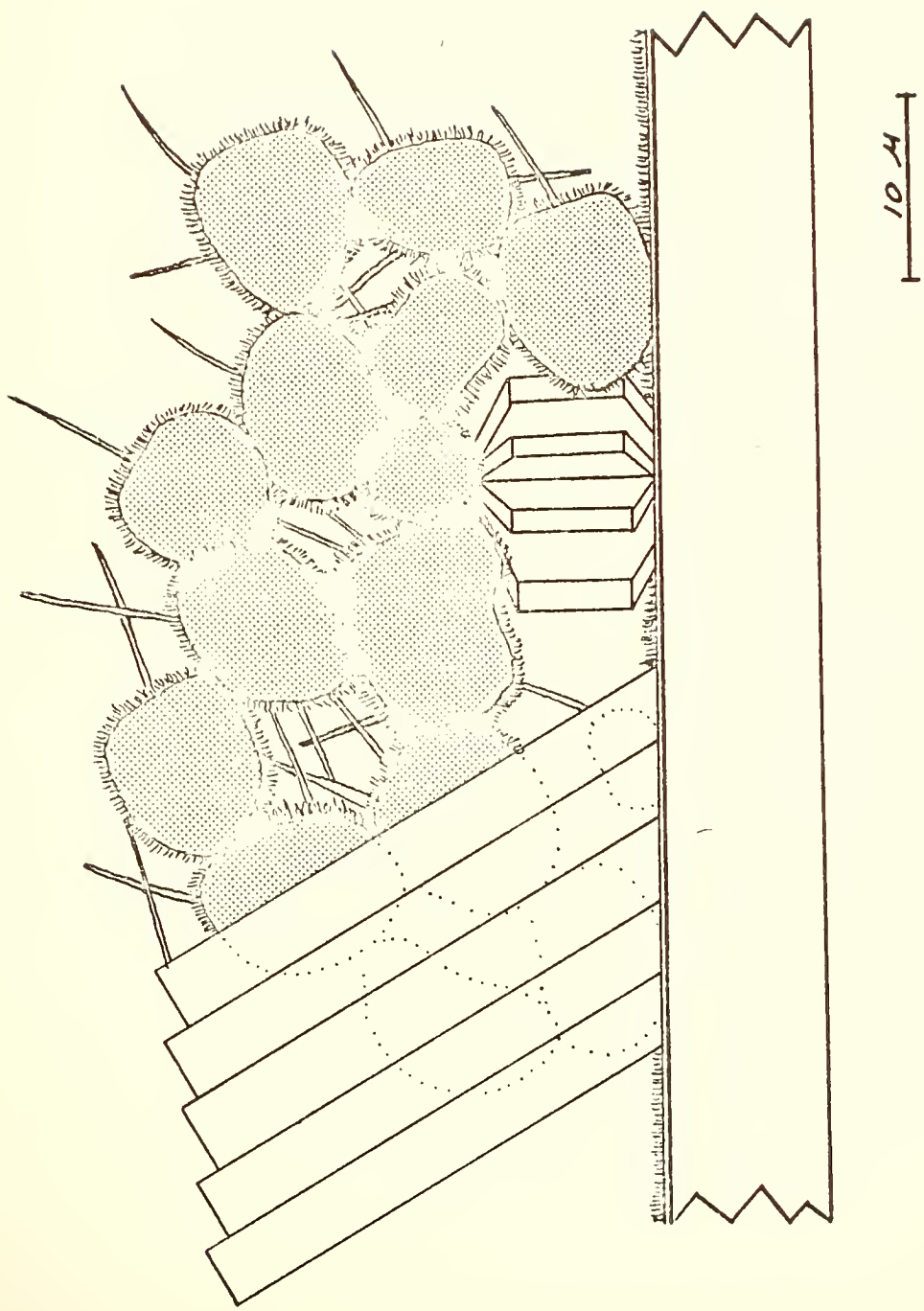

Figure 103. Interface After Three Days

the mineral cleavages within the rock. In no instance does fracture occur at the true paste-aggregate interface.

It was found that the orientation of the aggregate surface has no influence on the structure or mode of fracture at the interface. Water-cement ratio influences bond only by affecting the amount of void space at the interface. The lower the water-cement ratio, the smaller the amount of void space present, and the greater the amount of the interfacial film tied to the bulk of the paste at early ages. The structure that develops at the interface seems to be independent of the aggregate type. Surface roughness does not influence the structure at the interface or the type of fracture that is produced.

It is not known whether the essentially hollow hydration shells that were a prominant feature near the interface are also present in the interior of the paste. It is also not known whether or not these features are filled at later ages, although no sign of filling was seen on samples up to twenty-eight days of age.

Conclusions

1. A characteristic structure with several distinct features develops in a definite sequence at the cement paste-aggregate interface.

2. The structure that develops is independent of aggregate type, surface texture, substrate orientation, and water-cement ratio.

3. At least in the immediate vicinity of the interface, cement hydration takes place almost entirely through solution and the subsequent precipitation of hydration products.

4. The mode of fracture depends on the age of the material and the nature of the aggregate. At early ages the fracture surface will pass largely through void space lying near the interface. At later ages, when the void space has filled, it will pass either through a highly oriented lime film that forms on the aggregate surface, or through the rock with aggregates made up of minerals with well developed cleavages.

The above conclusions are based on the results and apply to the materials studied in this investigation. They are presumed applicable to most commonly used natural aggregates and portland cements, but not necessarily to other combinations.

LIST OF REFERENCES

LIST OF REFERENCES

1. Alexander, K. M., "Strength of the Cement-Aggregate Bond," ACI Journal, Proceedings, V. 56, No. 5, Nov. 1959, pp. 377-390.

2. Alexander, K. M. and Taplin, J. H., "Analysis of the Strength and Fracture of Concrete Based on the Unusual Insensitivity of Cement-Aggregate Bond to Curing Temperature," Australian Journal of Applied Science, V. 15, No. 3, Sept. 1964, pp. 160-170.

3. Alexander, K. M., Wardlaw, J., and Gilbert, D. J., "Aggregate-Cement Bond, Cement Paste Strength, and the Strength of Concrete," The Structure of Concrete, The Cement and Concrete Association, London, 1968, pp. 59-81.

4. Chatterji, S., and Jeffery, J. W., "Strength Development in Calcareous Cements," Nature, V. 214, May 1967, pp. 556-561.

5. Farran, J., "Mineralogical Contributions to the Study of Adhesion Between the Hydrated Constituents of Cement and the Imbedded Material," Revue des Materiaux de Construction et de Travaux Publics, (Paris), Nos. 490-492, 1956, pp. 155-172 and 191-209.

6. Hsu, T. T. C. and Slate, F. O., "Tensile Bond Strength Between Aggregate and Cement Paste or Mortar," ACI Journal, Proceedings V. 60, No. 4, April 1963, pp. 465-485.

7. Kaplan, M. F., "Flexural and Compressive Strength of Concrete as Affected by the Properties of Coarse Aggregates," ACI Journal, Proceedings V. 55, No. 11, May 1959, pp. 1193-1208.

8. Munger, E. L., "Bond Between Portland Cement Paste and Aggregate," Ph.D. Thesis, Iowa State College, 1957.

9. Shah, S. P. and Slate, F. O., "Internal Microcracking, Mortar-Aggregate Bond, and the Stress-Strain Curve of Concrete," The Structure of Concrete, The Cement and Concrete Association, London, 1968, pp. 82-92.

10. Taylor, M. A. and Broms, B. B., "Shear Bond Strength Between Coarse Aggregate and Cement Paste or Mortar," ACI Journal, Proceedings V. 61, No. 8, Aug. 1964, pp. 939-958.

11. Scholer, C. F., "The Role of Mortar-Aggregate Bond in the Strength of Concrete," Joint Highway Research Project, Purdue University, No. 1, Jan. 1967.

12. Hsu, T. T. C., Slate, F. O., Sturman, G. M. and Winter, G., "Microcracking of Plain Concrete and the Shape of the Stress-Strain Curve," ACI Journal, Proceedings V. 60, No. 2, Feb. 1963, pp. 209-224.

13. Jones, R. and Kaplan, M. F., "The Effect of Coarse Aggregate on the Mode of Failure of Concrete in Compression and Flexure," Magazine of Concrete Research, V. 9, No. 26, Aug. 1957, p. 89.

14. Shah, S. P. and Winter, G., "Inelastic Behavior and Fracture of Concrete," ACI SP-20, Causes, Mechanism and Control of Cracking in Concrete, 1969, pp. 5-27.

15. Nepper-Christensen, P. and Nielsen, T. P. H., "Modal Determination of the Effect of Bond Between Coarse Aggregate and Mortar on the Compressive Strength of Concrete," ACI Journal, Proceedings V. 66, No. 1, Jan. 1967, pp. 69-72.

16. Darwin, D. and Slate, F. O., "Effect of Paste-Aggregate Bond on the Behavior of Concrete," Unpublished Manuscript, 1969.

17. Bache, H. H., Ioorn, G. M., Nepper-Christensen, P., and Nielsen, J., "Morphology of Calcium Hydroxide in Cement Paste," Highway Research Board, Special Report 90, 1966, pp. 154-174.

18. Lyubimova, T. Y. and Pinus, E. R., "Crystallization Structure in the Contact Zone Between Aggregate and Cement in Concrete," Colloid Journal (U.S.S.R.), V. 24, No. 5, 1962, pp. 491-498.

19. Mather, K., "Applications of Light Microscopy in Concrete Research," Symposium on Light Microscopy, S.S.T.M. Sp-143, 1952, pp. 51-69.

20. Assarson, G. and Sundius, N., "Redogorelse for Undersokninger Angaende Orsakerne Till Forstorelse av Betong i Vattenbygnader," Tekniske Meddelander fran Kungl Vattenfallsstyrelsel, Series B., No. 16, 1929.

21. McConnell, D., Mielenz, R. C., Holland, W. Y. and Greene, K. T., "Cement-Aggregate Reaction in Concrete," ACI Journal, Proceedings V. 19, No. 2, Oct. 1947, pp. 93-128.

22. Terrier, P., and Moreau, M., "Examens au Microscope de Pates de Ciment Portland," Revue des Materiaux de Construction et de Travaus Publics, No. 584, May 1964, pp. 129-137.

23. Colony, R. J., "Petrographic Study of Portland Cement," Columbia School of Mines Quarterly, V. 36, No. 1, 1914, pp. 1-21.

24. Hedin, R., "Saturation Concentration of Calcium Hydroxide," Swedish Cement and Concrete Research Institute, Royal Inst. of Technology, Proceedings No. 27, Stockholm, 1955, pp. 1-14.

25. Martin, H., "Die Bindung im Beton," Betonstein-Zeitung, No. 11, 1963, pp. 539-533.

26. Chatterji, S. and Jeffery, J. W., "Three-Dimensional Arrangement of Hydration Products in Set Cement Paste," Nature, V. 209, March 1966, pp. 1233-1234.

27. Chatterji, S. and Jeffery, J. W. "Strength Development in Calcareous Cements," Nature, V. 214, May 1967, pp. 559-561.

28. Chatterji, S. and Jeffery, J. W., "Further Studies of the Three Dimensional Arrangement of the Hydration Products of Portland Cements," Indian Concrete Journal, V. 45, April 1971, pp. 167-172.

29. Chatterji, S., and Jeffery, J. W., "The Nature of the Bond Between Different Types of Aggregates and Portland Cement," Indian Concrete Journal, V. 45, Aug. 1971, pp. 346-349.

30. Diamond. S., "Application of Scanning Electron Microscopy to the Study of Hydrated Cement," Third Annual Scanning Electron Microscope Symposium, Chicago, Ill., April 1970, pp. 385-392.

31. Diamond, S., "Analysis of Hydrated Cements Using a Scanning Electron Microscope - Energy Dispersive X-ray Spectrometer Combination," Joint Highway Research Project, Purdue University, No. 21, Dec. 1971.

32. Williamson, R. B., "Constitutional Supersaturation in Portland Cement Solidified by Hydration," Journal of Crystal Growth, V. 3, 1968, pp. 787-794.

33. Taplin, J. H., "A Method for Following the Hydration of Portland Cement Paste," Australian Journal of Applied Science, V. 10, 1959, pp. 329-345.

34. Williamson, R. B., "Pseudomorphs of Original Cement Grains Observed in Hardened Pastes," Science, V. 164, May 2, 1969, pp. 549-551.

35. Williamson, R. B., "Solidification of Portland Cement," Report No. UC-SESM 70-23, University of California, Berkeley, 1970, 109 pp.

36. Mills, R. H., "Influence of Water in Areas of Restricted Adsorption on Properties of Concrete," Materials and Structures, V. 1, Nov.-Dec. 1968, p. 553.

37. Berger, R. L., Cahn, D. S. and McGregor, J. D., "Calcium Hydroxide as a Binder in Portland Cement Paste," Journal American Ceramic Society, V. 53, No. 1, Jan. 1970, pp. 57-58.

38. Mason, B., Principles of Geochemistry, John Wiley and Sons, Inc., New York, 1966, p. 167.

39. "Symposium on Alkali-Carbonate Rock Reactions," Highway Research Record, No. 45, 1964, 244 pp.

40. Russ, J. C., "Use of the Scanning Electron Microscope in Materials Science," Applications of Modern Metallographic Techniques, A.S.T.M. STP 480, 1970, pp. 214-248.

41. Hansen, W. C., "Actions of Calcium Sulfate and Admixtures in Portland Cement Pastes," A.S.T.M. STP No. 266, 1960, pp. 3-37.

APPENDIX

APPENDIX

Ottawa Sand Mortars

To study the structure at the interface in a system more closely resembling concrete, a series of mortars was prepared using standard Ottawa sand as aggregate.

Figures 104 and 105 show the surface of one of the sand grains on the mortar that was hydrated for one day before being broken. Fracture was for the most part close to the surface of the grain, presumably largely in the void space between the interfacial film and the main body of the paste. There is little or no evidence of any fracture in the interfacial film itself, however, indicating that in spite of the vibratory compaction, the void space at the interface with the mortars was greater than that found with the paste-substrate samples.

Figures 106 and 107 show the surface of a sand grain exposed by breakage after three days. The amount of fracture at the interface is still small.

Figures 108 and 109, taken of the seven day sample, show that the amount of fracture through the interfacial lime film is slowly increasing. Figure 108 shows little of the exposed fracture surface lying in the body of the

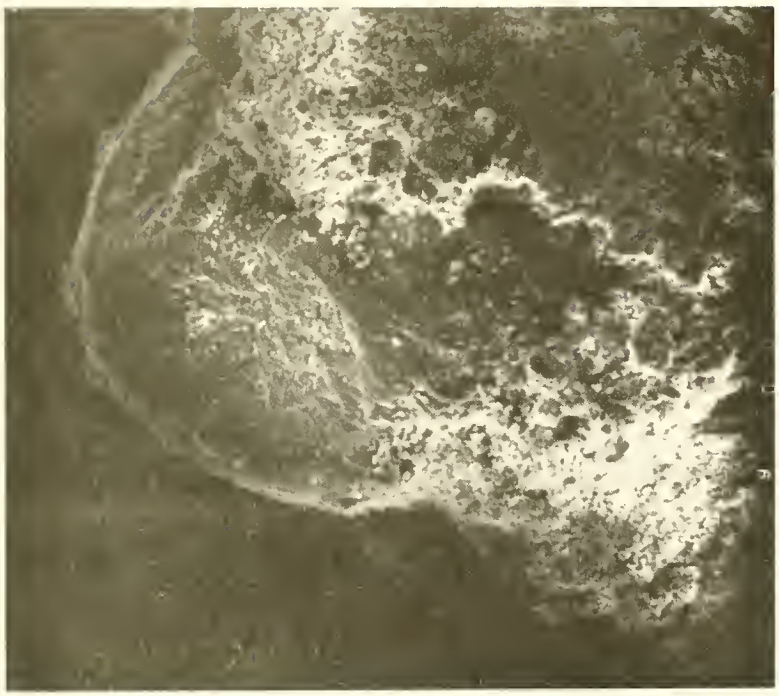

100 μ

Figure 104. Ottawa Sand Mortar - 1 Day

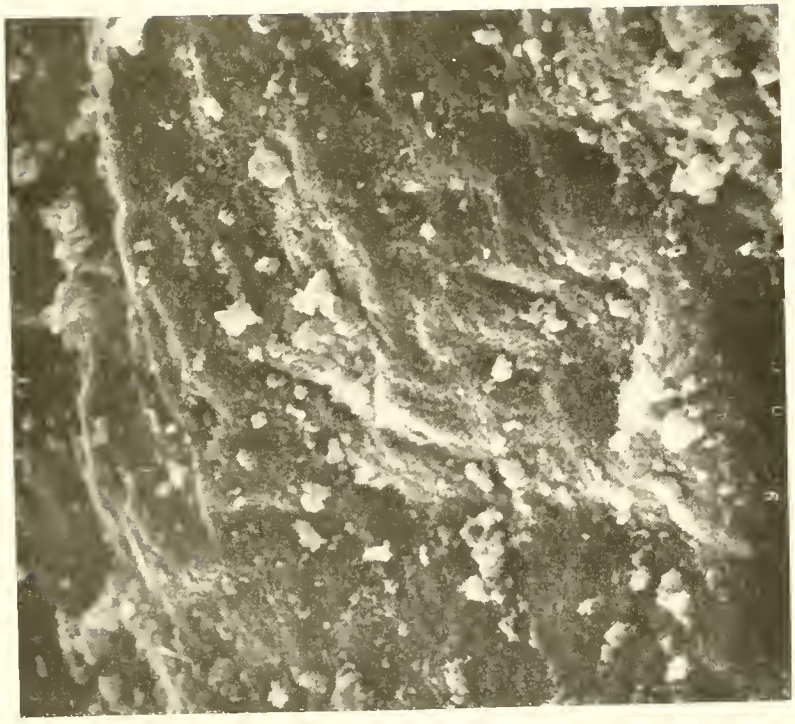

Figure 105. Ottawa Sand Mortar - 1 Day

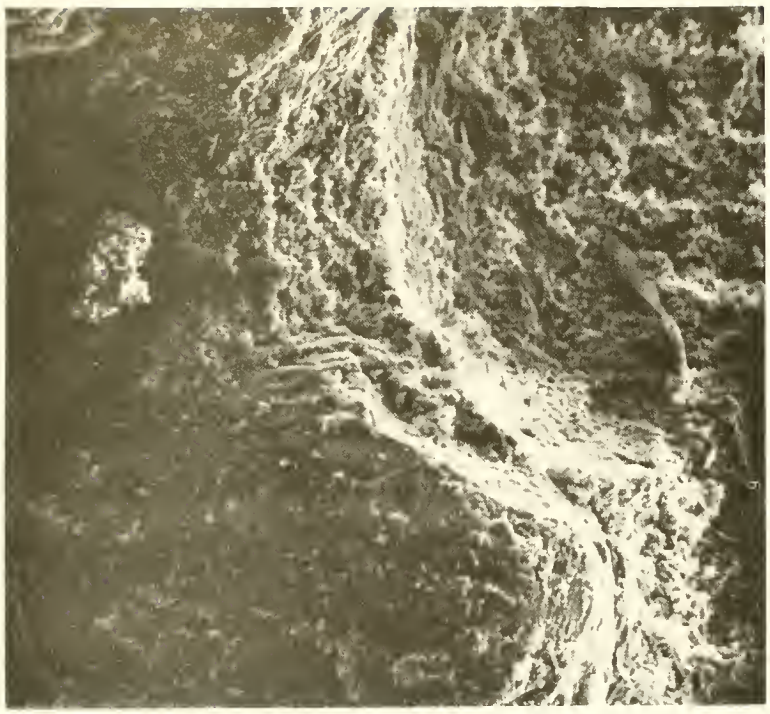

100 μ

Figure 106. Ottawa Sand Mortar - 3 Days

10 μ

Figure 107. Ottawa Sand Mortar - 3 Days

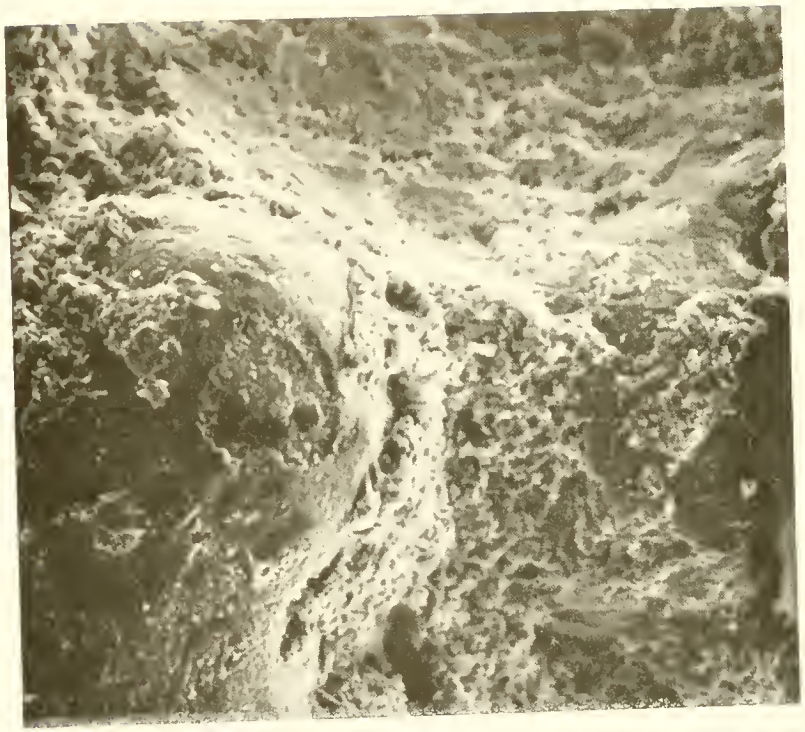

100 μ

Figure 108. Ottawa Sand Mortar - 7 Days

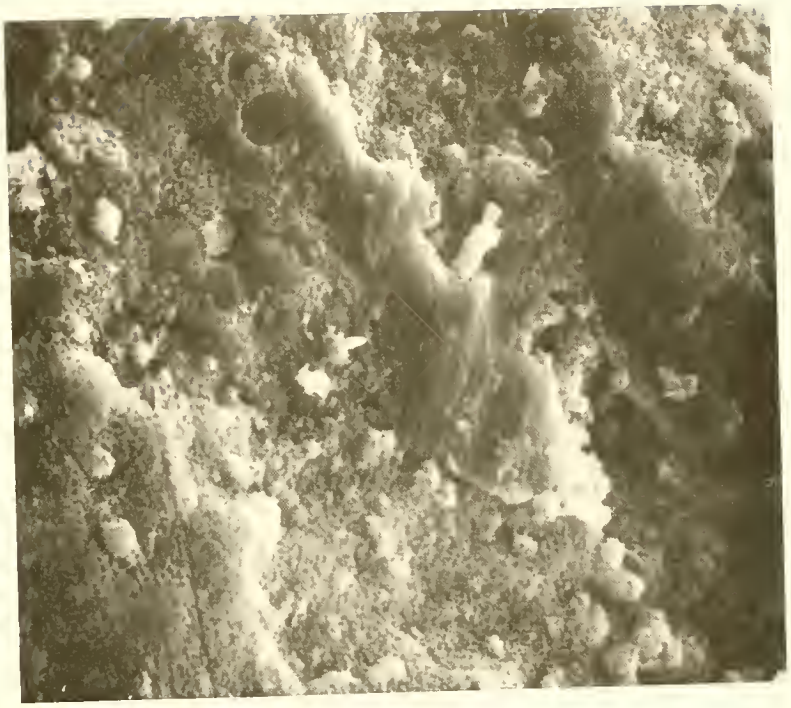

10μ

Figure 109. Ottawa Sand Mortar - 7 Days

paste, but rather in the void spaces near the interface.

Figures 110 and 111, taken of the fourteen day sample, show that although there has been some increase in the amount of fracture taking place in the interfacial film, the total amount is still small. In contrast, at fourteen days the surface of the roughened quartzite substrate was largely free of paste.

X-ray spectrometry once again confirmed that separation at the interface took place within the oriented lime film rather than at the true paste-aggregate interface.

Manufactured Calcite Sand Mortars

Mortar samples were also prepared using a manufactured calcite sand as aggregate. Study of these samples showed that with all of the mortar cylinders, regardless of age, the fracture surface passed through the aggregate grains. The fracture surface of the one day old mortar is shown on Figures 112 and 113.

The nature of the fracture surface would indicate that once a crack was initiated and began to propagate, the path of least resistance was through the calcite cleavages, rather than in the void spaces around the periphery of the sand grain as was the case with the silica sand mortars.

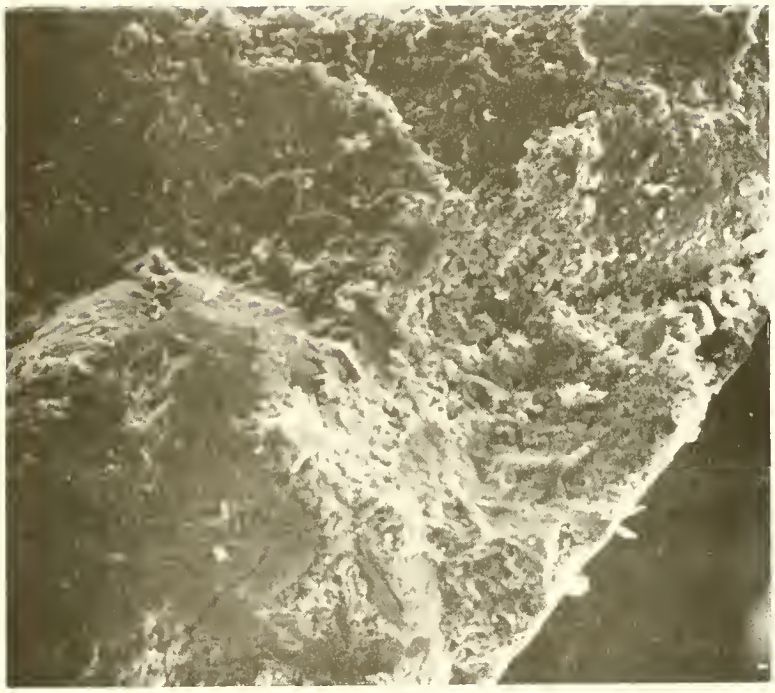

100μ

Figure 110. Ottawa Sand Mortar - 14 Days

10μ

Figure 111. Ottawa Sand Mortar - 14 Days

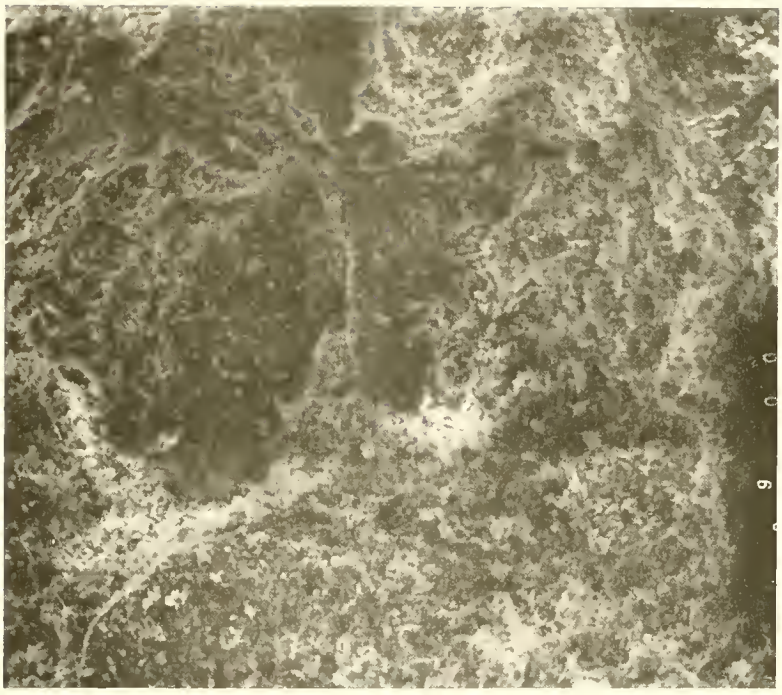

100 μ

Figure 112. Manufactured Calcite Sand Mortar - 1 Day

10 μ

Figure 113. Manufactured Calcite Sand Mortar - 1 Day

VITA

VITA

David Watson Hadley was born in Chicago, Illinois on September 10, 1929. He obtained his primary and secondary education in the Chicago public schools, graduating from South Shore High School in 1947. He served in the U.S. Army in 1948-49, and received a B.S. with honors in geology from the University of Illinois in 1953.

After working for a number of years as an engineering geologist, he joined the staff of the Research and Development Laboratories of the Portland Cement Association as Research Geologist in 1958. He is senior author of a number of papers in the field of concrete and concrete aggregates, and in 1964 was awarded the Highway Research Board Award for his work on the alkali reactivity of carbonate rocks.

He received an M.S. in geology from the University of Chicago in 1967, and in 1968 joined the staff of Purdue University as a Graduate Instructor in Research.

Mr. Hadley is married, and the father of three children.